

**A conserved and essential motif in the pre-mRNA
splicing factor Snu66 and *SRC1* alternative splicing
factors in *S. cerevisiae***

A Thesis

Submitted
By

POULAMI CHOUDHURI
MP12004

For the partial fulfilment of
DOCTOR OF PHILOSOPHY



Department of Biological Sciences
Indian Institute of Science Education and Research (IISER) Mohali
Sector-81, Mohali-140306, Punjab, India

January, 2021

Dedicated to Pishan

Declaration

The work presented in this thesis entitled “**A conserved and essential motif in the pre-mRNA splicing factor Snu66 and SRC1 alternative splicing factors in *S. cerevisiae*.**” has been carried out by me under the supervision of Dr. Shravan Kumar Mishra at the Indian Institute of Science Education and Research (IISER) Mohali. This work has not been submitted in part or full for a degree, a diploma, or a fellowship to any university or institute. Whenever contributions of others are involved, every effort is made to indicate this clearly, with due acknowledgement of collaborative research and discussions. This thesis is a bona fide record of original work done by me and all sources listed within have been detailed in the references.

Date:

Poulami Choudhuri

Place:

(Candidate)

In my capacity as the supervisor of the candidate's thesis work, I certify that the above statements by the candidate are true to the best of my knowledge.

Date:

Dr. Shravan Kumar Mishra

Place:

(Supervisor)

Acknowledgement

The process of earning a doctorate and writing a thesis is long and arduous and it is certainly not done singlehandedly. On the very onset of this report, I owe my greatest debt from the core of my heart to all those without whom I would not have reached this far.

*First and foremost, I express my deepest gratitude to my Ph.D. supervisor **Dr. Shravan Kumar Mishra**, who is a great mentor and I am fortunate enough to get the chance to work with him. His cordial nature, guidance, scientific knowledge, experience and dedication made my work enjoyable and comprehensive. His excellent mentorship has immensely helped me in a better understanding of science and academics. The feeling of him being my side always gave me immense support and confidence to pursue this endeavour. He taught me that experiments should be thoughtfully designed, carefully analysed, and controls are as important as the test samples. I admire him for being a person who always makes sure that everything should be done perfectly. I learned from him that one should be focused, organized, and disciplined. Under his guidance, I learned that one should always give 100% to your job and as they say to believe that perseverance is the key. Whenever problems got me demotivated, he always became the light at the end of the tunnel.*

*I express my sincere thanks to my doctoral committee members, **Prof. Anand Kumar Bachhawat** and **Prof. Purnananda Guptasarma** for their time, support, and valuable suggestions. Their critical comments and guidance have always been very helpful for the timely progress of my doctoral study and enhanced the quality of my work.*

*I profoundly thank **Dr. Jeffrey A. Pleiss** at Cornell University, Ithaca, USA for sharing the splicing-sensitive microarrays design, helping us to perform the experiment and **Dr. Nishant KT** for hosting me in his lab in IISER Thiruvananthapuram for some experiment. I acknowledge **Mrs. Ulla Cramer** from Prof. Stefan Jentsch laboratory at the Max Planck Institute of Biochemistry, Martinsried, Germany for materials and strains used in this study. I am also thankful to **Dr. Saikat Ghosh** and **Dr Soumitra Mitra** for helping me with the microscopy facility.*

*I would like to thank **Director**, IISER Mohali, for giving me the opportunity to work at this premier research institute and permitting me to use the excellent infrastructure for carrying out my research work. I express my immense gratitude to all faculties and members of **Department of Biological Sciences, IISER Mohali** for providing me access to departmental facilities, for the exciting discussions and encouraging interactions during seminars and presentations.*

I would like to thank IISER Mohali, Ministry of Human Resource and Development (MHRD), Centre for Protein Science, Design and Engineering (CPSDE), Ministry of Human Resource and Development (MHRD), and Wellcome-DBT India Alliance, for fellowship during my PhD tenure.

I am very thankful to all non-teaching staff members, administration, library staff, store and purchase sections, accounts sections, hostel caretakers, mess peoples, cleaning staff and entire IISER Mohali community for their help and cooperation.

*I am extremely thankful to all my lab members for their incredible support, fruitful scientific discussions, and all the parties we enjoyed together. Special thanks to **Balashankar R** for his immense contribution in the successful completion of the project and for being a great emotional support. My sincere thanks to the seniors **Poonam, Prashant, and Kiran** who gave me hands on training in the lab. Two people who need special mention are **Rakesh**, and **Anupa** who picked me up every time I broke down and felt I could not do better. I thank all the other members **Manu, Praver, Karan, Sumanjit, Ankita, Bhavya, Bhargesh, Amjad, Nivedha, Sugata, and Azeem** for their valuable inputs for the project and creating a homely environment. I am really grateful to **Mr. Baidnath Mandal** (Vidhya) for his efforts and support in the lab work.*

*Getting through this journey required more than academic support, and I have many many people to thank, for listening to and, at times having to tolerate me over the past years. I cannot begin to express my appreciation for their friendship. I would like to extend my gratitude to the 1st batch of the **Int. PhDs (2012)** for coming together at the very beginning. I thank **Manaoj** and **Vikash** for always being with me, giving me confidence, sharing the love of food, and our little trips. For many memorable crazy days out and in, I must thank **Sujoy, Ayushi, Samiridhi, Ankit, Shivam Mayank** and **Meenakshi**. I would also like to thank*

Drishya, Richa, Charu, and Ambika who were far but helped me believe in myself a bit more every time we talked.

Finally, I owe my deepest gratitude and love to my parents (**Maa and Babu**). They are the people behind all my achievements and are the pillar of my strength. Thank you for being the coolest parents that you are. I am extremely lucky to have such a supporting family (**Dadu-Didara Kaku-Kakira, Mani-Meshora, Mamu-mamira, Pishimani, Pishan, and the amazing young bunch**) who encouraged me through phone calls – despite my own limited devotion to correspondence. This thesis stands as a testament to your blessings, unconditional love, prayers, support, sacrifices, and faith. Thanks a lot for being the driving force and the cushion to fall back on.

Last but not least, my heartfelt gratitude goes to **Shyamal Uncle** who has been the person to give that little required nudge to my academic career. From admission in DU to IISER-Mohali you have been the bearer of good news and I thank you from the bottom of my heart for everything you helped me with. This journey would not have been possible without you.

I hope to make you all proud.

Thanking You

Poulami

Contents

List of Figures	i
List of Tables	iii
List of Boxes	iii
Abbreviations	v
Synopsis	ix

Chapter 1: Introduction

1.1 RNA Splicing	1
1.2 The spliceosome	2
1.3 Intron and Exon Definition	8
1.4 Splicing Fidelity	9
1.5 Alternate Splicing	11
1.6 AAA-ATPase	14
1.7 Homologous Recombination	15

Chapter 2: Snu66 function and mechanism

2.1 Introduction	21
2.2 Objective	23
2.3 Results	23-36
2.2.1 <i>An essential conserved motif of Snu66</i>	21
2.2.2 <i>Genetic interactors of Snu66-CM</i>	27

2.2.3 <i>Spliceosome architecture in Snu66-CM mutant</i>	29
2.2.4 <i>Role of Snu66-CM in splicing</i>	31
2.2.5 <i>Snu66-CM in S. pombe</i>	33
2.4 Conclusion and Discussion	37

Chapter 3: Sap1-Snu66 Function and Regulation

3.1 Introduction	41
3.2 Objective	43
3.3 Results	43-66
3.3.1 <i>Snu66-Sap1 interactions</i>	43
3.3.2 <i>Sap1 isoforms</i>	44
3.3.3 <i>Sap1 isoform expression by alternate transcription</i>	46
3.3.4 <i>Phenotype for Sap1</i>	48
3.3.5 <i>Genetic interactors of Sap1</i>	50
3.3.6 <i>Different localisation of isoforms</i>	51
3.3.7 <i>Regulation of Sap1_C by Tup1</i>	53
3.3.8 <i>Tup1 binds the internal promoter directly</i>	54
3.3.9 <i>Sumoylation of Tup1 inhibits Sap1_C expression</i>	55
3.3.10 <i>Role of Sap1 in splicing</i>	56
3.3.11 <i>Does Sap1 has any other function?</i>	59
3.3.12 <i>Sap1-Snu66 complex in splicing fidelity</i>	60
3.3.13 <i>Sap1-Snu66 in homologous recombination</i>	64
3.4 Conclusion and Discussion	67

Chapter 4: *SRC1* alternative splicing factors and mechanism

4.1 Introduction	71
4.2 Objective	73
4.3 Results	73-86
4.3.1 <i>Specific spliceosomal proteins promote SRC1 alternative splicing</i>	73
4.3.2 <i>SRC1 alternative splicing is defective in prp8-101 allele</i>	76
4.3.3 <i>The RES complex promotes SRC1 alternative splicing</i>	77
4.3.4 <i>Mechanism of SRC1 alternative splicing</i>	83
4.4 Conclusion and Discussion	86

Methods

5.1 Materials	91-108
5.1.1 <i>Chemicals and plastic wares</i>	91
5.1.2 <i>Molecular biology reagents</i>	91
5.1.3 <i>Antibodies and antibody-coupled beads</i>	92
5.1.4 <i>Media</i>	92
5.1.5 <i>Buffers and stock solutions</i>	93
5.1.6 <i>Yeast strains and plasmids</i>	95
5.1.7 <i>Primers</i>	104
5.1 Methods	109-122
5.2.1 <i>Strain maintenance</i>	109
5.2.2 <i>Yeast genomic DNA isolation</i>	109
5.2.3 <i>Yeast competent cell preparation</i>	110

<i>5.2.4 Yeast transformation</i>	110
<i>5.2.5 Quik Change Site-directed mutagenesis</i>	110
<i>5.2.6 Overlap extension (SOE) PCR</i>	111
<i>5.2.7 Deletion and tagged strain generation</i>	111
<i>5.2.8 Trichloroacetic acid (TCA) precipitation</i>	112
<i>5.2.9 Western blot assays (WB)</i>	112
<i>5.2.10 Co-immunoprecipitation (Co-IP) assay</i>	113
<i>5.2.11 RNA isolation and RT-PCR</i>	114
<i>5.2.12 Real time quantitative PCR</i>	115
<i>5.2.13 Splicing reporter assays</i>	115
<i>5.2.14 Growth assay</i>	116
<i>5.2.15 Splicing sensitive microarray</i>	116
<i>5.2.16 ONPG assay</i>	116
<i>5.2.17 Northern blot assay</i>	117
<i>5.2.18 Microscopy</i>	119
<i>5.2.19 Ni-NTA pull-down assay</i>	119
<i>5.2.20 Chromatin immunoprecipitation (Ch-IP) assay</i>	120
Appendix	123
References	129
Publication	141

List of Figures:

Figure 1.1 Schematic for RNA splicing.

Figure 1.2 Spliceosome assembly and transition.

Figure 1.3 Structural comparisons between the human and yeast B^{act} complexes.

Figure 1.4 Structural comparisons between the human and yeast C complexes.

Figure 1.5 Structure of the *S. cerevisiae* spliceosomal C* complex.

Figure 1.6 Mechanism of intron and exon definition.

Figure 1.7 Mechanism of proofreading via DEAD/H-box ATPases in the splicing pathway.

Figure 1.8 Mechanism of Alternative splicing.

Figure 1.9 Cryo EM-structure of Cdc48.

Figure 1.10 Repair of DNA double-strand breaks by DSBR and SDSA

Figure 1.11 Repair of DNA double-strand breaks by SSA and BIR.

Figure 2.1: Views of an atomic model of the *Saccharomyces cerevisiae* U4/U6.U5 tri-snRNP.

Figure 2.2: Conserved domains of Snu66/SART1.

Figure 2.3: Identification of a conserved C-terminal domain of Snu66 essential for cell survival.

Figure 2.4: Genetic interaction of the Snu66-CM.

Figure 2.5: Role of Snu66-CM in spliceosome architecture.

Figure 2.6: Role Snu66-CM in splicing.

Figure 2.7: Snu66-CM in *S. pombe*.

Figure 2.8: Splicing defects in *S. pombe* snu66 mutant.

Figure 2.9: Change in level of spliceosome components.

Figure 2.10: Schematic of Snu66 and its interacting domains.

Figure 3.1 Sap1 a novel interactor of splicing factor Snu66.

Figure 3.2: Two isoforms of Sap1.

Figure 3.3: Expression by alternate transcription via internal promoter.

Figure 3.4: Phenotype in $\Delta sap1$.

Figure 3.5: Genetic interactors of Sap1.

Figure 3.6: Localisation of Sap1 and Sap1_C.

Figure 3.7: Role of Sap1 in pre-mRNA splicing.

Figure 3.8: Other probable functions of Sap1.

Figure 3.9: Role of Sap1-Snu66 complex in splicing fidelity.

Figure 3.10: Complementation of $\Delta sap1$ by different variants of Sap1.

Figure 3.11: Regulation of Sap1_C by Tup1.

Figure 3.12: Mechanism of repression by Tup1.

Figure 3.13: Level of Tup1 sumoylation.

Figure 3.13 Sap1-Snu66 complex in homologous recombination (HR).

Figure 3.14: The Sap1-Snu66 complex.

Figure 4.1 *SRC1* alternative splicing via Hub1, Snu66, and Prp38.

Figure 4.2: Proximity probing of splicing factors with *hub1(D22A)* to monitor their role in *SRC1* alternative splicing.

Figure 4.3: Excess of Hub1 does not alter *SRC1* alternative splicing pattern.

Figure 4.4: *SRC1* alternative splicing requires functional *Prp8-101* surface.

Figure 4.5: Screening for factors involved in *SRC1* alternative splicing.

Figure 4.6: RES complex facilitates *SRC1* alternative splicing.

Figure 4.7: Mutants defective in mRNA export do not show *SRC1* alternative splicing defects.

Figure 4.8: Splicing defects in RES complex mutants is distinct from *hub1Δ*.

Figure 4.9: U1, U5, and U6 snRNA binding of *SRC1* 5' ss.

Figure 4.10: Mechanism of *SRC1* alternative splicing with additional factors.

List of Tables:

Table 2.1 Splice site analysis for *snu66-1* targets

Table 4.1: *SRC1* alternative splicing factors and proposed mechanisms

Table 4.2 Affinity of *SRC1* 5'ss binding to U1, U5, and U6 snRNAs.

Table 5.1: Strains used for Chapter 2

Table 5.2: Strains used for Chapter 3

Table 5.3: Strains used for Chapter 4

Table 5.4: Plasmids used for Chapter 2

Table 5.6: Plasmids used for Chapter 3

Table 5.7: Primers used for RT-PCR and ChIP assay

List of Boxes:

Box 1: Ubiquitination

Box 2: Sumoylation

Box 3: SIM

Box 4: Alternate Transcription

Abbreviations

AS- Alternative Splicing

AAA-ATPase- ATPase Associated with diverse cellular Activities

BIR- Break-Induced Replication

bp- Branch Point

DBSR- Double-Stranded Break Repair

EDA-Exon Defined A

ESE- Exonic Splicing Enhancer

ESS- Exonic Splicing Silencer

HIND- Hub1 Interaction Domain

HR- Homologous Recombination

ISE- Intronic Splicing Enhancer

ISS- Intronic Splicing Silencer

ILS- Intron Lariat Spliceosome

MS- Mass spectrometry

NTC- Nineteen Complex

OD- Optical Density

ORF- Open Reading Frame

PCNA- Proliferating Cell Nuclear Antigen

PD- Post Diauxic

RES- Retention and Splicing

SDSA- Synthesis-Dependent Strand Annealing

SIM- SUMO Interaction Motif

snRNA- Small nuclear RNA

snRNP- Small nuclear Ribonucleoprotein

Snu66-CM- Snu66 Conserved and Essential C-terminus Motif

ss- Splice Site

SSA- Single-Strand Annealing

SUMO- Small Ubiquitin-like Modifier

U2AF- U2 Auxiliary Factors

UTR- Untranslated Region

WB- Western Blot

WT- Wild Type

SYNOPSIS

A conserved and essential motif in the pre-mRNA splicing factor Snu66 and *SRC1* alternative splicing factors in *S. cerevisiae*

Poulami Choudhuri (MP12004)
Indian Institute of Science Education and Research Mohali,
Sector 81, SAS Nagar, Mohali
Punjab, India, 140306

INTRODUCTION

Pre-messenger RNA splicing is an essential step in eukaryotic gene expression wherein mRNAs are generated by removing non-coding intron and joining protein-coding exons. The process is executed by a dynamic ribonucleoprotein (RNP) complex called spliceosome in two sequential transesterification reactions. Through these reactions the machinery excises introns harbouring the splicing signals like 5' splice site (5'ss), branch point (bp), 3' splice site (3'ss), polypyrimidine tract. These cis-acting RNA signals are detected by trans-acting factors of the spliceosome comprising of small nuclear RNAs (snRNAs) and snRNA-associated proteins. Together, they form the five spliceosomal snRNPs (U1, U2, U4, U5 and U6). Additional regulatory factors participate in spliceosome assembly and activation thereby accomplishing constitutive and regulated splicing of the diverse intron-containing pre-mRNAs¹.

The U4/U6.U5 tri-snRNP complex is an important component of the spliceosome as it forms the catalytic centre. It consists of core splicing factors like Prp8, Brr2, Snu114, Prp6, Prp3, including Snu66 which help in attaining its proper conformation². Snu66 (SART1 mammalian homolog) appears to function like a scaffold and is important for the tri-snRNP assembly. Unlike in the budding yeast *Saccharomyces cerevisiae*, where Snu66 is non-essential under standard growth conditions, the protein is indispensable in intron richer organisms³. Recent cryo-EM studies have confirmed multiple interactions of Snu66 with splicing factors such as Prp8, Brr2, Prp6, and the ubiquitin-like modifier Hub1^{4,5}.

Alternative splicing is a process of generating variably spliced mRNAs (proteins) from a parent pre-mRNA. The process is critical for increasing the complexity of gene expression and cell proteome. Snu66 has been reported to regulate alternative splicing of *SRC1* in *S. cerevisiae* by binding non-covalently to the ubiquitin-like modifier Hub1⁶. *S. cerevisiae SRC1* pre-mRNA has one intron with two overlapping competing 5'ss //GCAA//GUGAGU. Splicing using the downstream 5'ss GUGAGU is constitutive and Hub1-independent that generates Src1-L encoding transcript while splicing using the upstream 5'ss GCAAGU is alternative and Hub1-dependent that generates transcript encoding Src1-S protein. In a recent article, researchers have shown an important role of Hub1-mediated

spliced Src1-S form of protein in regulation of endosomal sorting complexes required for transport (ESCRT) (Chm7) recruitment to the nuclear envelope and interaction with Src1-L⁷.

In brief, I have studied and report the following results in my PhD thesis:

- i) **Function and mechanism of Snu66 in pre-mRNA splicing:** This part of the study was performed both in the budding yeast *S. cerevisiae* and the intron-richer fission yeast *Schizosaccharomyces pombe*. The protein has an essential motif at the C-terminus which is critical for pre-mRNA splicing and cell survival. I also found a novel interactor of Snu66, a SUMO binding AAA-ATPase Sap1 and explored possible role of the Sap1-Snu66 complex in *S. cerevisiae*.
- ii) **SRC1 alternative splicing factors in *S. cerevisiae*:** I screened, identified, and studied splicing factors that promote alternative splicing of *SRC1* in *S. cerevisiae*. I have also studied mechanism of *SRC1* alternative splicing via the two overlapping 5' splice sites.

RESULTS AND DISCUSSION

- i) **Function and mechanism of Snu66:** I found that Snu66 has a C-terminal Motif (abbreviated as Snu66-CM), from amino acid residues 531-554, which is conserved from *S. cerevisiae* to *H. sapiens*. By contrast to the previously characterised motifs in Snu66, its CM is an essential motif and its absence imparted partial cold sensitivity in *S. cerevisiae*. The region helped in the constitutive splicing as well as splicing using non-canonical splice signals such as GUAUAU. Interestingly, Snu66-CM was indispensable in the intron-richer yeast *S. pombe*. Point mutants, such as *D600A*, and the deletion of Snu66-CM were lethal to cells and the mutation *K613A* led to temperature-sensitive growth defects in *S. pombe*. The *K613A* mutant also showed a significant reduction in splicing efficiency and defects in the recognition of introns with non-canonical splice signals.

To understand Snu66 function better, we carried out a yeast two-hybrid screen using Snu66 as bait and found Sap1 as an interactor in *S. cerevisiae*. Sap1 is a SUMO-conjugate binding AAA-ATPase. I found that two protein isoforms of Sap1, Sap1 full length (Sap1) and Sap1 shorter form (Sap1_C), of 100 kDa and 50 kDa respectively, were expressed from alternatively transcribed mRNAs in a carbon source-dependent manner. Interestingly, Sap1 bound Snu66 through its CM. I discovered multiple interesting properties of Sap1, however the function of Sap1-Snu66 complex remains to be explored further.

- ii) **SRC1 alternative splicing factors in *S. cerevisiae*:** In this part of my thesis, I have identified additional regulators in *SRC1* alternative splicing in *S. cerevisiae*. These include spliceosomal complex B proteins, RES complex subunits, and Nam8. I found core splicing factors, like Prp6

and Prp3, also play a role in the regulation of alternative splicing. I further elucidated the role of Prp8 and identified the *prp8-101* allele that was specifically defective in *SRC1* alternative splicing. Since Hub1 is also required for *SRC1* alternative splicing, the data suggest that the newly identified factors function via mechanisms related to Hub1. I also identified the role of RES complex subunits (Snu17, Bud13, Pml1, and Urn1), and factors like Nam8, Ecm2 in *SRC1* alternative splicing. These proteins appear to function via a mechanism independent of Hub1. By using different mutants of 5'ss of *SRC1*, I found that the usage of the two overlapping splice sites of *SRC1* pre-mRNA depends on the strength of its binding to U1, U6 and/or U5 snRNAs. And, the newly identified protein factors might modulate binding efficiencies of the snRNAs.

CONCLUSION

The findings of my PhD thesis have demonstrated that the conserved splicing factor Snu66/SART1 has a highly conserved essential functional motif at the C-terminus. While the absence/mutation of Snu66-CM affects the pre-mRNA splicing (constitutive and of introns containing non-canonical splice sites) in both *S. cerevisiae* and *S. pombe*, the effect of this motif on cell viability is striking in intron-rich *S. pombe*. Snu66 also interacted with SUMO-binding AAA-ATPase Sap1 via Snu66-CM. These data suggest that splicing function Snu66 must be understood in light of the newly identified motif.

SRC1 alternative splicing requires multiple core splicing factors, and regulators. Based on their mechanism of function they can be broadly divide into two categories; Hub1-dependent and Hub1-independent. The selection of the *SRC1* 5'ss depends on their strengths of binding to U1, U6, and/or U5 snRNAs. In wild type cells, these splicing factors might 'slow down' spliceosome to promote the usage of both the non-canonical and competing 5'ss. These data suggest that different types of alternative splicing might require distinct set of splicing core and regulatory factors.

REFERENCES

1. Will, C. L. & Lührmann, R. Spliceosome structure and function. *Cold Spring Harb. Perspect. Biol.* **3**, a003707 (2011).
2. Stevens, S. W. *et al.* Biochemical and genetic analyses of the U5, U6, and U4/U6 x U5 small nuclear ribonucleoproteins from *Saccharomyces cerevisiae*. *RNA* **7**, 1543–1553 (2001).
3. Gottschalk, A. *et al.* Identification by mass spectrometry and functional analysis of novel proteins of the yeast [U4/U6.U5] tri-snRNP. *EMBO J.* **18**, 4535–4548 (1999).
4. Zhan, X., Yan, C., Zhang, X., Lei, J. & Shi, Y. Structures of the human pre-catalytic spliceosome and its precursor spliceosome. *Cell Res.* **28**, 1129–1140 (2018).
5. Nguyen, T. H. D. *et al.* CryoEM structure of the yeast U4/U6.U5 tri-snRNP at 3.7 Å resolution. *Nature* **530**, 298–302 (2016).
6. Mishra, S. K. *et al.* Role of the ubiquitin-like protein Hub1 in splice-site usage and alternative splicing. *Nature* **474**, 173–178 (2011).
7. ESCRT recruitment by the inner nuclear membrane protein Heh1 is regulated by Hub1-mediated alternative splicing. **49**, (2020).

Chapter 1

1. Introduction

1.1 RNA Splicing

Pre-messenger RNA splicing is an essential step in eukaryotic gene expression wherein mRNAs are generated by removing non-coding intron and joining protein-coding exons¹. It takes place in two sequential trans-esterification reactions, which depend on splicing signals in the pre-mRNA molecule like 5' splice site (5'ss), branch point (bp), 3' splice site (3'ss), poly-pyrimidine track, etc. In the first reaction, the branch site nucleophilic adenosine (UACUAAC) attacks the 5' splice site (GUAUGU), yielding a 5' exon and a lariat intermediate. In the second reaction, the 5' exon imposes the next nucleophilic attack on the 3' splice site (UAG), yielding a spliced mRNA and a free lariat^{2,3,4}. These reactions are carried out by the dynamic ribonucleoprotein complex called spliceosome (Figure 1.1). The spliceosome is composed of five small nuclear RNAs (U1, U2, U4, U5, and U6) and associated proteins⁵. Unlike conventional enzyme catalysis, the spliceosome assembles into the active catalytic complex and disassembles during each cycle of splicing. During this process, the spliceosome undergoes multiple rearrangements of the snRNPs to form different intermediate complexes and the active catalytic core.

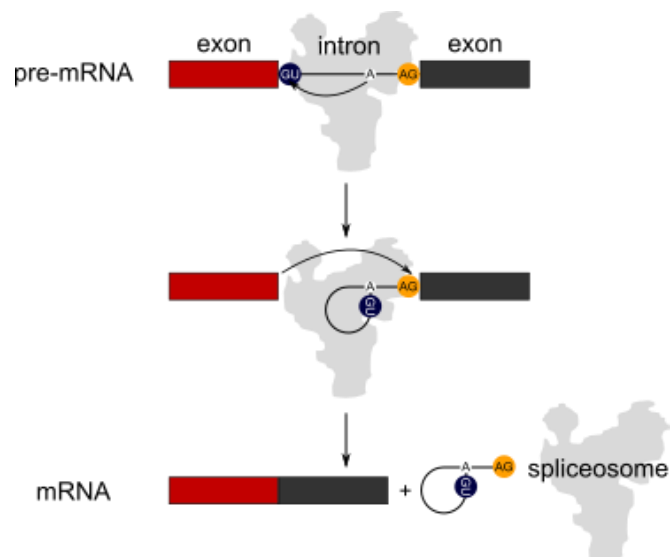


Figure 1.1 Schematic for RNA splicing. The two trans-esterification reactions required for removal of the intron from pre-mRNA and ligation of the exons in a spliced mRNA molecule carried out via the spliceosome. Splice sites are shown as small circles with different colours on the intron.

2

1.2 The Spliceosome

Assembly: The recruitment of the spliceosome on a pre-mRNA takes place in a stepwise manner (Figure 1.2). Firstly, the U1 snRNA recognises the 5' ss forming an early complex E, followed by recognition of the bp sequence by U2 snRNA, converting to complex A. Next, the U4/U6-U5 tri-snRNP gets recruited and forms the complex B, which is still catalytically inactive⁶⁻⁸. The 5' ss-U1 snRNA interaction is broken, and U1 is replaced by U6 snRNA. Subsequently, U4 gets disassembled from the complex B, transforming it to catalytically activated complex B^{act}⁹. In complex B^{act} the U2 and U6 snRNA base-pair, forming U2/U6 helix I, the catalytic RNA core. It also marks the incorporation of the NineTeen complex (NTC) and REtention and Splicing (RES) complex proteins. The B* complex is formed by bringing the 5' ss and bp adenosine nearby for the 1st reaction. Following the first trans-esterification reaction, the spliceosome converts to complex C. The 5' and 3' exons are brought in proximity, forming complex C* where the 2nd trans-esterification reaction takes place. The mRNA is released from the P complex. Finally, the intro-lariat spliceosome (ILS) is disassembled for the next round of splicing reaction^{10-12 13}.

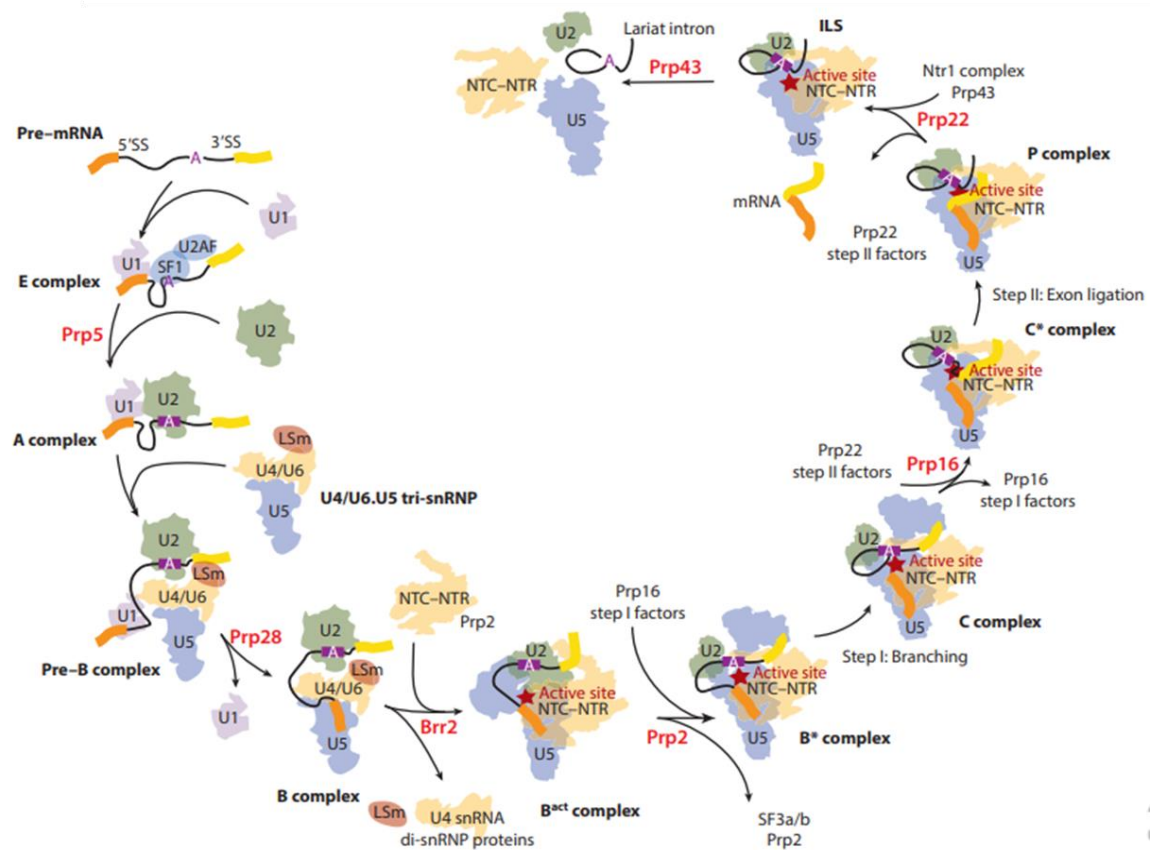


Figure 1.2 Spliceosome assembly and transition. The schematic depicts how the spliceosome assembles on the pre-mRNA molecule, the different transition states (complex E-complex P and ILS), and *trans*-acting factors regulating these transitions (helicases Prp5-Prp43, shown in red). (Image directly adapted from Zhan et al. 2018)

Transition: Several helicases are involved in the smooth functioning of the spliceosome. They are the key players in spliceosomal transitions and are also called the DExD/H-ATPases (e.g., Prp5, Prp16, Prp43, etc.) (Figure 1.2)^{10,14}. Prp5 is needed for the formation of the pre-spliceosome by bridging U1 and U2 snRNA. It carries out the transition from E complex to A complex¹⁵. Next, helicase is Prp28, which facilitates the exchange of 5'ss-U1 snRNA to 5'ss-U6 snRNA interaction^{16,17}. This marks the entry to the tri-snRNP complex-forming pre-catalytic complex B. Here, Brr2 unwinds and releases U4 snRNPs^{18,19}. Prp2 comes in next and changes the B^{act} complex to catalytically active complex B*. It unwinds and removes the SF3 proteins, and exposes the bp and 5'ss to each other for the first trans-esterification (branching)²⁰⁻²². After the first step, Prp16 brings the 5'exon and 3'ss in proximity for the second reaction in C* complex. Prp16 removes proteins such as Yju2 and Cwc25, in an ATP-dependent manner, which is required for the first step. This also results in the binding of the

next helicase Prp22^{23,24}. After the second reaction, Prp22 unwinds the U5 snRNA and ligated exon, releasing the mRNA and the intron-lariat spliceosome from the post catalytic P complex^{25,26}. Finally, the ILS is disassembled by helicase Prp43, a member of NTC, and the lariat and spliceosomal components are released²⁷⁻²⁹.

Structure: Recently, interesting cryo-EM structural studies of the spliceosome in different organisms (*Saccharomyces cerevisiae*, *Schizosaccharomyces pombe*, and human) have confirmed many snRNP interactions. Though the basic backbone stays similar, there are certain differences in how spliceosome behaves in these organisms. The *S. cerevisiae* U4.U6/U5 tri-snRNP structure is highly comparable to the *S. pombe* ILS cryo-EM structure and shows various conserved interaction patterns such as Snu114 and N-terminal domain of Prp8. In *S. cerevisiae*, the structure of the tri-snRNP has been well studied. It has a head, body, and foot region, majorly comprising of Prp8, Brr2, and Snu114. Brr2 interacts with Prp8 and translocates along U4 snRNA. It unwinds U4/U6 duplex and detaches itself and U4 snRNA from the main body of Prp8. The presence of other splicing factors likes Snu66, Prp3, Prp31, and Prp4, has also been shown through electron density mapping^{30,31}.

4

Although the tri-snRNP components are present in an activated spliceosome (B^{act}), they show marked differences in conformation. For example, the core protein Prp8 exists in a closed conformation in the activated complex rather than an open conformation. The β -hairpin switch loop gets rearranged and comes closer to the exons. The position of Brr2 is rotated by 45° in B^{act} compared to the tri-snRNP structure. The U4 snRNA is removed, and U2/U6 snRNAs are rearranged in the B^{act} complex. The *S. cerevisiae* activated complex has 38 proteins, 10 from U5 snRNP, 7 from U2 snRNP, 6 from NTC, 6 from NTR, 3 from the RES complex (Pml1, Bud13, and Snu17); four known splicing factors (Cwc21, Cwc22, Cwc24, and Cwc27); the adenosine triphosphatase (ATPase)/helicase Prp2; and the step 2 factor Prp17. These arrangements are very similar in *S. cerevisiae* and human activated spliceosome except for some minor differences^{32,33}.

The human activated spliceosome (hB^{act}) has 52 proteins, 11 from U5 snRNP, 19 from U2 snRNP, five from the NTC, seven from the NTR, three from the retention and splicing (RES) complex (SNIP1, Bud13, and RBMX2), three splicing factors (SRm300, Cwc22, and

RNF113A), two peptidyl-prolyl isomerases (PPIs, NY-CO-10, and CypE), the ATPase/helicase Prp2, and the step II factor Prp17. The U2/U6 helix II is bent by about 40° in hB^{act}, Brr2 positioning changes drastically from early to late hB^{act} spliceosome, and also an extra turn of the U6/intron duplex²² (Figure 1.3).

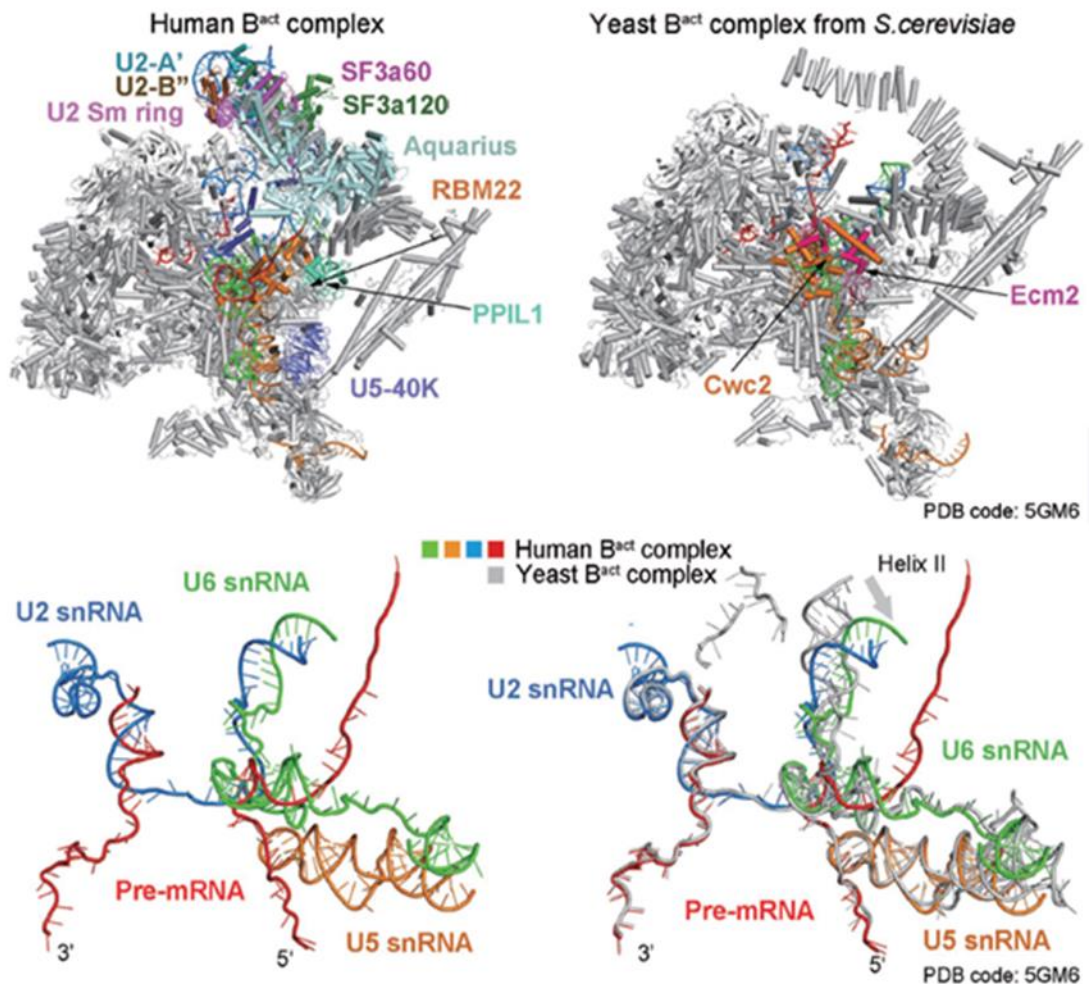
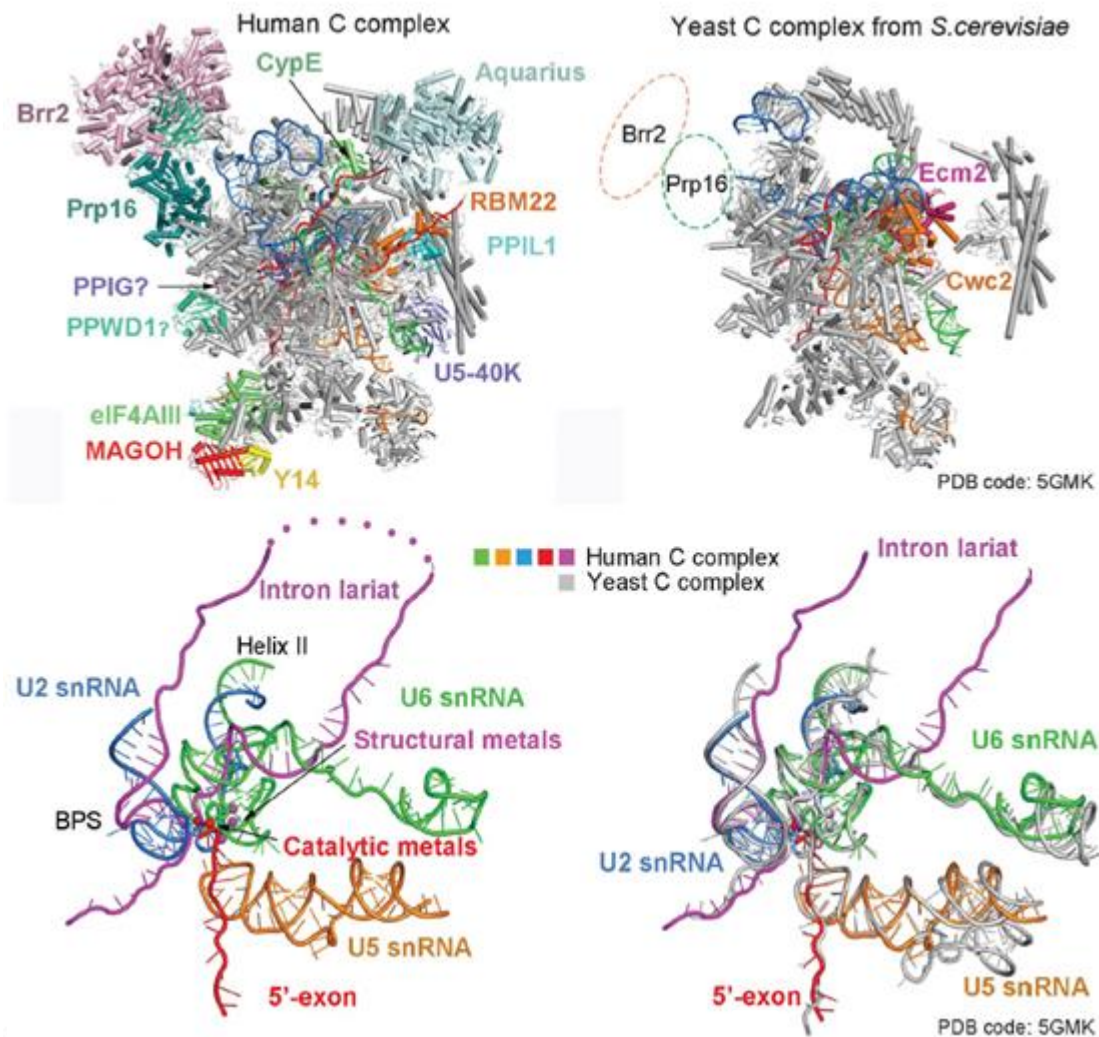


Figure 1.3 Structural comparisons between the human and yeast B^{act} complexes. While most of the basic backbone stays similar, the spliceosome varies in specific components among the two organisms. The upper panel shows the unique component of each spliceosome in a different colour, whereas the common components are in grey. The lower panels represent the RNA components in the two spliceosomes. The left lower panel shows the human spliceosome, and the right panel is an overlay of human and yeast B^{act} spliceosome. (Image directly adapted from Zhang et al. 2018).

After the incorporation of the tri-snRNP spliceosome obtains a conformation for the first reaction named complex B*, which sees the incorporation of NTC (Cef1, Isy1, and Syf2), NTR (Cwc2, Ecm2, and Bud31) proteins, and step 1 factors (Cwc21, Cwc22, Cwc25, and Yju2) to their positions in both yeast and humans. The SF3a and SF3b proteins, which shield 5'ss and bp are removed such that the spliceosome is activated for 1st trans-esterification to occur^{34,35} (Figure 1.4).



6

Figure 1.4 Structural comparisons between the human and yeast C complexes. The upper panel shows the unique component of each spliceosome in a different colour, whereas the common components are in grey. There are few more proteins in the human C complex (upper left panel). The density map for Brr2 and Prp16 is better resolved in the human complex compared to its yeast counterpart (upper right panel). The lower panels represent the RNA components in the human and yeast spliceosome. The left lower panel shows the human spliceosome, and the right panel is an overlay of human and yeast C complex. (Image directly adapted from Zhan et al. 2018)

Following the 1st step, the major change from B* to C* via C complex is the displacement of the intron bp/U2 duplex by 90° and translocation of the lariat junction by about 20°. The first step splicing factors Cwc25, Yju2, NTC component IsyI are dissociated. The second step splicing factors Prp17, Prp18, and Prp8 (RNase H like domain) align to their new position. Similar rearrangements also occur in human C* complex varying mostly in the degree of rotations compared to yeast C*^{36,37} (Figure 1.5).

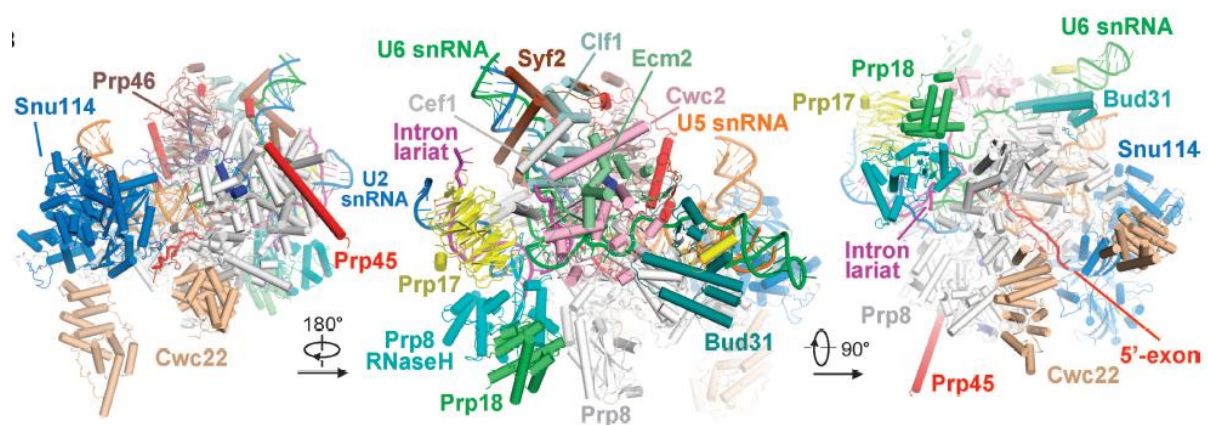


Figure 1.5 Structure of the *S. cerevisiae* spliceosomal C* complex. Proteins and RNA components of yeast C* complex ready for exon ligation reaction, surrounding the active catalytic site. (Image directly adapted from Yan et al. 2017)

These cryo-EM structures of the different stages of the spliceosomal complex have validated the mechanism of the two reactions during splicing and their regulation by the various spliceosomal RNA and protein molecules. Following this, the ILS is formed, and finally, the spliceosome is completely dissociated for another round of splicing.

1.3 Intron and Exon definition

Due to the degeneracy of the 5' and 3' splice site consensus sequences, the identification of *bona fide* vs. pseudo splice sites becomes a critical function for the spliceosome. For the spliceosome to differentiate the two splice sites, it is essential to define the region as introns and exons in the pre-mRNA. While lower eukaryotes mostly have long exons interspersed with small introns, higher eukaryotes have small exons separated by long introns. Due to this variation in the size of exons and introns, intron definition is more common in the lower eukaryotes, including yeasts. In the intron definition pathway (Figure 1.6A), the spliceosome assembles on the small intron by recognising the 5' splice site via U1 and branch point via U2. They can also interact with 3' splice sites recognising auxiliary factors, etc.^{7,38}. On the other hand, in higher eukaryotes, since the exons are smaller, the splicing machinery assembles on the exon first rather than on long introns. This is termed as exon definition (Figure 1.6B). In this mechanism, the U1 bound to 5' splice site of an intron interacts with downstream U2/U2 auxiliary factors (U2AF), and the U2AF bound to the 3' splice site of the intron interacts to an upstream U1 bound to the 5' splice site of the next intron. The exon defined pre-mRNA with snRNPs form exon defined A complex (EDA), which changes conformation and finally converts to an intron defined structure and forms the spliceosomal A complex³⁹⁻⁴¹.

8

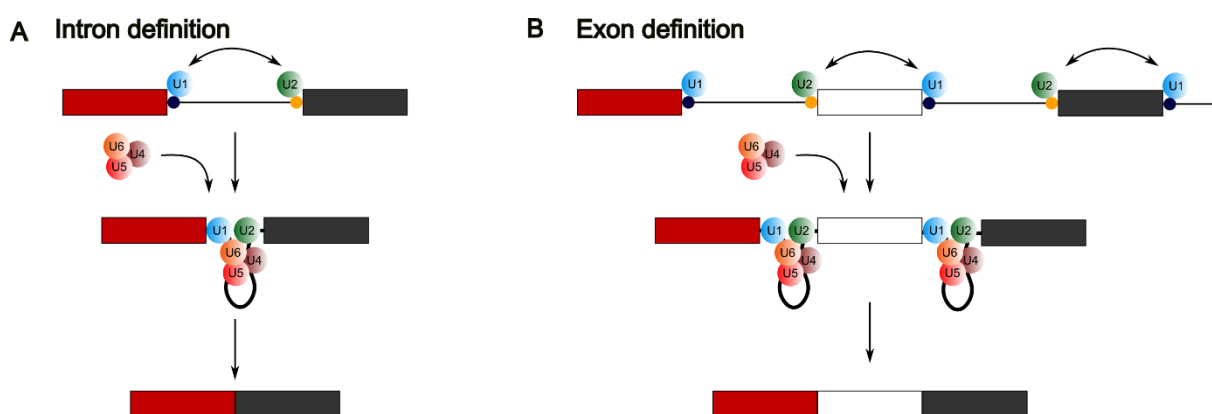


Figure 1.6 Mechanism of intron and exon definition. (A) Intron definition model where splice sites pairing happens across an intron. It happens when long exons are separated by short introns. (B) Exon definition model where splice sites pairing happens across the short exons. It happens when shorter exons are separated by long introns.

1.4 Splicing Fidelity

Splicing fidelity refers to the selection of an optimal splice site over a suboptimal one. As evident from the above discussion, splicing is a highly regulated and complex process. Despite such complexity, splicing is a high fidelity process. Similar to replication and transcription, proofreading is indispensable in the removal of introns during pre-mRNA splicing but is reversible. Splicing fidelity is improved by the DExD/H-ATPases, in addition to their remodeling activity. Out of the eight helicases involved in splicing, five (Prp5, Prp28, Prp16, Prp22, and Prp43) have been shown to regulate splicing fidelity^{24,42–45} (Figure 1.7).

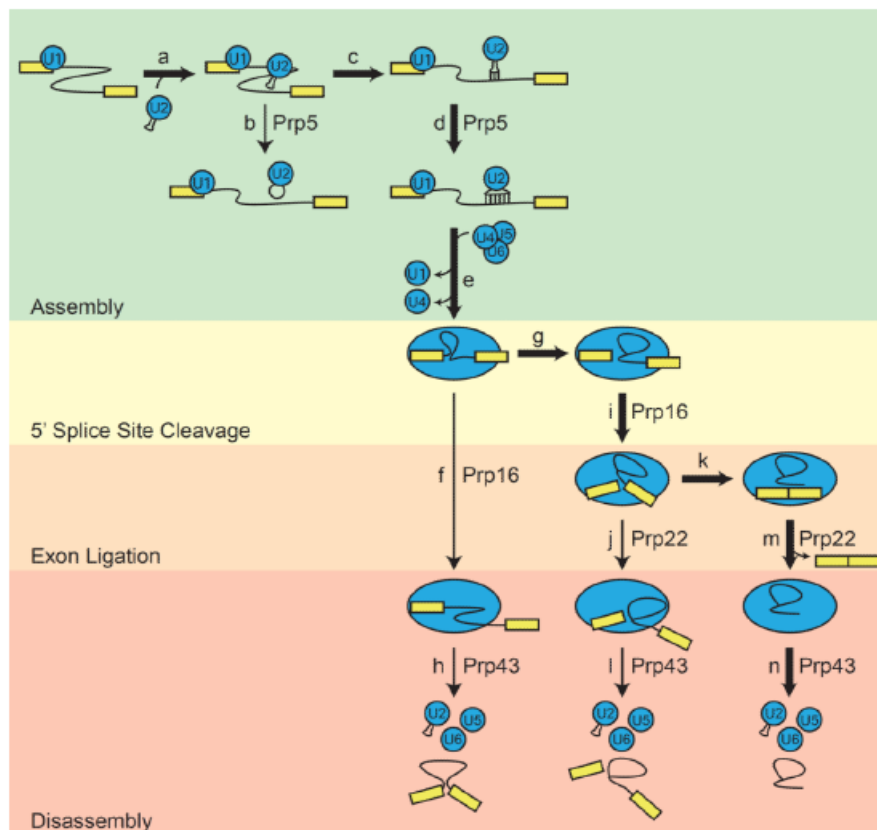


Figure 1.7 Mechanism of proofreading via DEAD/H-box ATPases in the splicing pathway. (A) Shows improper binding of U2 snRNP. (B) Prp5-dependent rejection if it is suboptimal branch site. (C) Proper binding of U2 to optimal branch point. (D) Prp5 stabilises U2 association with the optimal substrate. (E) Incorporation of the U4/U6•U5 tri-snRNP, (F) Prp16-dependent rejection of suboptimal 5' ss- branch site interaction. (G) Optimal 5' ss- bp interaction leads to branching reaction. (H) If rejected by Prp16, the complex enters Prp43-mediated discard pathway. (I) In optimal 5' ss-bp interaction, Prp16 promotes transition to the exon ligation conformation. (J) Prp22-

dependent rejection of sub-optimal 5' splice site - 3' splice site interaction. **(K)** Optimal 5' splice site - 3' splice site interaction leads to exon ligation, **(L)** if rejected by Prp22 5' exon and lariat intermediate enters Prp43-mediated discard pathway. **(M)** In optimal exon ligation, Prp22 promotes release of the newly synthesised mRNA. **(N)** And finally, Prp43 promotes the release of the lariat intron and dissociation of the spliceosome into its component. Heavy arrows indicate the canonical splicing pathway on optimal splice signals via the helicases. (Image adapted from Semlow and Staley 2012)

These helicases antagonise the use of suboptimal splice sites and promote optimal splice site usage. Though the molecular mechanism of their function is not very well understood, it is reported that the helicases usually work either by a thermodynamic and/or a kinetic pathway. The thermodynamic mechanism argues that the spliceosome binds the suboptimal splice site and forms a non-productive stable conformation that inhibits the occurrence of the reaction/rearrangement. The helicases then unwind this conformation and push the pre-mRNA towards the discard pathway. Whereas the kinetic proofreading mechanism states that, spliceosome with the help of the helicases, rejects the suboptimal introns. The DEAD/H-box ATPase promotes the usage of optimal splice sites by acting after the productive reaction/recognition step and antagonises suboptimal splice sites by acting before the reaction/recognition step. This means that in the case of suboptimal splice sites, which forms a less stable spliceosome structure, the helicases work faster, whereas in the case of optimal splice sites, which forms stable spliceosome conformation delays the action of the helicases^{13,46,47}. These proofreading mechanisms have been well explained in for Prp5, Prp16, and Prp22, although they work at different stages of the splicing pathway but via a similar mechanism (Figure 1.7).

10

Apart from the DEAD/H-box ATPases, there are other proteins that have been shown to play an important role in splicing fidelity. One such protein is Hub1 (Homologous to Ubiquitin-1). It is non-essential for growth and viability in *S. cerevisiae* but in higher eukaryotes such as *S. pombe*, it becomes indispensable. Hub1 has been shown to bind the tri-snRNP protein Snu66 at a conserved region called HIND. Mishra et al (2011) also demonstrated that Hub1 is required for alternate splicing in *S. cerevisiae*.

Box 1: Ubiquitination (conjugation of Ubiquitin) is a well-established post-translational modification carried out by enzymatic cascades in stepwise reactions. Ubiquitination consists of three main steps namely activation, conjugation and ligation brought about by enzymes E1, E2 and E3 respectively.

Later, Karaduman et al (2017) showed that Hub1, through a second surface, binds to Prp5 and reduces splicing fidelity in yeast. It helps in the assembly of a pre-spliceosome on suboptimal ss by activating Prp5. Overexpression of Hub1 leads to error-prone splicing of suboptimal and cryptic ss causing inhibition of cell growth^{48,49}. An important outcome of reduced splicing fidelity is the occurrence of alternate splicing.

1.5 Alternate Splicing

Alternative splicing is a process of generating variably spliced mRNAs from a parent pre-mRNA. This helps in increasing the complexity of gene expression and cell proteome. Alternate splicing becomes critical in processes like cell differentiation, organism development, and evolution. Alternative splicing frequency is lesser in lower eukaryotes but increases significantly as we move up the ladder to higher and complex eukaryotes. Alternate splicing can happen through different modes. They are majorly classified into five modes:

- i. Exon skipping: where an exon is spliced out of the mRNA (Figure 1.8A).
- ii. Alternate 5'ss: where different 5'ss can be recognised, resulting in subtle changes in the product (Figure 1.8B).
- iii. Alternate 3'ss: different 3'ss can be recognised, resulting in variation in the downstream exon (figure 1.8C)
- iv. Intron retention: where an intron or a part of an intron is retained in the mature RNA molecule such that it comes in frame with the exon and codes a functional protein (Figure 1.8D).
- v. Mutually exclusive exons: where only one of two exons can be retained in the mRNA, not both (Figure 1.8E).

While exon skipping is largely observed in mammals, intron retention is more common in metazoans. Apart from these above-mentioned modes, alternate mRNAs can be generated using alternative polyadenylation site (changes the 3' end of the protein) and alternative promoters (more of transcription-based variation)^{50,51} (Figure 1.8F, G).

These mechanisms of alternative splicing are regulated via *cis*-acting elements or *trans*-acting factors. The *cis*-acting elements are present in the intron itself or neighboring exons. These can be splicing enhancers or silencers. If present on exon, they are called exonic splicing enhancers (ESE) signals or exonic splicing silencers (ESS) signals, and if present on introns, they are called intronic splicing enhancers (ISE) signals or intronic splicing silencer (ISS) signals. The *trans*-acting factors bind the enhancer (SR proteins) or silencer (hnRNPs) signals and regulate the assembly of spliceosome and recognition of splice site^{52,53}.

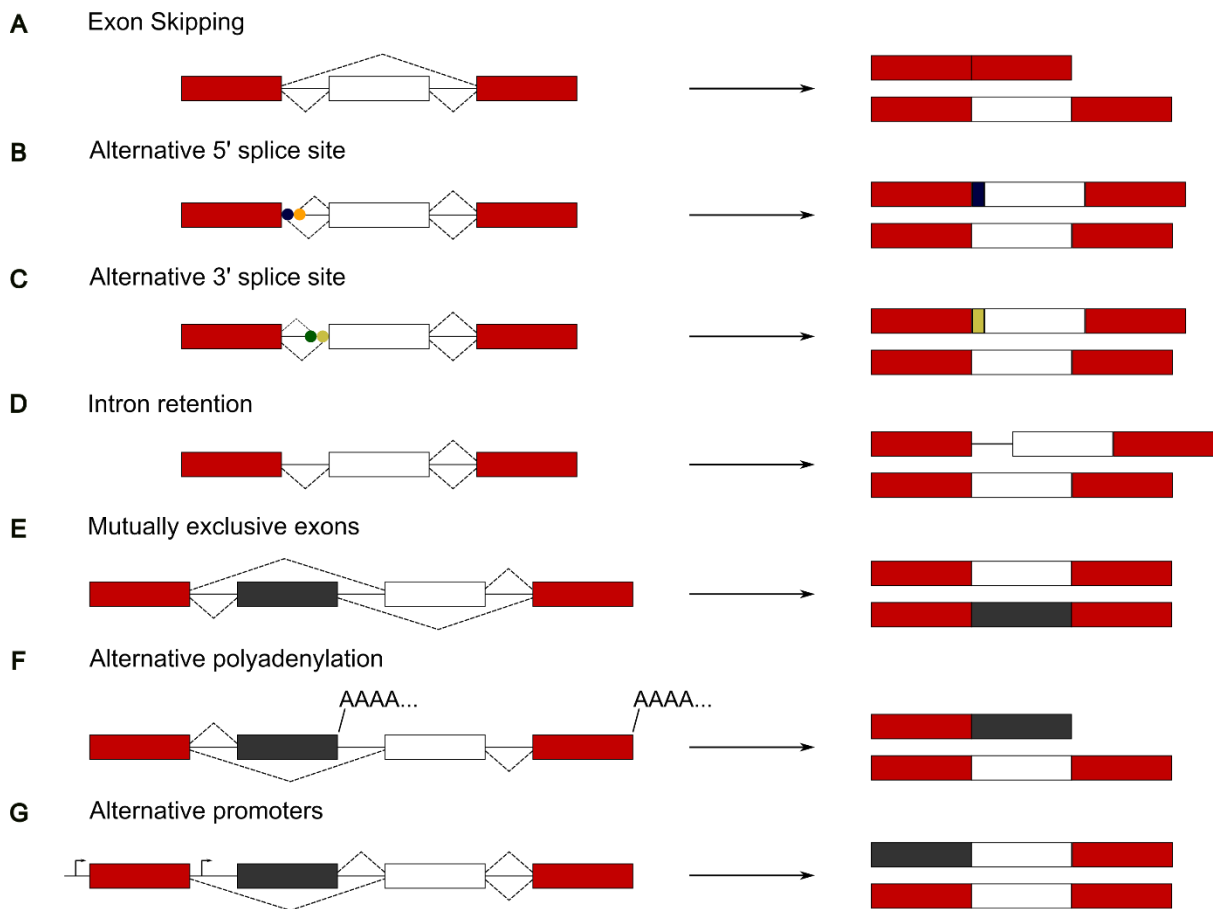


Figure 1.8 Mechanism of Alternative splicing. Alternative splicing where one pre-mRNA give rise to more than one mRNAs is mediated by multiple ways like (A) skipping of exons, (B), (C) using alternative 5' and 3' splice sites, (D) intron-retention, (E) inclusion of mutually exclusive exons, (F, G) alternative polyadenylations at different sites and alternative promoters.

Factors such as Hub1 help in recognition of the alternate 5'ss of *SRC1* and other weak splice sites in *S. cerevisiae*. It regulates alternate splicing while working along Snu66, Prp5, and Prp38 *trans*-acting factors. It does so by reducing the splicing fidelity in the cells, thus recognising weak ss. Similarly, various proteins work by different mechanisms and at different stages of splicing to regulate constitutive and alternate splicing^{48,49,54}.

PART II

1.6 AAA-ATPase

ATPase Associated with diverse cellular Activities (AAA-ATPase) is a family of proteins that shares a conserved domain of 230 amino acids forming a hexameric ring structure^{55,56}. A large number of member proteins of the family from different organisms (prokaryotes, lower and higher eukaryotes) have been identified. They have an $\alpha\beta\alpha$ core domain, which includes the walker A and walker B motifs⁵⁷⁻⁵⁹. AAA-ATPases are involved in DNA recombination, replication, and repair, protein degradation, membrane fusion, microtubule motor, signal transduction, etc. A few examples of such ATPases are as follows: (i) Pch2 which plays a role in Mec1-dependent phosphorylation of Hop1 (a meiotic checkpoint protein) in response to synaptonemal complex defects⁶⁰; (ii) Vps4 ATPase regulates membrane trafficking by catalysing the release of class E endosomal membrane-associated proteins (Vsp24 and Vsp32)⁶¹; (iii) Dynein with its six tandemly repeated AAA domains is required for minus-end-directed microtubular trafficking by use of ATPase activity for mechano-motor force generation⁶². (iv) A very well-studied member of the family is Cdc48/p97/VCP, which functions as a segregase of ubiquitin conjugates for their degradation by ubiquitin-proteasome system⁶³. In *S. cerevisiae*, Cdc48 works along with its cofactors Ufd1/Npl4 to remove the polyubiquitinated proteins from membranes and other complexes⁶⁴. It is involved in the apoptosis of cells from yeast to human and is an integral part of the ERAD pathway^{65,66}. Based on the crystal and cryo-EM structure (Figure 1.9) it has been confirmed that Cdc48 has an N-terminal (N) domain and two ATPase (D1 and D2) domains, which form stacked hexameric rings^{67,68}. Cdc48/p97 is also associated with inclusion body myopathy and Paget disease of bone and frontotemporal dementia⁶⁹. (v) Msg1 is another important member of the AAA-ATPase family in yeast. It is conserved in prokaryotes and eukaryotes. It is important for maintaining genome stability. It is a DNA dependent AAA-ATPase involved in regulating homologous recombination. It is recruited to sites of replication stress via ubiquitylated PCNA. It can process single-strand DNA annealing and regulate mitotic homologous recombination^{70,71}.

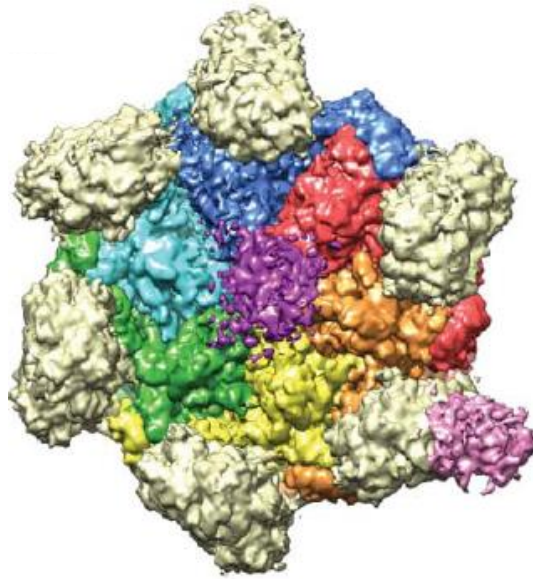


Figure 1.9 Cryo EM-structure of Cdc48. Low threshold density segmented view of the hexameric Cdc48 subunit ATPase cassette. (Image adapted from Cooney et al. 2019)

1.7 Homologous Recombination

Homologous recombination (HR) is a cellular process in which similar sequences between double or single-stranded nucleic acid molecules are exchanged. The cell uses HR for creating genetic diversity, maintaining proper segregation of chromosomes during meiosis, telomere maintenance, and repairing certain DNA damages. HR has been mostly studied in bacteria *E. coli*. But it plays an essential role in eukaryotes, which is abundant and highly studied in yeast *Saccharomyces cerevisiae*. HR forms the basis of natural selection as it provides a platform for shuffling and selecting favourable and unfavourable mutations that occur in cells during meiosis. The importance of mitotic HR becomes clear by the occurrence of cancer that results from defective in DNA damage repair by HR protein. Mitotic HR is also important for a process called antigen switching in immune cells. Several genetic diseases and cancers are related to defects in HR or DNA repair in cells^{72,73}.

A double-stranded break (DSB) in DNA is crucial for the initiation of HR. While programmed double-stranded breaks occur during meiosis, spontaneous breaks during replication or due to ionising radiation leads to mitotic HR. Meiotic and mitotic HR differ in the events related to crossover formation, which are controlled via HR regulatory factors.

According to the DSB model (Figure 1.10 lower left), the ends of the broken DNA strand are first processed by an exonuclease, which generates a 3' single-stranded DNA tail. This single-stranded DNA invades a homologous DNA molecule, called the donor duplex, and displaces its counter from the donor duplex forming a D-loop. Strand exchange during the generation of degraded DNA regions leads to the formation of a DNA heteroduplex. If such a similar exchange happens for the 2nd double-stranded break end, the DNA heteroduplex becomes connected by forming two-holiday junctions. This phenomenon results in crossover or exchange of the DNA regions from donor duplex to recipient duplex and is called double-stranded break repair (DSBR)^{73,74}.

While the above-described pathway is common in meiosis, in the case of mitosis, it follows the synthesis-dependent strand annealing (SDSA) model (Figure 1.10 lower right). In this case, the 2nd DSB end is not captured in the recombination duplex; rather, the invading strand after synthesis is displaced and reanneals to the broken end. This strand then acts as the template for repairing the 2nd broken strand of the DNA double strand^{75,76}.

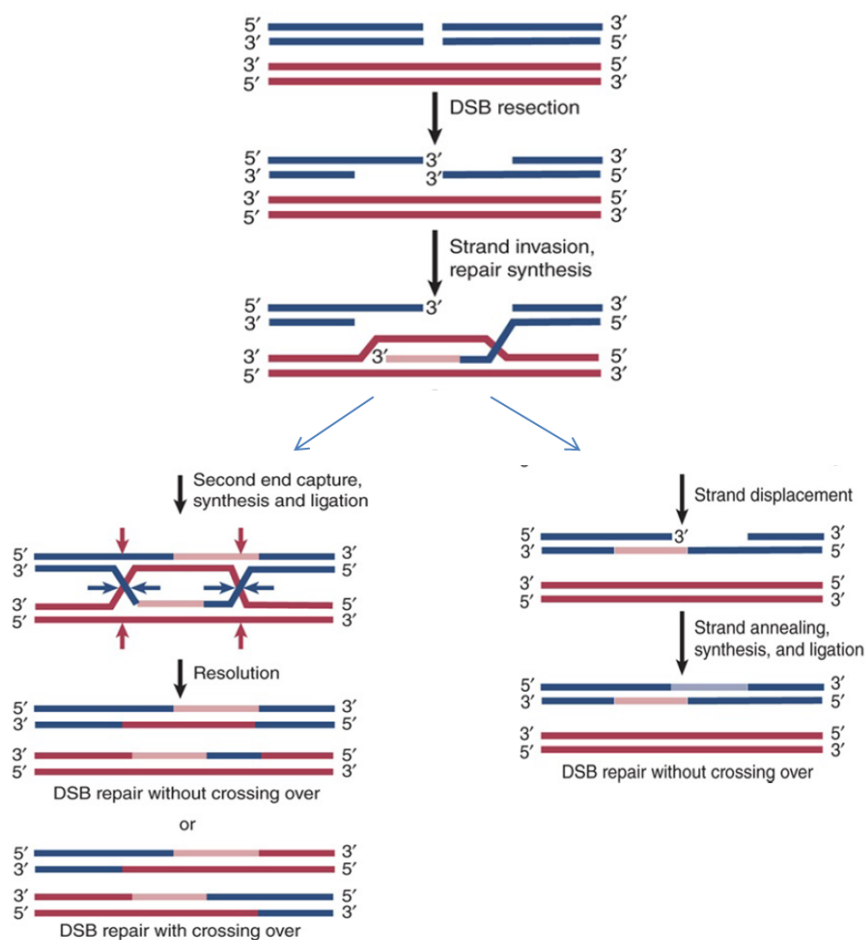


Figure 1.10 Repair of DNA double-strand breaks by DSBR and SDSA. (Top panel) the initiation of the repair pathway on the introduction of a break via ssDNA tail formation and invasion of the homologous DNA strand. This is common for DSBR and SDSA pathways. (Lower left panel) the DSBR pathway, which involves double holiday junction (HJ) formation and crossover. (Lower right panel) SDSA pathway uses the 1st repaired strand as a template for 2nd end repair and does not for crossover. (Image adapted from Lewin's Gene X)

Another mechanism for DSB processing is the single-strand annealing (SSA) pathway (Figure 1.11 left), where the ends forming ssDNA tails ligate to each other. This pathway is mainly observed in the case of closely repeated sequences and needs a subset of the HR proteins, not the complete cascade of regulators^{77,78}.

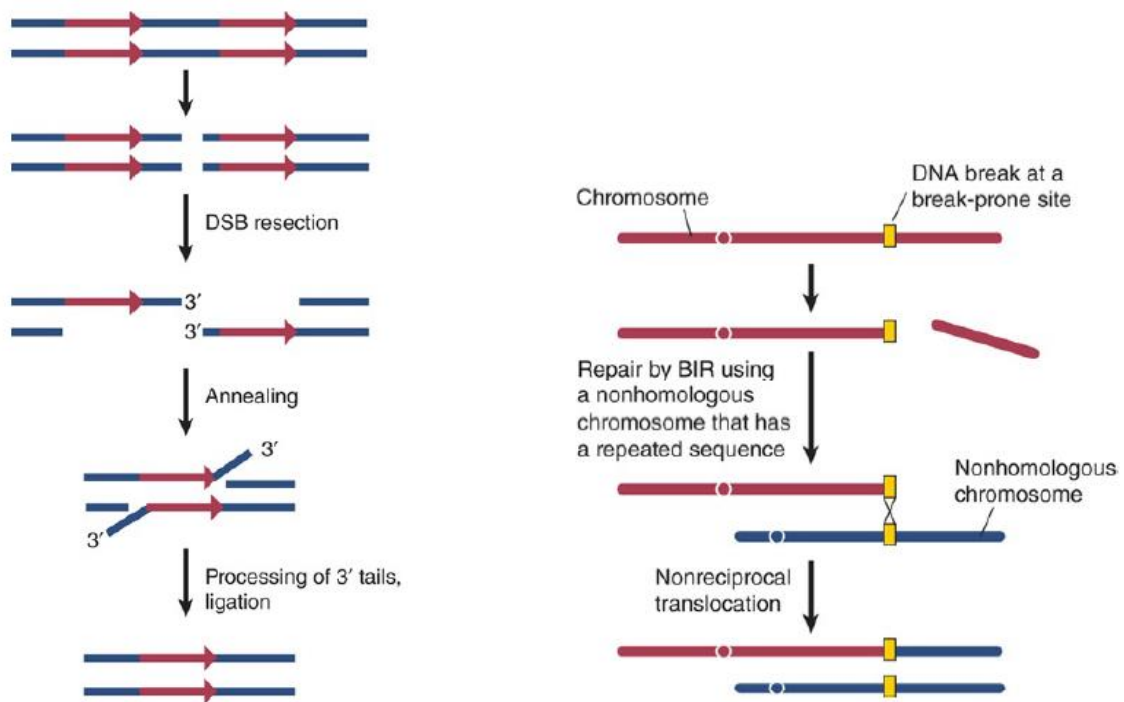


Figure 1.11 Repair of DNA double-strand breaks by SSA and BIR. (Left panel) shows the SSA pathway, which takes place in case of repeats where the broken ends ligate to each other, and the ssDNA is chopped off by endonucleases. (Right panel) shows the BIR pathway in which the one broken end generated recombines to a homologous/non-homologous DNA. (Image adapted from Lewin's Gene X)

Last but not least is the break-induced replication (BIR) pathway of HR (Figure 1.11 right). This pathway is observed if there is a replication fork collapse resulting in only one end DSB. In this pathway, the ssDNA tail invades a homologous or non-homologous chromosome with a repeated sequence for the DNA synthesis at the broken end. In the case of a non-homologous chromosome acting as the donor strand, it can result in non-reciprocal translocation between the chromosomes^{79,80}.

Chapter 2

Snu66-CM function and mechanism

2.1 Introduction

Snu66 (Small Nuclear ribonucleoprotein associated) is one of the 24 stably associated proteins of the tri-snRNP. It is a 66kDa protein with homologs in *S.pombe* (*snu66*) as well as humans (*SART1*). In *S. cerevisiae*, a null mutant of Snu66 shows cold sensitivity, i.e., although it grows at 30°C (permissible temperature), it becomes inviable at 16°C (restrictive temperature). The cold-sensitivity in Snu66 deletion is attributed to severe splicing defects indicated by the accumulation of U3A and U3B pre-mRNA⁸¹.

Snu66 provides a scaffold for various proteins to interact to form the spliceosome core and regulate different splicing steps⁸². For example, Snu66 binds Hub1 through the conserved arginine residue in the Hub1 Interaction Domain (HIND) and regulates alternate splicing^{48,83}. Cryo-EM studies of the tri-snRNP have also confirmed that the N-terminus of Snu66 has a globular domain that interacts with Prp8 endonuclease-like and Brr2 N-terminal ratchet domains. A long helical region is wedged between Prp8 Jab1/MPN and Brr2 N-terminal HLH domains, and the C-terminus of Snu66 wraps around Brr2 C-terminal cassette^{30,54,84} (Figure 2.1). In the human spliceosome Snu66/SART1 is a B complex specific protein. It acts as a bridge between Prp8 and U4 core domain. The U4 quasi-pseudoknot and core domain interact with the N-terminus helices of Snu66. In an extended conformation Snu66/SART1 also interacts with Prp6. In the B complex, Snu66 appears to stabilise the two catalytic motifs (Switch loop and β -finger) of Prp8 by restricting their movement prior to spliceosome activation. Therefore, Snu66 is important for tri-snRNP assembly and recruitment to spliceosome in *S. cerevisiae* and humans.

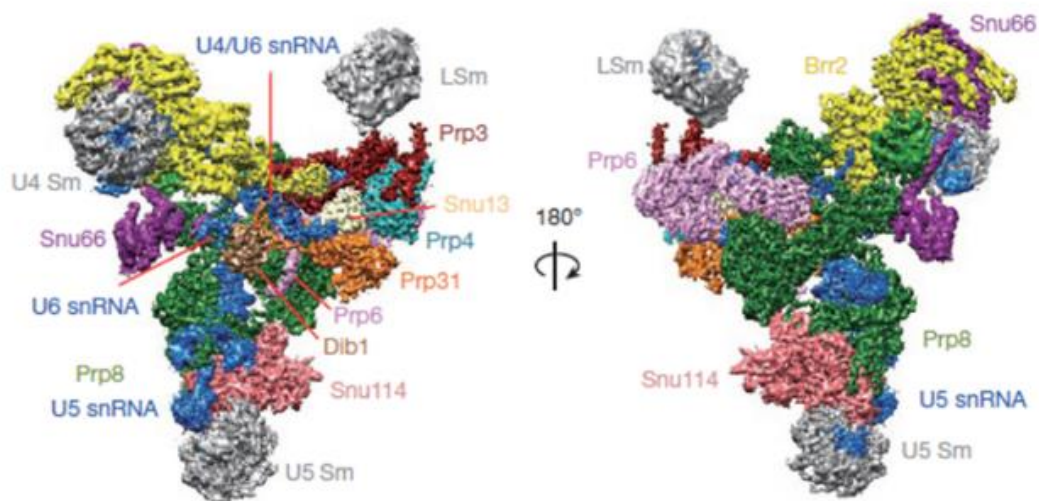


Figure 2.1: Views of an atomic model of the *Saccharomyces cerevisiae* U4/U6.U5 tri-snRNP. It appears like Snu66 is in contact with Prp8, Brr2, U4 Sm proteins, and the snRNAs. (Image adapted from Nguyen et al. 2016)

Human SART1 is expressed in two forms SART1 (800) and SART1 (259). However, most studies are restricted to the shorter form of the protein generated via -1 frameshifting during post-transcriptional regulation. The shorter SART1 (259) is involved in inducing cytotoxic T lymphocytes in cancer cells along with the recruitment of the tri-snRNP to spliceosome^{85,86}, and recent studies have concluded that the full-length SART1 (800) functions as an E3 ubiquitin ligase for HIF1 α in hypoxic condition⁸⁷. Both SART1 protein forms have a critical role in the regulation of cell proliferation. Multiple studies have found a possible role of SART1 in different diseases like cancer, retinitis pigmentosa, atopy, etc⁸⁸⁻⁹⁰.

Snu66/SART1 is essential in higher eukaryotes (starting from *Schizosaccharomyces pombe* to humans), which might be due to the simple reason of higher splicing events and/or parallel functions of Snu66. Like its mammalian homolog, Snu66 is known to function in multiple pathways. Even in yeast; for example, it is important for 5SrRNA biogenesis and processing of other rRNAs⁹¹.

Although Snu66/SART1 has been reported as a general splicing factor and as a part of the tri-snRNP, its precise role in the spliceosome and the function of the C-terminus of Snu66 still remains unclear. In this study, we try to understand the function of the C-terminus motif of Snu66, and explore, analyse, and compare the importance of this motif using various biochemical and genetics approaches

2.1 Objective

Function and mechanism of Snu66 in pre-mRNA splicing: I researched to understand the importance of the general splicing factor Snu66 with a focus on the C-terminus of the protein. This part of the study was performed both in the budding yeast *S. cerevisiae* and the intron-rich fission yeast *S. pombe*.

2.2 Results

2.2.1 An essential conserved motif of Snu66

Snu66 and its homologs are known in different organisms, but the similarity in their sequence is limited. Mishra et al. (2011) found that HIND (Hub1 Interaction Domain) is a conserved motif at the N-terminus of Snu66 across species. To find more such conserved regions of Snu66, we aligned Snu66 sequences of *S. cerevisiae*, *S. pombe*, and humans and visualised using jalview software (Figure 2.2). In the image, we can see that there are several scattered regions that are conserved among the homologs. Some of the regions at the N-terminus have been validated by Zhang et al. (2018) to interact with other core spliceosomal proteins (labelled in the figure); the C-terminus of Snu66 remains unexplored.

To understand the Snu66 splicing function better, we wanted to complement the cold-sensitive phenotype of $\Delta snu66$ by transforming cells with different truncated versions of the protein. We cloned different truncations of Snu66 (black boxes mark truncated regions) and performed complementation assays by spotting the different transformants on media plates and incubating them at different temperatures.

A

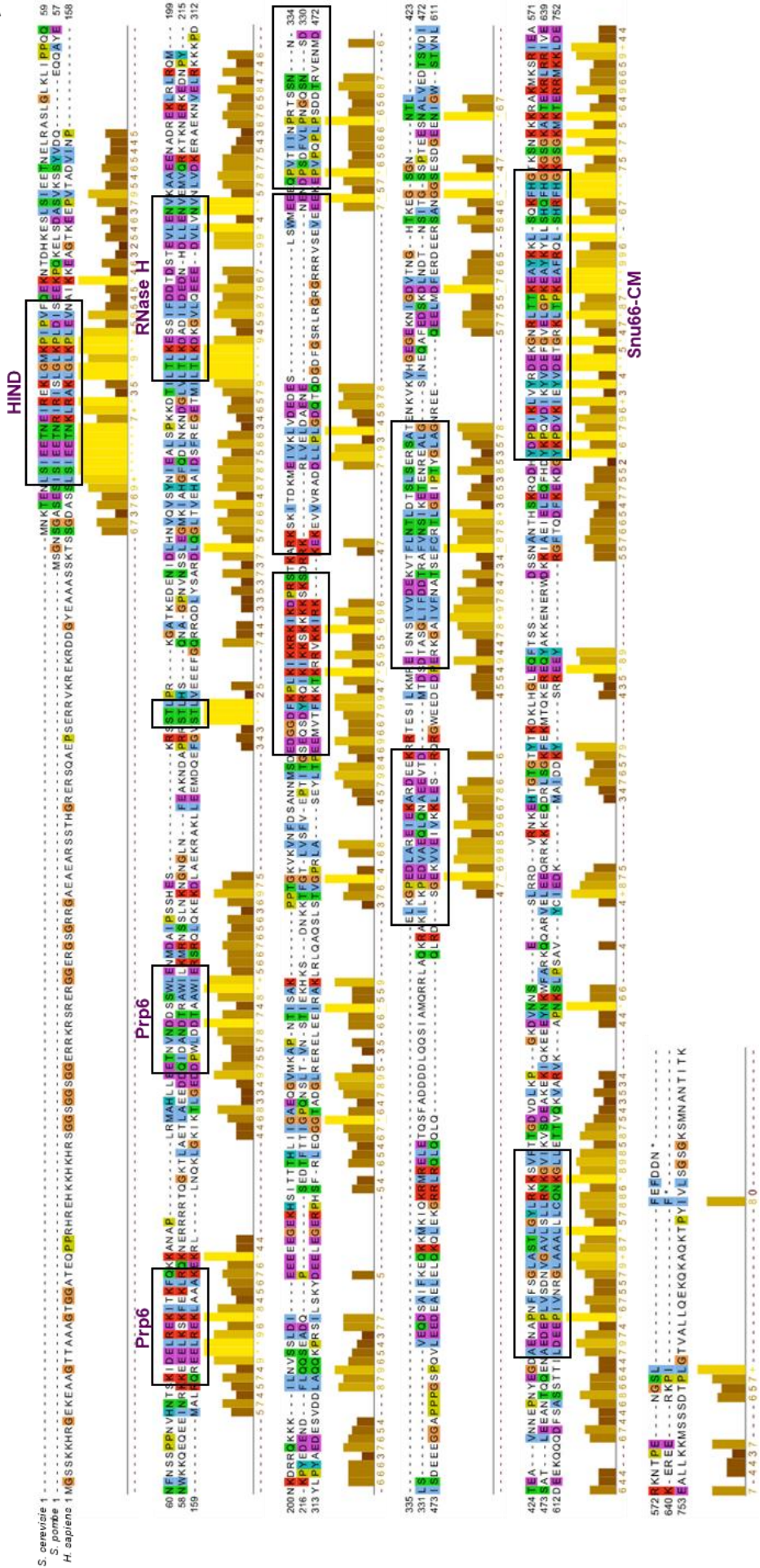


Figure 2.2: Conserved domains of Snu66/SART1. (A) The alignment of *S. cerevisiae* (Snu66), *S. pombe* (Snu66), and *H. sapiens* (SART1) shows the multiple scattered regions of homology among the proteins. Some of these conserved regions (marked in black boxes) interact with other splicing factors like Hub1, Prp6, RNase H domain of Prp8 that have been labeled in the image. Black rectangles also represent different truncations of Snu66 used for the experiment.

Interestingly, we observed that all the truncations complemented the phenotype, except for the fragment 531 to 554. The absence of this fragment showed a partial cold-sensitive phenotype (Figure 2.3A). We did a thorough analysis of the Snu66 C-terminus region from homologs in various eukaryotic organisms (mentioned in the figure) and found that the region appeared highly conserved throughout the spectra of organisms. So, we termed the region Snu66 Conserved and Essential C-terminus Motif (abbreviated as Snu66-CM) (Figure 2.3B).

Following that, we mutated each of the conserved residues of the Snu66-CM region and found that, except for the complete deletion of the region, none of the point mutants showed cold sensitivity. We also used a HIND mutant, *R9A*, and *R20A* (*RRAA*), defective in Hub1 binding for a better comparison of the two conserved domains (Figure 2.3D). These results showed that the C-terminus region is crucial for the *S. cerevisiae* survival at lower temperatures and might play a role in the splicing function of Snu66. Although point mutants grew normally, the region as a whole is critical at lower temperature, unlike any of the other conserved regions. Since this experiment was done in a plasmid-based background and might have different levels of expression, we wanted to validate our results using a chromosomal strain. We made chromosomal strains of a few of these mutants like *RRAA*, *D533A*, *K546A*, and Δ *Snu66-CM* and performed similar complementation assays. Our results were consistent, with only the deletion of the motif showing partial cold sensitivity phenotype (Figure 2.3D).

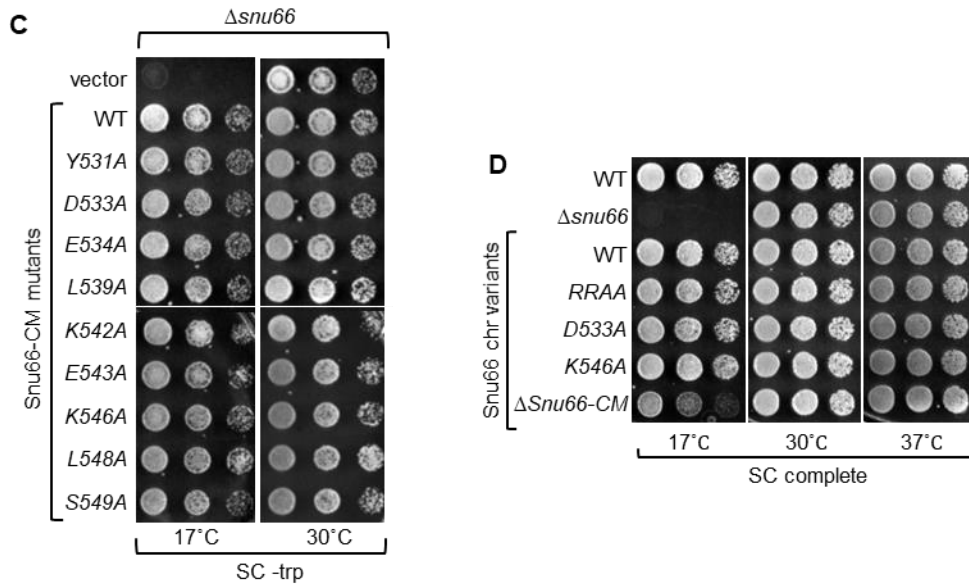


Figure 2.3: Identification of a conserved C-terminal domain of Snu66 essential for cell survival. (C) The point mutants of the highly conserved residues of the C-terminal region Snu66-CM do not show cold sensitivity. They all complement the effect of the null mutant. (D) In the chromosomal variants, too, only the complete deletion of Snu66-CM shows the phenotype, the point mutants of the domain (*D533A* and *K546A*) do not show cold or temperature sensitivity when grown at 17, 30, and 37°C.

2.2.2 Genetic interactors of Snu66-CM

Since we found a crucial motif of Snu66, we wanted to verify some of the genetic interactions of Snu66 with respect to this essential motif. It has been previously reported that Snu66 genetically interacts with the core splicing factor Prp8. We checked whether Snu66-CM would also show a similar genetic interaction with Prp8. We used the *prp8-101* mutant and checked the synthetic lethality with $\Delta snu66$. It was observed that the double mutant (*prp8-101* $\Delta snu66$) was sick at 25°C and 35°C (Figure 2.4A). We made double mutants of *prp8-101* with all the Snu66-CM point mutants as well as the $\Delta Snu66$ -CM. We observed that the Snu66-CM mutants (point mutants and deletion) did not show a similar sickness with *prp8-101* (Figure 2.4B). This showed that the C-terminus region might not be responsible for the genetic interaction of Snu66 and Prp8 and might have a different set of interactors.

We also checked another set of genes that showed synthetic sickness with Snu66 deletion in an SGA array⁹² screen. The two targets tested were *Lea1* and *Brr1*. *Lea1* is an important U2 snRNP component⁹³, and *Brr1* is a spliceosomal protein which helps in stabilising the newly synthesised snRNAs^{94,95}. As the Snu66-CM point mutants did not show any phenotype, we used just the Δ *Snu66*-CM to check the genetic interaction with *Lea1* and *Brr1*. We also took a HIND deletion and a HIND-Snu66 CM double deletion to compare the two different Snu66 conserved motifs. We transformed Δ *snu66* Δ *lea1* and Δ *snu66* Δ *brr1* with the Snu66 mutant plasmids and observed the cell growth at 30°C (Figure 2.4C). We found that the deletion of Snu66-CM showed synthetic sickness with both the splicing factors. The Δ *HIND* single deletion mutant, however, did not show any growth defect (we shuffled out the WT Snu66 plasmid on 5-FOA plates). These results suggested that only the C-terminus of Snu66 genetically interacted with these snRNP components. The interaction of Snu66 with the U2 component *Lea1* might be signifying that these proteins are important for the interaction of the U2 and U6 snRNPs which form the catalytic RNA helix I core, and the Snu66-CM interaction with *Brr1* might be required to stabilise the newly synthesised snRNAs which would be required for proper spliceosome complex formation and splicing.

28

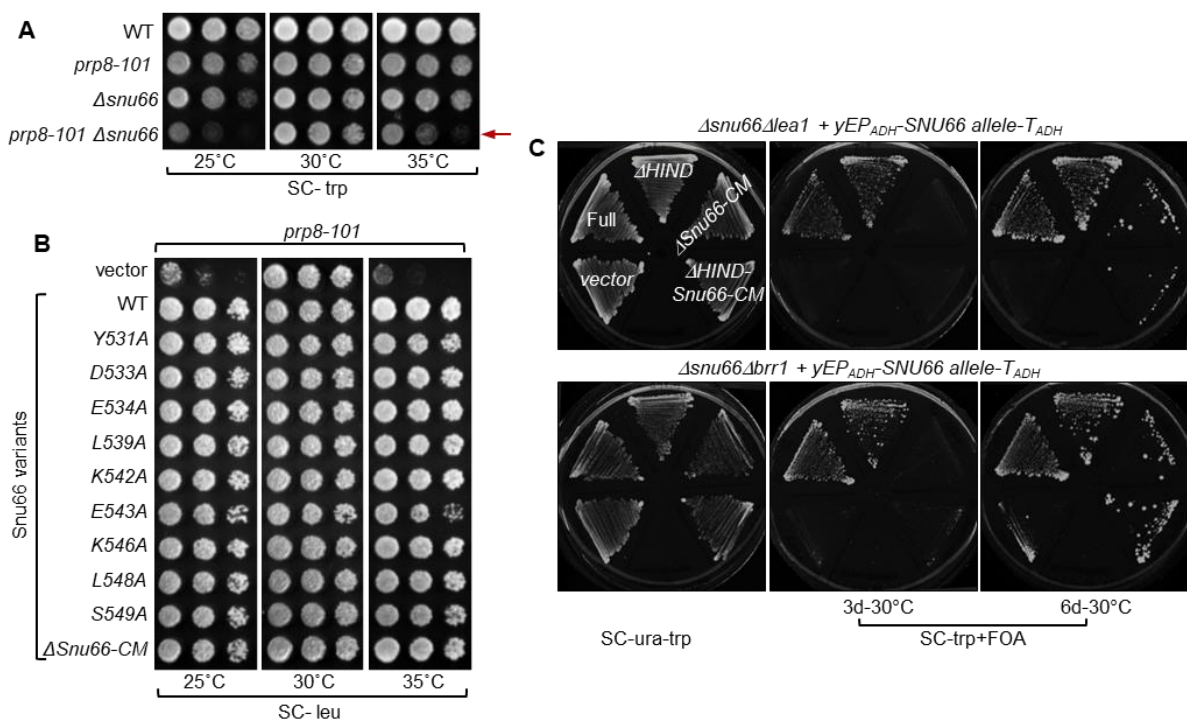


Figure 2.4: Genetic interaction of the Snu66-CM. (A) Snu66 genetically interacts with Prp8 and shows synthetic sickness with the *prp8-101* mutant at 25 and 35°C. (B) However, the Snu66-CM point mutants and deletion do not show synthetic sickness with *prp8-101* at 25°C and 35°C. (C) Genetic interaction of Snu66-CM with Leal and Brr1. The deletion of Snu66-CM with Leal and Brr1 makes the cell synthetically sick at 30°C but does not get affected on the removal of the HIND region. The mutant plasmids for Snu66 (Δ HIND, Δ Snu66-CM and Δ HIND –Snu66-CM) were transformed, and the WT type copy of Snu66 was shuffled out on 5-FOA plates.

2.2.3 Spliceosome architecture in Snu66-CM mutant

It is well established that Snu66 forms a scaffold interacting with several proteins to bring a proper conformation of the spliceosome. Therefore it was an important question whether Snu66-CM was required to maintain the proper architecture or conformation of the spliceosome? To answer that, we first checked if the incorporation of Snu66 itself into the spliceosome/tri-snRNP was dependent on its C-terminal motif. We performed CoIP experiments where we immuno-precipitated Prp4 to precipitate the spliceosome harbouring different mutants of Snu66 (chromosomal variants *RRAA*, *K546A*, and Δ *Snu66-CM*). In the immuno-precipitated samples, we checked the levels of these different mutants by western blot. We observed a reduction in the level of spliceosomal Snu66 in the Δ *Snu66-CM* mutant (Figure 2.5A). This proved that the C-terminus motif is important for the incorporation of Snu66 in the spliceosome.

Since Nguyen et al (2016). suggested in the cryo-EM study that the Snu66 C-terminus wraps around Brr2, we checked whether Snu66 mutants affected the incorporation, maintenance, or removal of Brr2 from the spliceosome? We performed another CoIP with Brr2 tagged in different mutants of Snu66. We immuno-precipitated the different mutants of Snu66 and checked for Brr2 levels by western blot. We observed that the levels of Brr2 remained unchanged, indicating that none of the Snu66-CM mutants affected Brr2 incorporation into the spliceosome (Figure 2.5B).

This showed that although these two proteins are known to interact via multiple domains, the Snu66-CM particularly was not responsible for the incorporation or maintenance of Brr2 levels in the spliceosome. This is indicative of the multivalent and complex interaction property of the interesting scaffold protein Snu66 in the spliceosome.

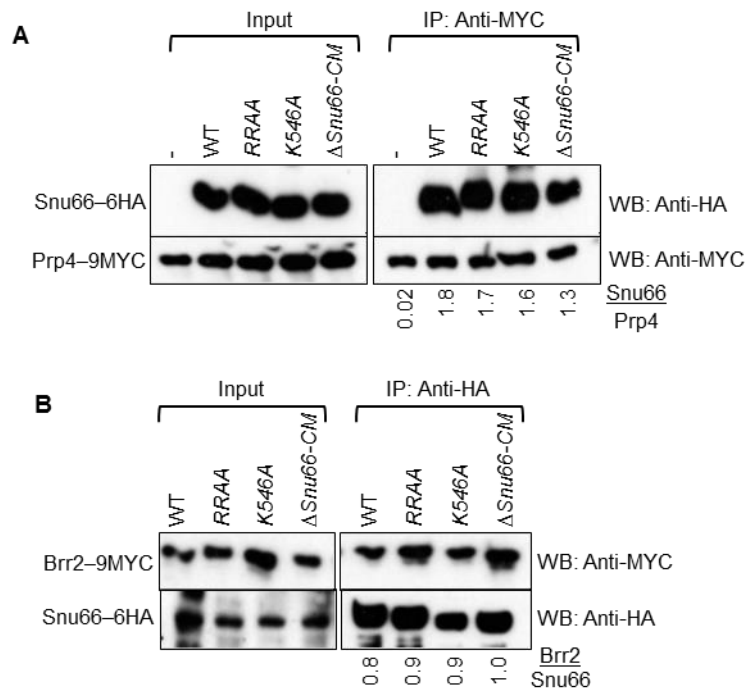


Figure 2.5: Role of Snu66-CM in spliceosome architecture. (A) IP of the spliceosome with Prp4 shows that the removal of the Snu66-CM region lowers the level of incorporation of Snu66 in the spliceosome, but the point mutants *RRAA* and *K546A* do not affect it. The quantification of the protein levels is given below the blot. (B) IP of spliceosome with different mutants of Snu66 shows that it does not affect the level of Brr2 incorporation or maintenance in the spliceosome. The quantification of the levels of protein is given below the blot (the smaller ratio in WT is because of experimental error in this specific blot and was not observed when the experiment was repeated).

2.2.3 Role of Snu66-CM in splicing

As it has been discussed before that the cold sensitivity of Snu66 null mutant is due to pre-mRNA splicing defect, we chose a few endogenous targets that showed splicing defects upon removal of Snu66. We analysed the splicing of these genes in the point mutants and $\Delta Snu66\text{-CM}$ in *S. cerevisiae*. We performed RT-PCRs and observed that the point mutants *D533A* and *K546A* did not show significant splicing defects, but $\Delta Snu66\text{-CM}$ showed splicing defects comparable to $\Delta snu66$. In some targets, the defect was almost equal in both $\Delta Snu66\text{-CM}$ and $\Delta snu66$ strains; in others, the defect in $\Delta Snu66\text{-CM}$ was slightly less compared to Snu66 null mutant. To confirm the specificity in the splicing defect of the targets to Snu66-CM, we used *Δhub1* as a negative control (Figure 2.6A). The absence of splicing defects in *Δhub1* confirmed that the defects are specific for Snu66 mutants. This signified a direct role of the Snu66-CM region in splicing and further validated its essentiality.

To find if Snu66-CM was also needed to recognize non-canonical splice signals, we did a growth-based assay using the *ACT1-CUPI* splicing reporter⁹⁶, which has a part of the *ACT1* gene fused to the *CUPI* gene that provides the cell copper resistance (Figure 2.6B). We took WT (GUAUGU) and two 5'ss mutants of *ACT1* intron (GUCUGU and GUAUAU) plasmids and transformed them into various Snu66 mutant strains (marked in the figure). We performed a spotting experiment and found that out of the two 5'ss mutants of *ACT1* intron, one (GUAUAU) showed growth defects on copper-containing plates (Figure 2.6C). This showed that Snu66-CM is important for the recognition of introns with certain non-canonical splice signals. Like the conserved region HIND, which has been shown to regulate alternative splicing/recognition of non-canonical ss, Snu66-CM also regulated splicing via certain non-canonical splice sites (5'ss GUAUAU).

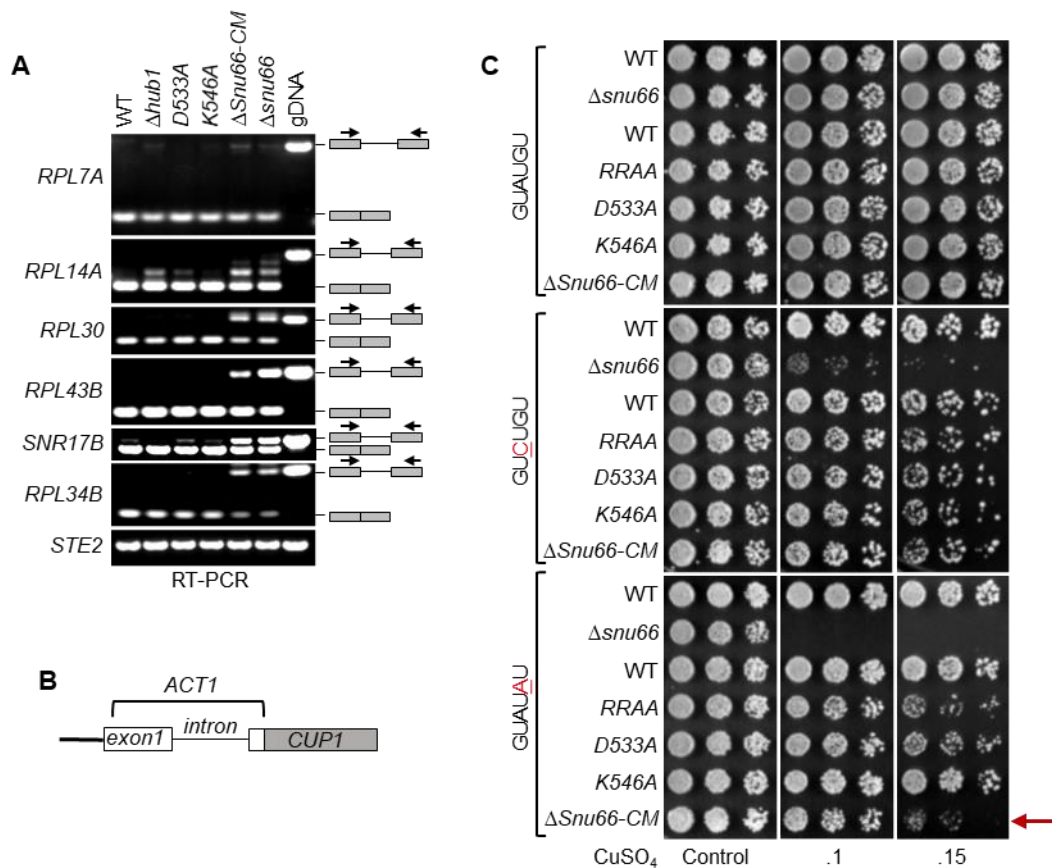


Figure 2.6: Role Snu66-CM in splicing. (A) RT-PCR assays with targets of Snu66 chosen from a microarray data show a defect in splicing for the genes in $\Delta Snu66-CM$. For most of the targets (*RPL7A*, *RPL30*, *SNR17B*, and *RPL34B*), the defect in $\Delta Snu66-CM$ is comparable to $\Delta snu66$, and in others (*RPL14A*, *RPL43B*), the defect is slightly varying. Although the point mutants of Snu66-CM do not show a drastic effect on splicing and are comparable to the negative control $\Delta hub1$. (B) *ACT1-CUP1* splicing reporter with exon1 intron and part of exon2 of *ACT1* gene fused to *CUP1* gene, which confers copper resistance to cells. (C) The *ACT1-CUP1* reporter (using CuSO₄ of .1mM and .15mM) with WT (GUAUGU) and non-canonical 5' ss (GUCUTU and GUAUAU) show copper sensitivity of $\Delta Snu66-CM$ with non-canonical 5' ss (GUAUAU). However, the point mutants do not show a similar amount of copper sensitivity. Also, in the case of the 5' ss mutant (GUCUGU), there is no such sensitivity, but both the mutants show copper sensitivity in the case of $\Delta snu66$. This indicates that the Snu66-CM domain is responsible for recognition of certain non-canonical splice sites.

Snu66-CM was involved in the regulation of constitutive splicing and splicing using a weak/non-canonical splice site.

To further validate the observation that Snu66-CM mutants are indeed defective in using non-canonical ss we tried to monitor splicing using an *ura4* based splicing reporter (Anil et al., unpublished) (Figure.2.8B). We made 5'ss, bp, and 3'ss mutants in the *tho5* intron interrupting the *ura4* reading frame. The western blot analysis for the reporters showed a difference in splicing of *ura4* in *snu66-1* compared to the WT strain in splice site mutants. It is said based on less amount of the full length functional *ura4* protein being formed in the mutants, and appearance of the lower bands corresponding to lower molecular weight peptides arising due to the translation of an *ura4* mRNA that has a pre-mature stop codon in it (Figure 2.8C). Compared to the wild type intron, the ss mutants showed higher splicing defects in *snu66-1*; however, the extent of defect also varies from mutant to mutant. This confirmed that Snu66-CM is important for splicing using non-canonical ss.

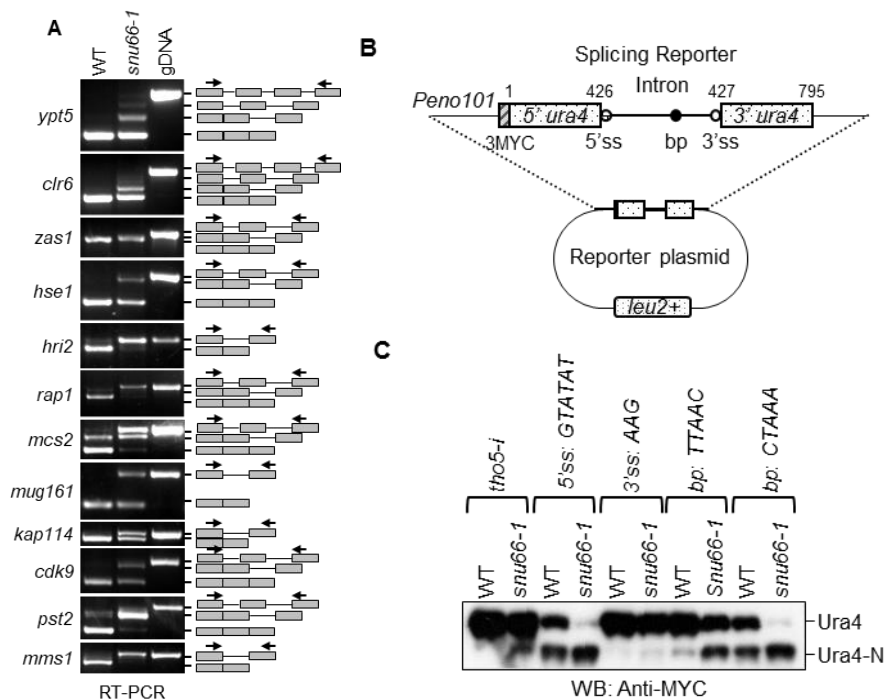


Figure 2.8: Splicing defects in *S. pombe* *snu66* mutant. (A) RT-PCR in *S. pombe* shows defects in constitutive splicing defects. It also shows defects in the splicing of an intron with non-canonical splice signals (5'ss, bp, 3'ss). (B) Schematic of *S. pombe* *ura4* splicing reporter (ss, splice site; bp, branch point). Numerical on the reporter shows the insertion site of introns in the *ura4* gene. (Anil et al., unpublished). (C) There are splicing defects for the different mutants of 5'ss, bp, and 3'ss in *snu66-1* strain. The defects in 3'ss TAG mutant is comparatively lesser than the other mutants used.

Table 2.1 Splice site analysis for Snu66-1 targets

	Gene name	Splicing defects	5'ss	Bps	3'ss	intron length
1	<i>hse1</i>	?	GTAAGT	CTAAC	TAG	44
		Yes	GTATGT	CTAAC	TAG	173
2	<i>hri2</i>	Yes	GTATGT	CTTAC	AAG	49
3	<i>rap1</i>	Yes	GTATGG	CTAAT	TAG	45
		Yes	GTATGA	CTAAC	TAG	82
4	<i>mcs2</i>	Yes	GTATGT	CTCAC	TAG	86
		Yes	GTATGT	CTTAC	TAG	50
5	<i>mug161</i>	Yes	GTATGA	CTAAC	TAG	113
6	<i>kap114</i>	Yes	GTATGC	CTAAC	AAG	56
7	<i>cdk9</i>	No	GTATGT	CTAAC	CAG	51
		Yes	GTAAGT	CTAAA	TAG	120
8	<i>pst2</i>	No	GTACGT	TTAAC	TAG	46
		Yes	GTATAT	TTAAC	TAG	78
9	<i>mms1</i>	Yes	GTGAGT	CTAAC	CAG	40
		Yes	GTAAGT	CTAAC	TAG	39

Lastly, we tried to look at the spliceosome architecture in *S. pombe* by a CoIP experiment in *snu66-1* strain. We tried to generate strains with *cdc5* and *brr2* double tags. But the strain *snu66-1* appeared to be sensitive to these double tags. So, we used a single tagged strain (*cdc5-6HA*) in wild type and *snu66-1* cells and performed an immuno-precipitation followed by a mass spectrometry analysis. In most cases, the data did not show significant change in the levels of splicing factor in WT vs. *snu66-1* (Figure 2.9). This could be because we used a point mutant, which might not be sufficient to hinder the interaction of Snu66 to any protein or that this conserved motif, although important for the splicing function of the protein, might not be crucial for its scaffolding function.

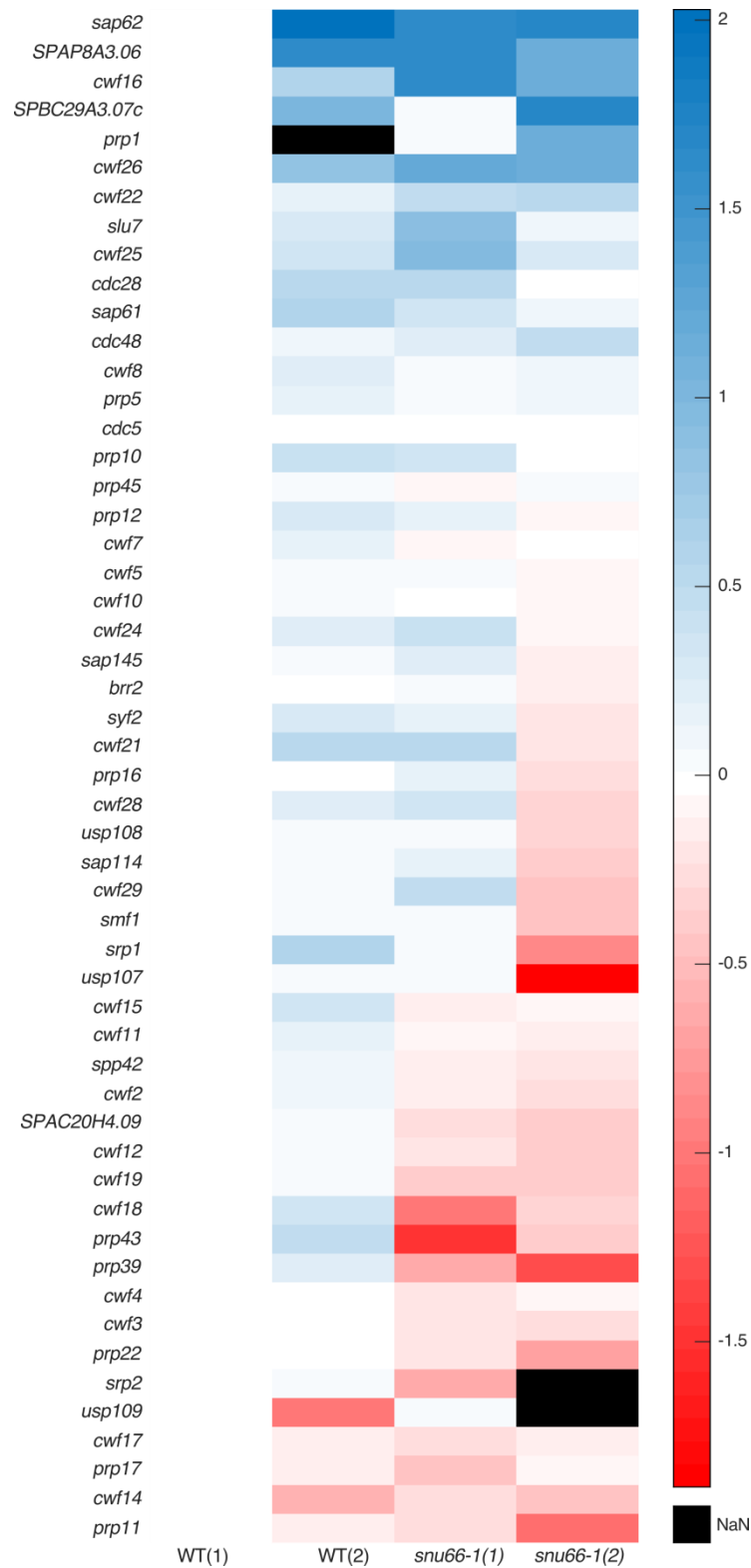


Figure 2.9 Change in level of spliceosome components. Heat map of mass spectrometry data of WT vs. *snu66-1* in replicates. It does not show a significant difference in level of the spliceosomal proteins mentioned along the Y-axis. The values for each indicated spliceosomal protein has been normalised with the immuno-precipitated *cdc5* value and with respect to its own value in the first WT replicate.

2.3 Conclusion and Discussion

From the results, it was concluded that the splicing factor Snu66/SART1 has a highly conserved essential functional motif at the C-terminus. While the absence of Snu66-CM imparted a partial cold sensitivity in *S. cerevisiae*, the effect on cell viability is striking in intron-rich *S. pombe*. A point mutation of the domain like *D600A* was deleterious for the cells. The Snu66-CM did not appear to affect the basic architecture of the spliceosome, as observed from the CoIP/MS data. But the region did show genetic interactions to snRNP proteins like Brr1 and Lea1. The failure in obtaining a double-tagged strain in the *S. pombe* *snu66-1* strain could also be indicative of a complex genetic interaction of the Snu66-CM region to other spliceosomal proteins like Cdc5 and Brr2 in higher organisms.

The density map from cryo-EM structural studies on this region of Snu66 has not been very clear in either *S. cerevisiae* or *H. sapiens*. Nguyen et al. (2016) showed a poly Ala chain represent most of Snu66-CM in *S. cerevisiae*, and Zhan et al. (2018) mostly remained confined to the N-terminus interaction of Snu66 in his human spliceosome structure studies. Although the Snu66-CM might not have a scaffolding role, the motif is critical for the Snu66 protein function in splicing itself (Figure 2.10). A better understanding of the Snu66-CM structure and interactor via cryo-EM in the future might help us further in deciphering this highly regulated and intriguing mechanism of splicing.

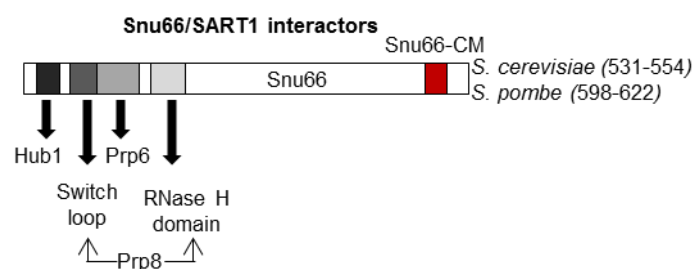


Figure 2.10: Schematic of Snu66 and its interacting domains. Regions of Snu66 interacting with various splicing factors (Hub1, Prp8, and Prp6). These regions at N-terminus (grey boxes) have been identified previously⁵⁴. In this study, we report the C-terminus conserved motif (*S. cerevisiae* 531-554, and *S. pombe* 598-622 red box) essential for cell viability and pre-mRNA splicing. The Snu66-CM genetically interacts with Lea1 and Brr1.

It can also be concluded that the region is crucial for pre-mRNA splicing (constitutive and non-canonical splice sites) in both *S. cerevisiae* and *S. pombe*. Both the organisms showed significant splicing defects for several targets. The significant amount of splicing defect in *S. pombe* in the point mutant (*K613A*) shows the vitality of the motif in intron-rich organisms. These results can be extrapolated to humans, a much complex organism with a complex splicing pathway. With a higher amount of alternative splicing, a larger number of exons and introns, which are also longer in size, and non-canonical splice signals, the Snu66-CM in human SART1 might play a crucial role in its splicing pathway.

Chapter 3

Sap1-Snu66 Function and Regulation

3.1 Introduction

Sap1 is an uncharacterised member of the AAA-ATPase family (discussed in section 1.7). It was identified as an interactor of transcription repressor Sin1⁹⁷. Sap1 also binds to SUMO (Box 2) conjugates non-covalently through a SIM (SUMO Interaction Motif)⁹⁸ (Box 3). But its function has not been explored yet. Obtained as an interactor of the splicing factor Snu66 in a yeast two-hybrid screen, Sap1 interested us, and we wanted to find its importance in RNA splicing. We started exploring the expression of the protein, looked at its phenotypes, interactors, localisation, plausible function, and regulation. While Sap1-Snu66 interaction indicated a role of this complex in RNA splicing, we could not find any splicing role for the complex. However, based on our results, we hypothesised that the Sap1-Snu66 complex has an unexpected and intriguing role in homologous recombination.

Box 2: Sumoylation is a reversible posttranslational modification and the SUMO (Small Ubiquitin-like Modifier) gene *SMT3* was first identified in *Saccharomyces cerevisiae*^{174,175}. SUMO was shown to bind covalently and alter the localization of modified proteins¹⁷⁶. Sumoylation is carried out by an enzymatic cascade in stepwise reactions like ubiquitination. It consists of three main steps namely activation, conjugation and ligation brought about by enzymes E1, E2 and E3 respectively.

Box 3: Besides covalent modification SUMO binds to proteins non-covalently. the best characterized mode of non-covalent interaction is via a SUMO Interaction Motif (**SIM**) present on the substrate which is recognized by the presence of few hydrophobic amino acid stretch¹⁷³.

Homologous recombination (HR) in yeast (*S. cerevisiae*) is a highly regulated process that depends on members of *RAD52* epistatic family of protein and multiple helicases. Double-stranded breaks, which arise because of external factors like ionising radiations or internal factors like replication errors, initiate HR. DNA damage leads to replication blockage and cell cycle arrest, providing a window for repair. Replication stalling leads to ubiquitination and/or sumoylation of PCNA^{99,100}, which acts as a signal for repair pathway activation. It starts with the DNA end resection by the heterotrimeric complex Mre11, Rad50, and Xrs2 (MRX). The complex interacts with Dna2 for endonuclease activity and exonuclease Exo1 to degrade 5' strands to yield 3' single-stranded DNA (ssDNA) tail. This resection of the ends is regulated by the helicase Sgs1, which unwinds the DNA for Exo1/Dna2 to cleave¹⁰¹⁻¹⁰³. 5'-3' resection is followed by homologous pairing to the donor duplex and strand invasion catalysed by Rad51 recombinase. Rad51 binds the ssDNA tail and dsDNA donor in an ATP-dependent manner^{104,105}. However, the efficient strand exchange by Rad51 requires other proteins like RPA (Replication Protein A), Rad52, Rad54, etc. RPA helps Rad51 in binding ssDNA and form the nucleoprotein filament, and this interaction is mediated by Rad52. Rad52 interacts indirectly with Rad51 and delivers it to RPA coated ssDNA^{106,107}. Rad54 helps in the D-loop formation where the synthesis of the cleaved region on the donor template is achieved¹⁰⁸. Following strand synthesis, carried out by DNA pol δ , the resolution of the D-loop and intermediates take place. This segregation is also regulated by the Sgs1-Top3-Rmi1 complex, which removes the supercoils and disrupts the strand invasion.

Along with Sgs1, another important helicase in HR regulation is Srs2. Srs2 checks the level of spontaneous recombination by displacing Rad51 and inhibiting nucleoprotein filament formation. Srs2 is recruited by the SUMO-modified PCNA to inhibit homologous recombination. Although Srs2 inhibits initiation of HR, after strand synthesis it acts as a positive regulator by unwinding the invading strand from the donor strand along with Sgs1 leading to distinct recombination outcomes. Thus, Srs2 behaves as both a positive and negative regulator of HR¹⁰⁹⁻¹¹¹. The basic mechanism and the major factors (recombinase, nuclease, and helicases) remain constant in the different modes of HR with additional factors specific to each mode^{78,112}.

3.2 Objective

Expression, Regulation, and Function of Sap1 and Sap1-Snu66 complex: I researched the expression and regulation of SUMO binding AAA-ATPase Sap1 in *S cerevisiae* and the function of the Sap1-Snu66 complex.

3.3 Results

3.3.1 Snu66-Sap1 interactions

Following our previous chapter, where we studied the role of Snu66, we did a yeast two-hybrid screen using Snu66 as bait. We found Sap1 as an interactor of Snu66 and wanted to map the specific region for this interaction. We made different mutants of Sap1 like a SIM point mutant (*I236A*), a deletion of the SIM, a point mutant of the AAA-ATPase domain (*K651A*), and three other truncations (Figure 3.1A). We observed that the C-terminal region from 568 to 897 was necessary for Sap1-Snu66 interaction. A fragment shorter than that abolished the interaction. However, the truncation 521 to 897 had the strongest intensity of interactions, more than the full-length protein. Mutating the SIM and AAA-ATPase domain did not disrupt the interaction between Sap1-Snu66.

43

As we found the region of interaction for Sap1, we mapped the region of Snu66 bound to Sap1. We did a similar directed yeast two-hybrid with various truncations of Snu66. Interestingly, we found that the region 531-554 at the C-terminus of Snu66, i.e., Snu66-CM (described in chapter 1), was necessary and sufficient for Sap1-Snu66 interaction (Figure 3.1B). To validate if this was a true interaction, we used the point mutants of the Snu66-CM conserved residues and checked whether they affect this Sap1-Snu66 interaction (Figure 3.1C). We found that the different mutants affected the interaction with different intensity. In mutants like *Y531A*, *D533A*, *L539A*, *K546A*, *L548A*, the interaction was lost almost completely, *E543A* had very weak interaction, and *E534A*, *K542A*, *S549A*, and *G554A* did not affect the binding of Sap1 to Snu66.

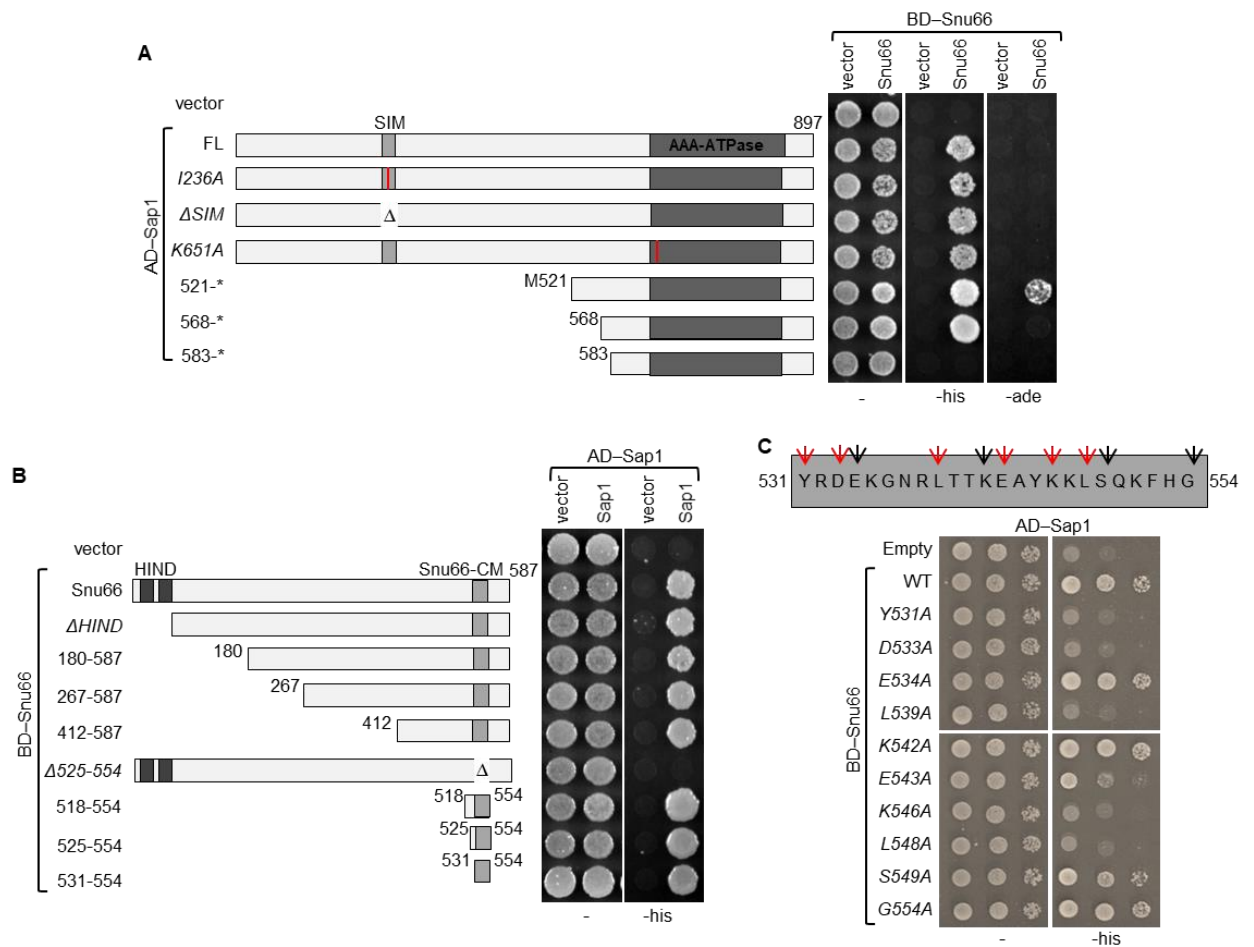


Figure 3.1 Sap1 a novel interactor of the splicing factor Snu66. (A) Snu66 interacts with Sap1 at the C-terminus. The region 521-897 has the strongest interaction, but the region 568-897 is sufficient for the proteins to interact. *I236A* is a point mutant of the SIM and *K651A* is an ATPase domain mutant. (B) A yeast two hybrid, with series of Snu66 truncation mutants, shows that the Snu66-CM is necessary (Δ 525-554) and sufficient (531-554) for Sap1-Snu66 interaction. (C) Various Snu66-CM residue point mutants affect the interaction between Sap1-Snu66 differently *Y531A*, *D533A*, *L539A*, *K546A*, *L548A* mutant: no interaction, *E543A*: weak interaction, *E534A*, *K542A*, *S549A*, *G554A*: no effect on Sap1-Snu66 interaction. (Data obtained with Balashankar)

3.3.2 Sap1 isoforms

To check the expression and protein levels of C-terminally 9MYC tagged Sap1, we scraped some cells from a freshly growing plate, isolated the total protein by TCA prep, and ran the sample on an SDS PAGE for a western blot analysis. It was surprising to find not only the 100kDa protein band (as mentioned in high-throughput studies) but another unknown 50kDa protein band (Figure 3.2A). To understand it further and check the specificity of the shorter

band, we performed a timeline-based expression check. We grew the cells in liquid culture and harvested them at different time points over a period of 36 hours, and performed a western blot analysis with anti-MYC antibody. We observed two signals, one for the 100kDa protein and another signal for a 50kDa protein, which only appeared after a certain time point during the cell growth (Figure 3.2B).

A diauxic shift is a mechanism where cells growing in glucose-rich media undergo a change in the carbon source usage from glucose to another compound¹¹³. We speculated that Sap1_C might be expressed after the cells undergo a diauxic shift or when cells grow using a non-fermentable carbon source. We mimicked the condition of the diauxic phase of growth and grew the cells in glycerol + lactate (non-fermentable carbon) media and did a similar experiment as before. As speculated, when grown in a non-fermentable carbon source, the shorter form of the protein started expressing from the initiation of the cell growth (Figure 3.2B). Thus, this observation confirmed that the expression of Sap1_C is carbon source dependent. To know the identity of the shorter form of Sap1, we looked at its amino acid composition by Edman-degradation reaction. In an Edman-degradation reaction, we can N-terminally sequence a peptide by cleaving the N-terminal amino acids one by one¹¹⁴. By this experiment, we found the protein sequence of Sap1_C and that it starts with a methionine residue at 521st position (Figure 3.2C).

As the Sap1-Snu66 interaction studies were yeast two-hybrid based, we wanted to validate the physical interaction of the two proteins in an *in-vitro* system. Since we identified a shorter isoform of the protein starting from Methionine⁵²¹, the fragment of Sap1 that interacted strongest with Snu66; we performed a GST-pull down assay with different variants of Snu66 and Sap1 recombinant proteins. We found that the recombinant Snu66-CM fragment of Snu66 interacted with the different recombinant forms of Sap1 (Figure 3.2D). But the recombinant HIND fragment of Snu66, known to interact with the splicing factor Hub1, did not pull down any of the Sap1 recombinant proteins. This proved that Snu66 indeed interacts with Sap1 via Snu66-CM even physically.

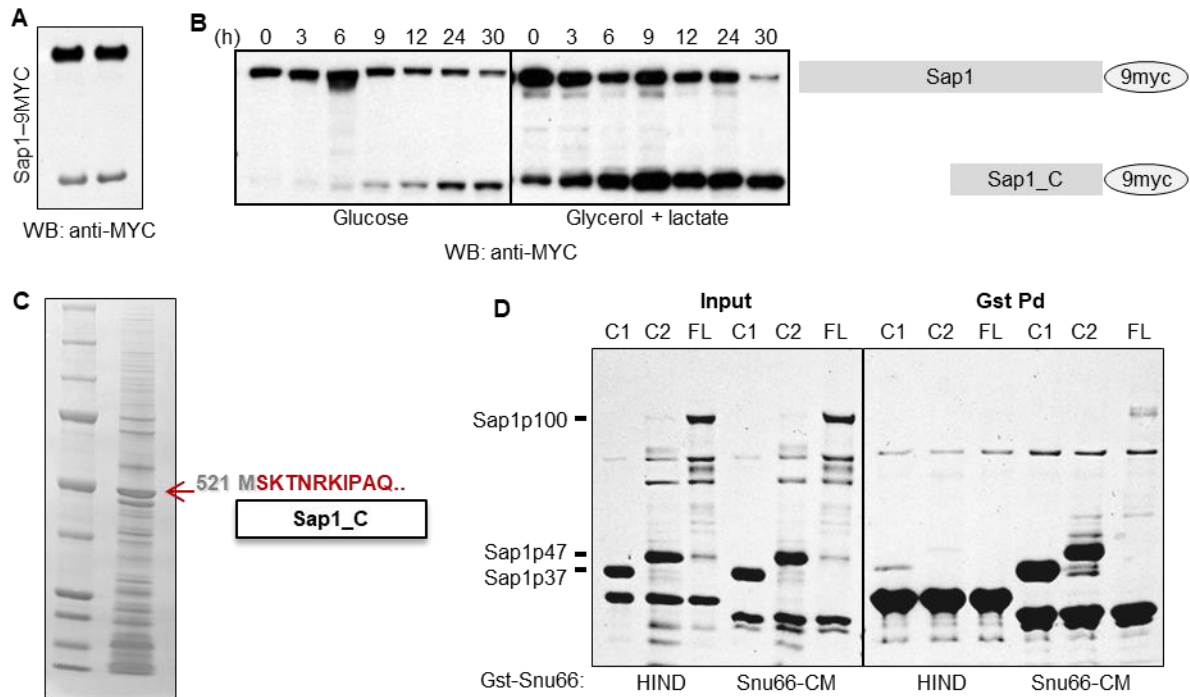


Figure 3.2: Two protein isoforms of Sap1. (A) Two bands for Sap1-9MYC at 100 and 50kDa. (B) The shorter form (Sap1_C) was expressed after diauxic shift in glucose-containing media or constitutively in non-fermentable carbon sources. (C) Amino acid sequence for Sap1_C from Edman degradation assay. Sap1_C starts with Methionine 521st. (D) *In-vitro* confirmation of Sap1-Snu66 interaction. Snu66-CM recombinant protein pulls down Sap1, but HIND recombinant protein does not. (Image C and D obtained from Shravan)

46

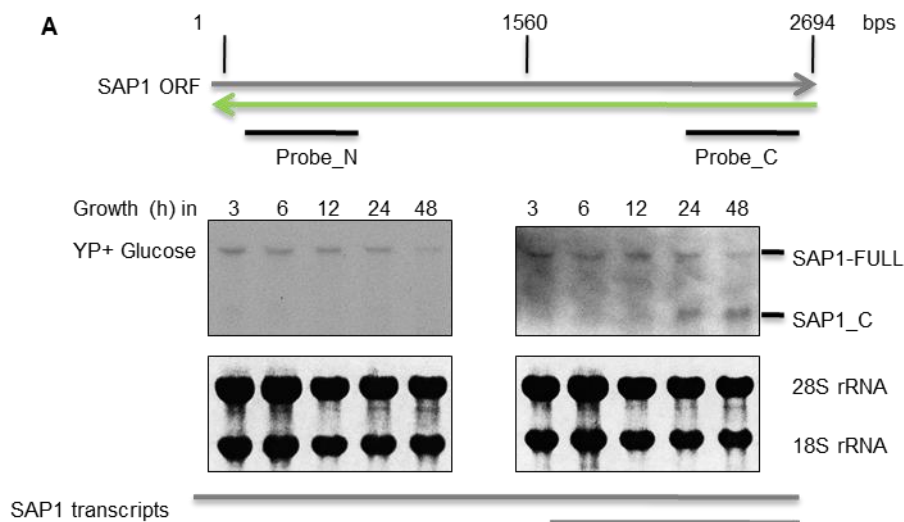
3.3.3 Sap1 isoform expression by alternate transcription

The next question was, how were the two isoforms made? The possible options for the two isoforms expression are: (a) alternate splicing (section 1.1.5); (b) post-translational modification; and (c) alternate transcription (Box 4). We ruled out alternate splicing because the gene does not have any intron. Since we found the shorter protein starts with a methionine from the Edman degradation experiment, we hypothesised that the two proteins are isoforms expressed from two different transcripts. To validate our hypothesis, we did a northern blot analysis using a probe for N terminus and C terminus of

Box 4: Alternate transcription is involved in the biogenesis of different mRNA (transcript) molecules from a common DNA sequence. It helps in generating transcripts with different first exon, start site, ORFs, varying lengths of 5'UTRs thus leading to formation of protein isoforms. Alternate transcription with use of alternate promoters can generate isoforms with different start sites¹⁷⁷.

the Sap1 ORF. Both the probes gave us a signal for the full-length mRNA, but the C terminus probe gave us another signal smaller in size, which is the mRNA for the shorter form of the protein (Figure 3.3A). Thus, we concluded that there are two separate transcripts for the two isoforms indicating that they are formed by alternate transcription of the ORF.

Next, we checked whether the two transcripts have two promoters for their transcription. As we know that a gene promoter is usually 100-500 base pairs upstream of the start site*, we speculated if the 2nd promoter for Sap1_C lay within the ORF of the full-length protein. To check that we fused the 500 base pairs above the 2nd start site, i.e., methionine⁵²¹, to a lacZ gene and observed its expression pattern by β -galactosidase assay. We indeed found that the expression of the lacZ mimicked Sap1_C expression in fermentable (glucose) and non-fermentable (glycerol + lactate) carbon sources (Figure 3.3B), which confirmed that an internal promoter just above the 521st methionine is responsible for the expression of Sap1_C after diauxic shift / in non-fermentable carbon source.



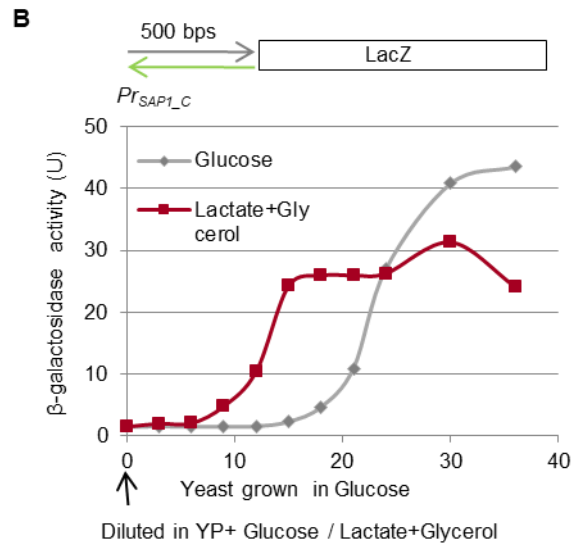


Figure 3.3: Expression by alternate transcription via internal promoter. (A) Northern blot showed the presence of two transcripts for Sap1 full length and shorter form. The N-term probe detects the longer transcript and the C-term probe detects both transcripts for isoform with the common C-terminus region (B). The 500bp region upstream of Met⁵²¹ fused to LacZ. ONPG assay showed that in glucose (grey curve) containing medium, lacZ expression starts after diauxic shift, whereas in lactate + glycerol media, LacZ expresses from the starting of the log phase (red curve). The expression of LacZ mimics that of Sap1_C. (Data obtained by Shravan)

3.3.4 Phenotype for Sap1

After finding out the interesting expression pattern of Sap1, we studied the phenotype of the cell upon the deletion of Sap1, which could help us in functional and mechanistic studies. We took WT and $\Delta sap1$ cells and did growth assays under several growth conditions. We used different media plates such as synthetic and rich media, different carbon sources (fermentable and non-fermentable), different temperatures, and oxidative stresses. But the $\Delta sap1$ did not show any phenotype, and both the strains grew similarly in all conditions (Figure 3.4A). It is reported by Gaytan et al. (2013) and Connor et al.(2012) that $\Delta sap1$ showed decreased resistance to chemicals like benzo-a-pyrene (Bap- carcinogen) and dieldrin (insecticide)^{115,116}. Hence, we used these two chemicals to verify the sensitivity/phenotype for $\Delta sap1$. But even with different concentrations of these chemicals, both WT and $\Delta sap1$ grew healthy (Figure 3.4A).

We speculated whether there is a difference in the rate of growth of WT and $\Delta sap1$ cells; although on a plate, they finally reach an identical density? To check this hypothesis, we did a growth curve analysis over 48 hours with an interval of 3 hours for O.D.₆₀₀ measurement in different culture media (Figure 3.4B). But, there was a negligible difference in the growth rate of the cells in rich media or with non-fermentable carbon sources.

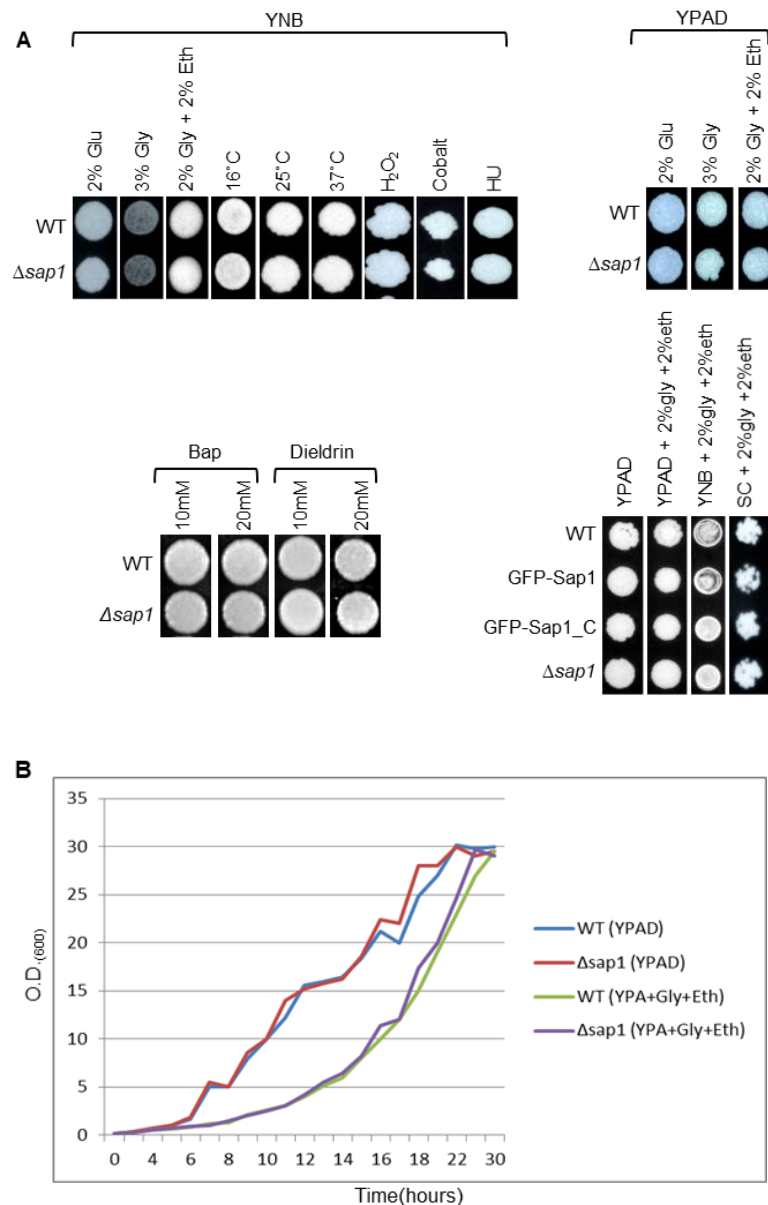


Figure 3.4: Phenotype in $\Delta sap1$. (A) No phenotype for $\Delta sap1$ in any of the conditions tested (media composition, carbon source, temperature, oxidative stress, and chemicals like deldrin and Bap). (B) The rate of growth for WT and $\Delta sap1$ remains similar in different media compositions and carbon sources.

3.3.5 Genetic interactors of Sap1

Since a single gene deletion with Sap1 did not give a visible phenotype, we looked at the interactors of Sap1 from high-throughput data (available on SGD), which in combination might provide a synthetic phenotype. Out of 60 listed genetic interactors, we choose *CLA4*, *ELM1*, and *GIN4* as all of them had been shown to help in septin ring formation during budding and work in the same pathway¹¹⁷⁻¹¹⁹. Septins are a group of five proteins Cdc3, Cdc10, Cdc11, Cdc12, and Sep7/Shs1, which form a ring-like structure at the bud neck during cell division (budding) in *Saccharomyces cerevisiae* that determines the balance of exchange between a mother and daughter cell¹²⁰⁻¹²². An important modification in septin ring formation is the sumoylation of certain septin proteins¹²³. Since Sap1 had a SIM, it is possible that it might be a part of the complex and required in the septin ring formation (Figure 3.5). To validate the hypothesis, we made single and double deletion strains of Sap1 and the three targets followed by spotting assay. But the double deletions did not show any synthetic sickness or growth advantage compared to the single deletions.

50

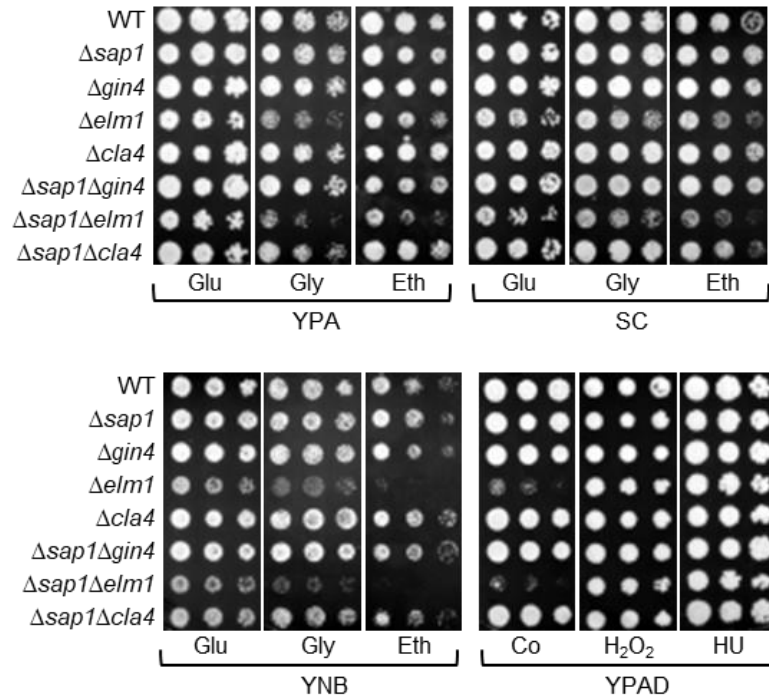


Figure 3.5: Genetic interactors of Sap1 Single and double deletion of Sap1, Cla4, Elm1, and Gin4 on rich and synthetic media plates with varying carbon sources (glucose, glycerol, and ethanol) and oxidative stress (cobalt, hydrogen peroxide, and hydroxyl-urea). The double deletions do not show any phenotype. However, $\Delta sap1\Delta elm1$ is moderately sick, but so is the single $\Delta elm1$ mutant.

3.3.6 Different localisation of isoforms

As we found that there are two isoforms of Sap1, we were curious to look at the localisation of the two forms. We N-terminally tagged Sap1 with GFP under the pADH promoter (Figure.3.6A), such that the expression of the two isoforms becomes constitutive, and observed their localisation in the cell. The two isoforms showed very different localisation in the cell; the full length (Sap1) localised as a punctate at the bud neck and/or at the opposite end of bud, and the shorter form (Sap1_C) diffused throughout the cytoplasm and nucleus (Figure.3.6B). With such different localisation, we speculated that the two forms might be involved in different pathways or regulate each other's expression for the proper functioning of the pathways they might be involved in.

51

As the full-length protein harbouring the SIM localised at the bud neck, we wanted to check whether septin sumoylation (they are present at the bud neck in ring structure) played a role in the bud neck localisation of Sap1 full-length. We imaged GFP tagged Sap1 in $\Delta siz1$, an E3 ligase, mutant¹²⁴ (septin, and most of the sumoylation inhibited in the deletion background). The localisation of the Sap1 in the $\Delta siz1$ deletion strain changed and got diffused (Figure 3.6C). We also wanted to check whether the localisation of Sap1 was cell cycle dependent. So; we arrested cells at various stages of the cell cycle (G₀, S, and G₂M phase) using different chemicals such as α -factor, hydroxyurea, and nocodazole^{41,124,125}. We observed that the localisation of Sap1 full-length did not change in wild type cells on cell cycle arrest, however the protein was diffused in the cytoplasm on in $\Delta siz1$ also after cell cycle arrest treatment (Figure 3.6D). This showed that the localisation of Sap1 full-length protein was related to septin sumoylation but did not depend on the stage of cell cycle. Upon inhibition of septin sumoylation in $\Delta siz1$ cell, the localisation of the Sap1 became like that of the shorter form Sap1_Cat all stages of the cell cycle.

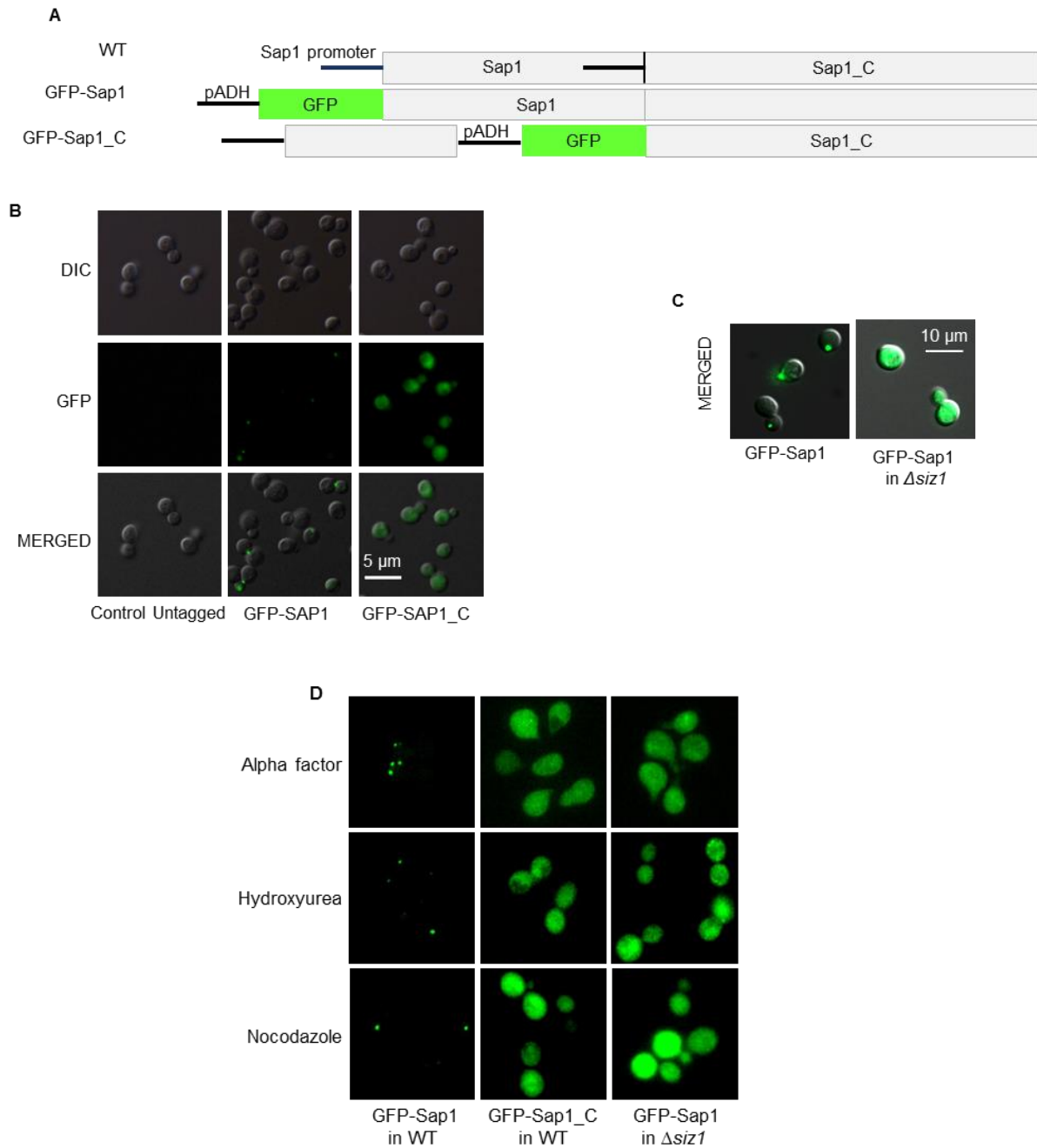


Figure 3.6: Localisation of Sap1 and Sap1_C. (A) Schematic of N-terminally tagged Sap1 with GFP under ADH promoter. This makes both the proteins Sap1 and Sap1_C constitutively expressed in the cells. In the case of GFP-Sap1_C, the ORF for the full length is interrupted. (B) The full-length Sap1 localised at the bud neck and/or at distal end of the bud as a punctate, and the shorter form Sap1_C diffused in the cytoplasm, and the nucleus is monitored by the green fluorescent signal. (C) The localisation of Sap1 changed and became diffused in the cytoplasm in $\Delta siz1$ mutants (D) Cell cycle arrest with alpha-factor, hydroxyurea, and nocodazole did not change the Sap1 localization in WT and in $\Delta siz1$ it remained diffused like the shorter form Sap1_C.

3.3.7 Regulation of Sap1_C by Tup1

Now, we wanted to check the regulation of Sap1_C expression. As the shorter form expresses only after a diauxic shift or in non-fermentable carbon sources, how does the cell maintain such specificity? To answer, we designed a reporter strain where we put the LacZ gene under the internal Sap1_C promoter and crossed it to the deletion library. We then carried out X-gal overlay assay with the spores from the diploids. We found that the LacZ expression was very high in the Tup1 deletion strain (Figure 3.7A). Tup1 is one of the first proteins to be identified as a transcription regulator and is conserved throughout all eukaryotes. It was initially identified as a corepressor and later suggested to also act as a coactivator. Tup1 shows dual activity based on its interacting partner proteins. Tup1 works in association with other co-repressor molecules in various pathways, such as carbon source regulation, mating-type switching, etc.

To validate the screen, we looked at the expression of Sap1 and Sap1_C in wild type and Tup1 deletion strains (*S. cerevisiae* deletion library, Euroscarf). We tagged Sap1 at the C terminus with 9MYC and did a western blot analysis. As per our screen, we observed that the shorter form of Sap1 expresses from the start of the growth in the $\Delta tup1$ mutant, whereas in WT cells, it expressed after diauxic shift (Figure 3.7B).

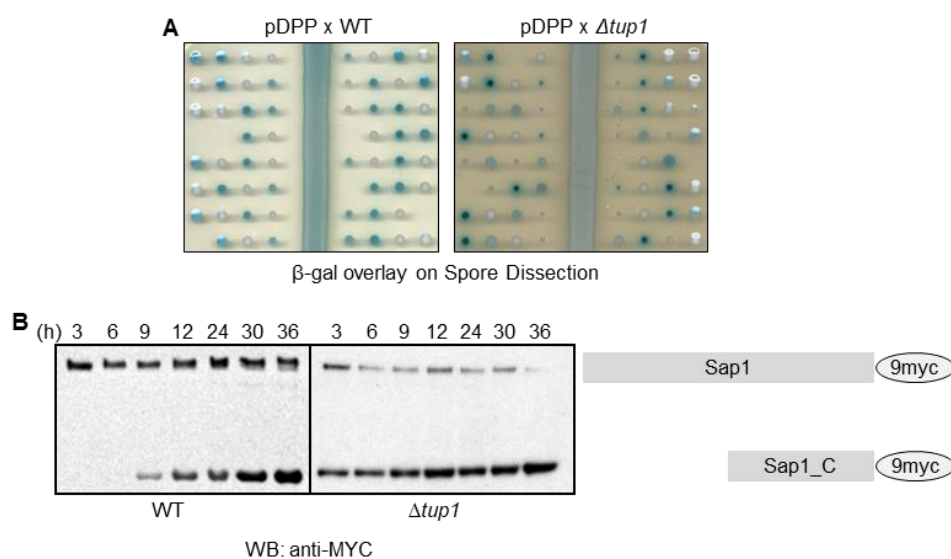


Figure 3.7: Regulation of Sap1_C by Tup1. (A) X-gal overlay assay on solid agar plates with spores dissected from the indicated cross shows higher LacZ expression under Sap1_C promoter in $\Delta tup1$ (Data in A obtained from Shravan). (B) Expression of Sap1 monitored by MYC western blot shows the expression of Sap1_C after a diauxic shift in wild type cells and constitutively in $\Delta tup1$ deletion mutant. The different time points for harvest are marked along X-axis in hours.

3.3.8 Tup1 binds the internal promoter directly

The mechanisms by which the Tup1 and its partner protein complex repress transcription are as follows:

- i) By direct interference with the activator.
- ii) By altering the local chromatin structure.
- iii) By interacting with the general transcription machinery.

The mechanism of co-repression of various genes by Tup1 is well studied along with its co-molecules^{126–128}. But what we obtained from the screen indicates a solo role of Tup1 in Sap1_C regulation. To further understand this mechanism of regulation, we performed a ChIP (chromatin immune-precipitation) experiment to locate the binding region of Tup1 along the entire Sap1 ORF and parts of the promoter and terminator region. We observed that the Tup1 bound mostly at the promoter region of Sap1_C in between the SIM and the start of the 521st Methionine (Figure 3.8A). Tup1 did not bind at all to the promoter of Sap1 full length. Thus, we could infer that the binding of Tup1 specifically to the promoter region of Sap1_C results in its carbon source dependent regulation.

We wanted to analyse the expression of Tup1 in exponentially growing cells, for which we performed a western blot analysis with 1 O.D.₆₀₀ C-terminally 6HA tagged Tup1 cells harvested over 36 hours. We observed that, interestingly, the expression of Tup1 gradually decreases towards the later phase of growth. We also observed in the blot that bands with higher molecular weight, which showed a similar reduction in expression/modification (Figure 3.8B). This observation made me question what those higher bands were, and could that be responsible for Sap1_C carbon source dependent regulation?

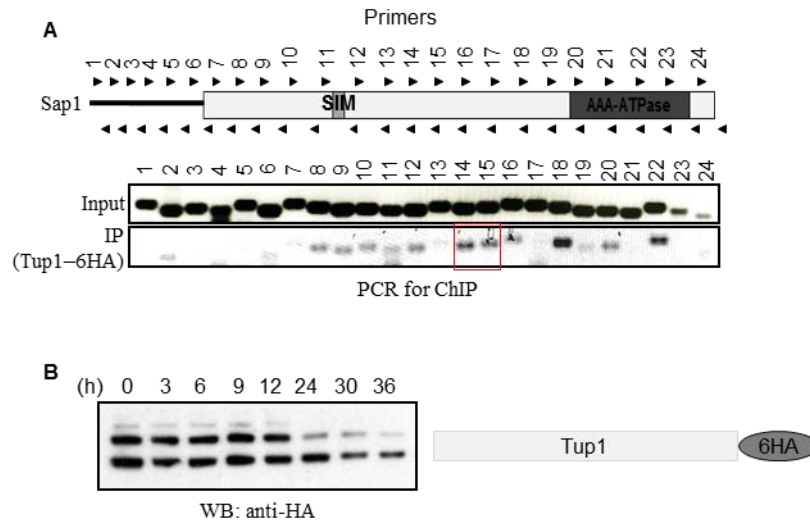


Figure 3.8: Mechanism of repression by Tup1. (A) PCR from ChIP sample shows Tup1 binds the Sap1_C promoter region highly but not the promoter for full-length Sap1. The Sap1_C starts at the region marked near number 18. The highest signals in the PCR come from regions numbered 14 to 18. The numbers represent the primer set and the region along Sap1; the primers amplify. The small light grey box denotes the SIM and the dark grey box denotes the AAA-ATPase domain. The red box shows the high signals in the ChIP PCR. (B) Expression of Tup1 monitored by HA western blot shows the reduction in its level during growth. It also shows the presence of sumoylated Tup1 and its reduction over time. The time points for cell harvest are marked along X-axis in hours.

3.3.9 Sumoylation of Tup1 inhibits Sap1_C expression

Scientists have shown that sumoylation has inhibitory effects on transcription. Such as, the sumoylation of H4 and H2B prevented acetylation of H4 and ubiquitination of H2B to repress transcription, and tethering SUMO to histone tails was sufficient to inhibit transcriptional activation¹²⁹. It has also been studied that the sumoylation of Gcn5 (HAT protein) inhibits transcription¹³⁰. Apart from histones and histone-modifying enzymes, which can remodel the chromatin structure to regulate transcription, transcription factors, and co-regulators (co-repressor/co-activator) also get sumoylated. For example, the sumoylation of Ssn6/Tup1 is shown to repress the transcription of galactose inducible gene *GALI* in the presence of glucose. Authors also proposed that Tup1 sumoylation mediates the transcriptional deactivation that is required to down-regulate *ARG1* expression^{131,132}.

We speculated that sumoylation might be regulating the binding of Tup1 to the promoter of *Sap1_C*. On the diauxic shift, Tup1 sumoylation is inhibited, which results in the removal of Tup1 from the promoter, thus, exposing the promoter to RNA polymerase. To validate our hypothesis, we conducted a denaturing Ni-NTA pull-down assay of 6His tagged Smt3 (SUMO gene) in the Tup1–6HA tagged strain and thereafter an anti-HA western blot to detect Tup1. The samples were harvested at different time points of growth, as mentioned in the figure (Figure 3.9). We observed that indeed, as the cells grew, there was a reduction in Tup1 sumoylation (mostly after the diauxic shift), which regulates the *Sap1_C* expression.

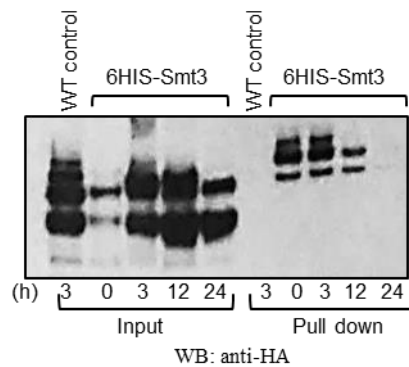


Figure 3.9: Level of Tup1 sumoylation. Level of Tup1 sumoylation monitored by HA western blot in Ni-NTA pull-down of 6His-Smt3. It shows that the amount of sumoylation goes down in cells harvested during the later phase of growth after the diauxic shift, which helps regulate the expression of *Sap1_C*.

3.3.10 Role of *Sap1* in splicing

Since *Sap1* was found as an interactor of general splicing factor *Snu66*, we also investigated *Sap1*'s role in RNA splicing. We performed a splicing sensitive microarray analysis (done in collaboration with Jeff Pleiss by Shravan at Cornell University). We took two strains wild type, and $\Delta sap1$ grew them at 30°C (control condition), 37°C (temperature stress), in glycerol, containing media (non-fermentable carbon source for *Sap1_C*) and cells post diauxic shift and performed the microarray with these varying conditions. The microarray analysis did not show a significant change in the splicing efficiency of the gene in any of the conditions provided (Figure 3.10A).

However, with thorough analysis we found a couple of candidates that appeared to get slightly affected by the absence of Sap1 under particular conditions (cells in glycerol media or post diauxic). One of the candidates was *TAD3*, a tRNA-specific adenosine deaminase, a multi-intron containing gene (2 introns)¹³³. We know that the number of multi-intronic genes in *Saccharomyces cerevisiae* is very less. This might be the reason for the lack of phenotype as Sap1 was not involved in general splicing phenomena but for very specific conditional multi-intron containing gene splicing. To validate this difference for *TAD3* splicing from the microarray, we carried out RT-PCRs and checked for defects in the splicing of either of the two introns in WT vs. $\Delta sap1$ strain grown under different conditions (Figure 3.10B). But, there was no observable splicing defect under any condition for either of the two *TAD3* introns.

As the defect might have been very subtle, and in the saturated RT-PCR product, it went undetected; we tried to check for minor splicing defects through a different quantitative approach. We designed a reporter using *TAD3* ORF fused to a LacZ gene in pLGSD5 vector, such that only a spliced *TAD3* comes in frame and allows lacZ expression (Figure 3.10C). We used the reporter for the calorimetric ONPG assay, where the intensity of the colour obtained from each sample could be used as a measure of the splicing efficiency. We performed the experiment in WT, $\Delta sap1$, $\Delta snu66$, and $\Delta hub1$ and observed that the reporter gave an equal readout for both wild-type, and $\Delta sap1$. In contrast, there was a striking difference in the case of $\Delta snu66$, and a moderate difference in $\Delta hub1$ strain (Figure 3.10C). So, the reporter assay also indicated that Sap1 does not play a direct role in pre-mRNA splicing.

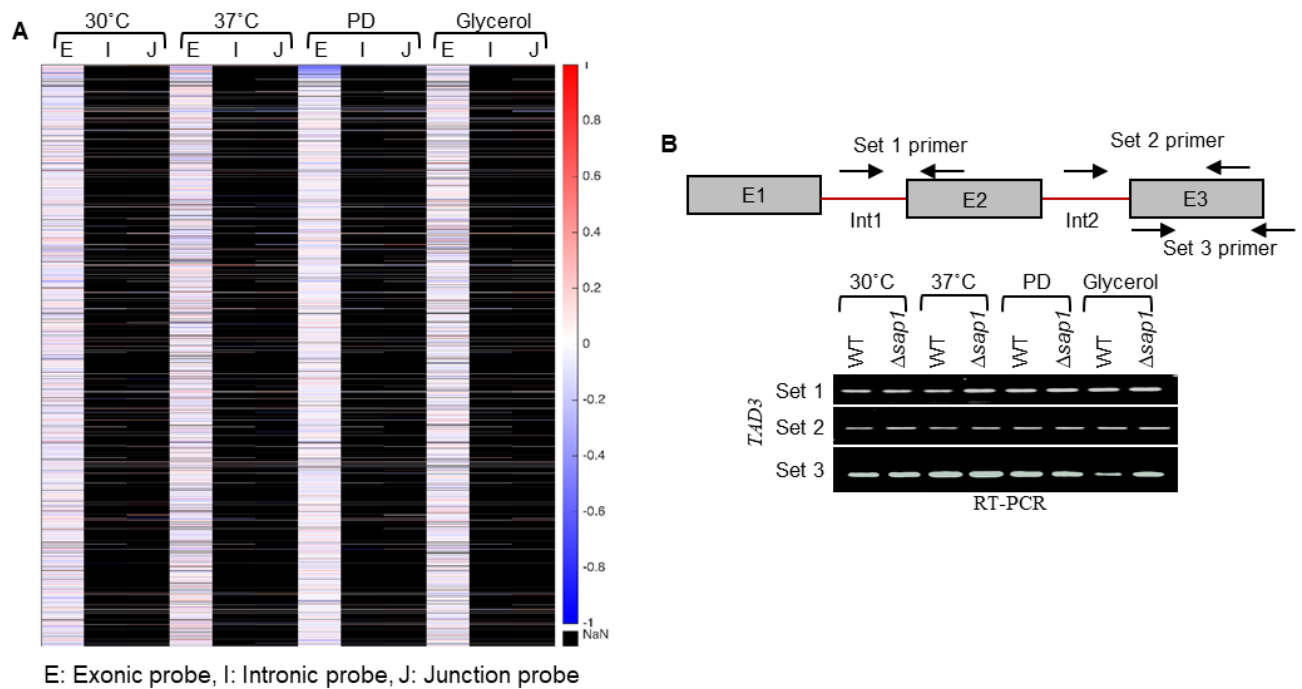


Figure 3.10: Role of Sap1 in pre-mRNA splicing. (A) Heat map of the splicing sensitive microarray of WT vs. $\Delta sap1$ under different growth conditions (PD-post diauxic). For most *S. cerevisiae* genes, the Intronic and junction probe did not have a value, and with the exonic probe, there was no significant difference in the ratio (B) RT-PCR for the two introns of *TAD3*, which showed a mild defect in splicing in PD and glycerol containing media. No observable difference in the level of intron retention under any evaluated condition. (C) ONPG assay with *TAD3* reporter in indicated strains. The reporter has complete exon 1, 2, and part of exon 3 and introns of *TAD3* fused to LacZ. LacZ comes in frame only on proper splicing. Sap1 deletion did not show a splicing defect for *TAD3*, whereas Snu66 and Hub1 deletion showed significant and mild defects, respectively.

3.3.11 Does Sap1 has any other function?

Since we did not find a direct role of Sap1 in splicing, we checked for other possible functions of Sap1. As Sap1 full length had a SIM motif, we checked if it plays a role in the sumoylation of substrates like septins. We used wild type, $\Delta sap1$, and $\Delta siz1^{124}$ strains to check the total sumoylation level (with SUMO antibody) and septin (Cdc3) sumoylation level (with HA antibody) in the cells. However, we observed that the sumoylation levels in $\Delta sap1$ were similar to wild-type, whereas our positive control $\Delta siz1$ showed a clear defect in total and Cdc3 sumoylation (Figure 3.11A).

As Sap1 localised at the bud neck, we also checked whether Sap1 is needed for bud/cell size regulation or the number of buds arising from a mother cell. We stained the WT and $\Delta sap1$ cells with calcofluor white (which fluorescently stains the cellulose and/or chitin in the cell wall), thus helping in visualisation. We grew the cells in different media and measured the size of 100 cells per sample, and observed that the cell/bud size and the number of buds from a mother cell were comparable in both strains. Microscopy images of WT and Sap1 deletion cells grown in synthetic media are shown in (Figure 3.11B).

At this point, we took a step back and gave our hypothesis a better thought. We found that Snu66 is also involved in the processing of 5SrRNA⁸². Hence, we tested if this Sap1–Snu66 interaction was involved in 5SrRNA processing. We performed a northern blot using a probe against the 5SrRNA sequence in wild type, $\Delta sap1$, and $\Delta snu66$ strains at both logarithmic and stationary growth phases. We did not observe any defective processing of the 5SrRNA bands could conclude that Sap1 does not play a role in 5SrRNA processing (Figure 3.11C).

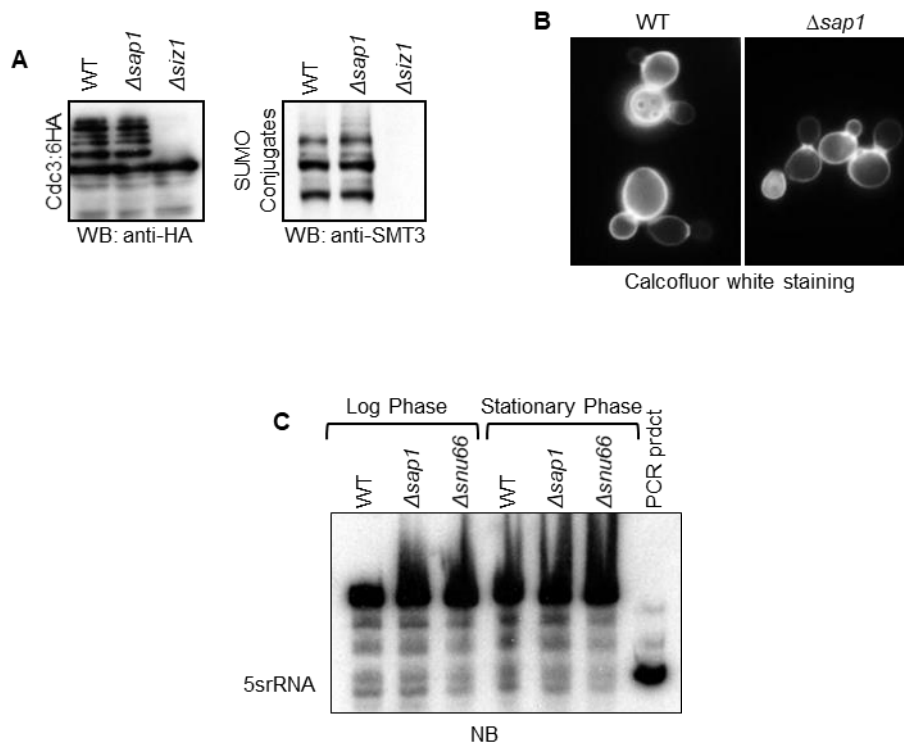


Figure 3.11: Results presented in the figure related to Sap1 function. (A) Level of septin (Cdc3) sumoylation and total sumoylation were monitored by HA and Smt3 western blot, respectively, in indicated strains. Sap1 deletion did not show any defect compared to E3 ligase Siz1 deletion (B) Calcofluor white stained WT, and Sap1 deletion strain did not show any difference in cell/bud size indicating that Sap1 does not have an effect on the cell size determination or differentiation. (C) Processing of 5SrRNA monitored by northern blot in indicated strains in the logarithmic and stationary phases. There was no defect in 5SrRNA processing in Sap1 deletion, Snu66 is a positive control. The PCR product lane marks the size for 5SrRNA signals.

3.3.12 Sap1-Snu66 complex in splicing fidelity

Following a similar line of speculations based on Sap1–Snu66 interaction, we questioned if Sap1 was involved in the regulation of splicing fidelity like Hub1. It has been shown previously that Hub1, which interacts with Snu66 at the N-terminus, is important for alternative splicing and plays a role in relaxing splicing fidelity in *Saccharomyces cerevisiae*⁴⁹. As we knew SNU66 and HUB1 both showed genetic interaction with PRP8 (a core splicing factor belonging to the tri-snRNP complex¹³⁴), we also checked for the synthetic phenotype in the double mutants of *prp8* and $\Delta sap1$. We took two Prp8 mutants (*prp8** and *prp8-101*^{48,135}) and deleted Sap1 in the cells. Interestingly, we observed that deleting Sap1 in

the Prp8 mutants rescued the temperature and cold sensitivity in both the Prp8 mutants (Figure 3.12A). Unlike Snu66 and Hub1, which show a synthetic sickness with these Prp8 mutants, Sap1 appeared to work in an antagonist way, and the deletion of Sap1 gave a growth advantage to the mutants.

This result got us excited, and we checked whether Hub1, which binds Snu66 N-terminally, and Sap1, which binds Snu66 C-terminally, had a complementary function or effect on cell phenotype. If Sap1 balanced/regulated the function of Hub1, an overexpression of Sap1 in Hub1 overexpressing cells would rescue its toxicity, so; we performed a dilution spotting with cells overexpressing both Hub1 and Sap1. However, the overexpressing cells did not show rescue of the Hub1 overexpression sickness rather a higher sickness in formamide containing media (Figure 3.12B), which could be because Hub1 and Sap1 did not function directly opposite to each other, i.e., their downstream targets were different, or they functioned at different stages of splicing.

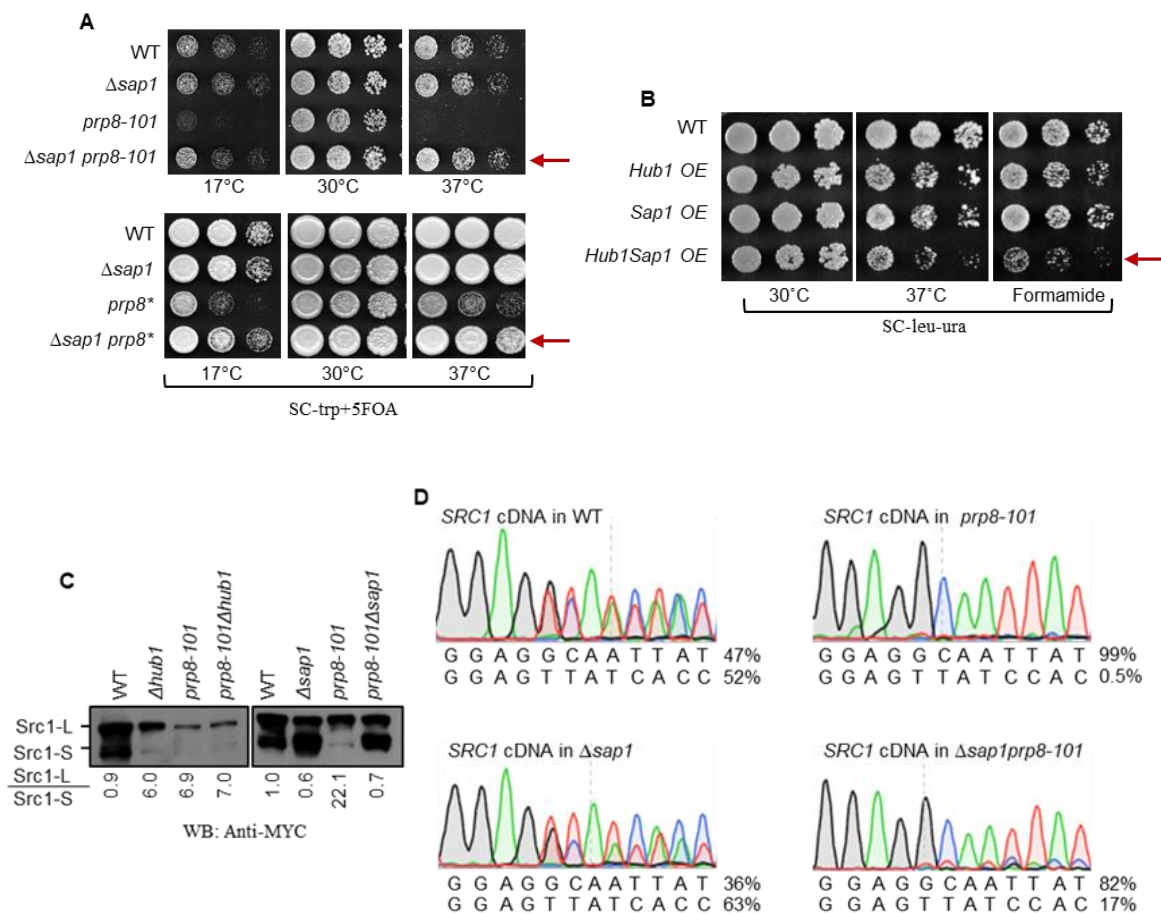
Now, since we observed that Sap1 deletion rescued *prp8-101* dependent temperature sensitivity, we wanted to validate the result further using the Src1 splice site usage in the cell. We transformed the cells with a plasmid containing 3MYC tagged Src1 under the *Gall-10* promoter. We grew cells in lactate + glycerol containing media till OD₆₀₀ 1 and then induced the cells with 2% galactose for half an hour to express Src1 protein. We observed that *prp8-101* single mutant expressed only the longer form of the protein (Src1-L), whereas *prp8-101Δsap1* cells expressed both the forms of the protein (Src1-L and Src1-S) similar to WT cells (Figure 3.12C). This made our hypothesis that Sap1 regulates splicing fidelity stronger, and we found that removal of Sap1 gave Prp8 mutants a growth advantage and also rescued the alternative splice site usage of *SRC1*.

Although we had shown it before at the level of Src1 protein expression, we wanted to extend our result to the RNA level. We isolated RNA from four strains (wild type, single mutants, and double mutant), synthesized cDNA, and sequenced them. We observed a rescue of *SRC1* alternative splicing or splice site usage in the absence of Sap1. We also observed that not only in the double mutant where there is a rescue of splicing but in the Sap1 deletion strain

too, there was a change in the proportion of splice site usage (Figure 3.12D). This further indicated that Sap1 might be involved in enhancing splicing fidelity, but the effect on cell phenotype was observable in a splicing compromised background.

Now to generalise this effect of Sap1 on splicing fidelity, we used the *ACT-CUP1* splicing reporter assay. We showed that while Snu66 interactor Hub1 reduced splicing fidelity in *prp8-101*, Snu66 interactor Sap1 enhanced splicing fidelity in *prp8-101*. 5'ss mutants (GUCUGU and GUAUAU) of the reporter removal of Hub1 increased *prp8-101* sensitivity in the case of the GUAUAU mutant, whereas removal of Sap1 decreased *prp8-101* sensitivity to even the GUCUGU mutant (Figure 3.12E). This was concluded by cell growth in copper-containing media. We also saw that the absence of the general splicing factor Snu66, however, made the cells copper-sensitive in either of the two 5'ss mutants, and recognition of non-canonical splice sites was defective in $\Delta hub1$ and $\Delta snu66$.

62



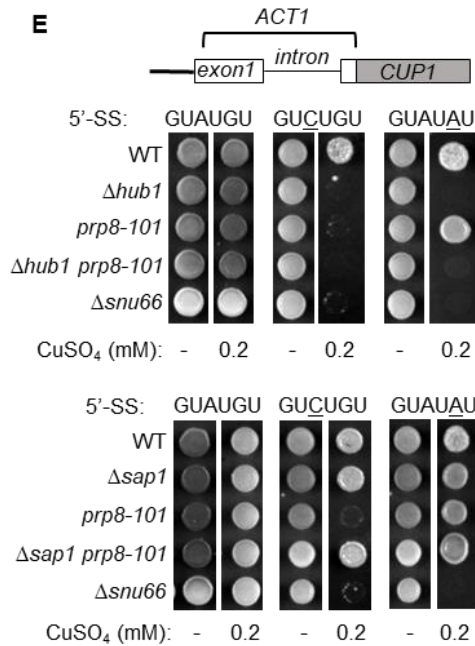


Figure 3.12: Role of Sap1-Snu66 complex in splicing fidelity. (A) Genetic interaction of Sap1 and Prp8 mutants. Deletion of Sap1 rescued *prp8-101* and *prp8** cold and temperature sensitivity. (B) Overexpression of Sap1 did not balance the sickness due to Hub1 overexpression; instead, it increased the sensitivity of cells to higher temperatures and formamide. (C) Alternative splicing of *SRC1* monitor by MYC western blot. The absence of Sap1 rescued the alternative splicing defect of *SRC1* in the *prp8-101* mutant. (D) The electropherogram of cDNA from wild type (WT) shows mixed peaks after *SRC1* exon-exon junction. By contrast, cDNA from the *prp8-101* allele shows sequencing peaks exclusively for Src1-L isoform, rescued in Δthe *sap1prp8-101* double mutant. Compared to WT, Sap1 deletion showed an increase in usage of *SRC1* alternative 5' ss too (E) *ACT1-CUP1* reporter assay on CuSO₄ plates (0.2mM) monitoring 5' ss usage defects in indicated strains (Data in E obtained with Balashankar). Unlike *hub1Δ*, which is defective in using both non-canonical 5' ss, *prp8-101* is defective only in using GUCUGU. But this defect of *prp8-101* was rescued by the absence of Sap1 and amplified by the absence of Hub1.

To validate these results, we had to do complementation assays, such that when we transformed Sap1 back in *prp8-101* mutants, they should show the temperature-sensitive phenotype again. Since we also wanted to find the functional domain to Sap1, we performed a plasmid-based complementation experiment. We took WT and *prp8-101* cells and transformed them with Sap1 wild type and mutant (*I236A*, *ΔSIM*, and *K651A*) plasmids. But the cells grew equally well even after transforming back Sap1. So, we made chromosomal strains with WT, and mutant Sap1 replaced in *prp8-101* mutants. But as evident from the

figure, even with the chromosomal copies of Sap1, the phenotype of *prp8-101* did not return (Figure 3.13). Hence, we isolated the Prp8 plasmid by shuttle prep and sequenced the *prp8-101* mutation region. Surprisingly the *prp8-101* mutation was not detected; rather, it was a WT sequence. At last, we concluded that Sap1 might not be involved in pre-mRNA splicing. On the basis of the sequencing result, however, we hypothesised that the Sap1-Snu66 complex might be required regulation of homologous recombination.

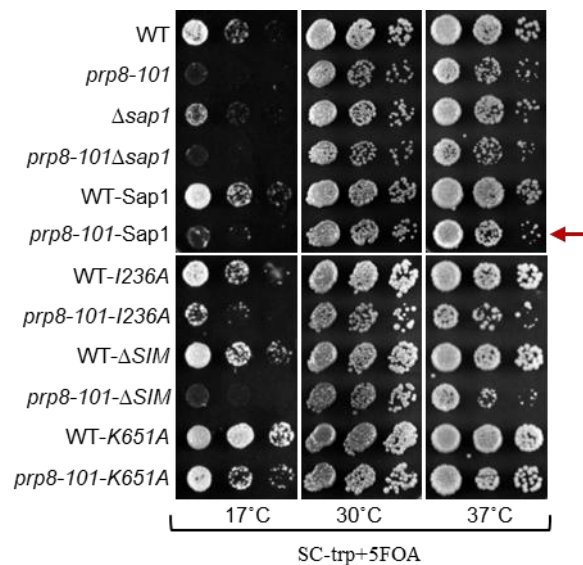


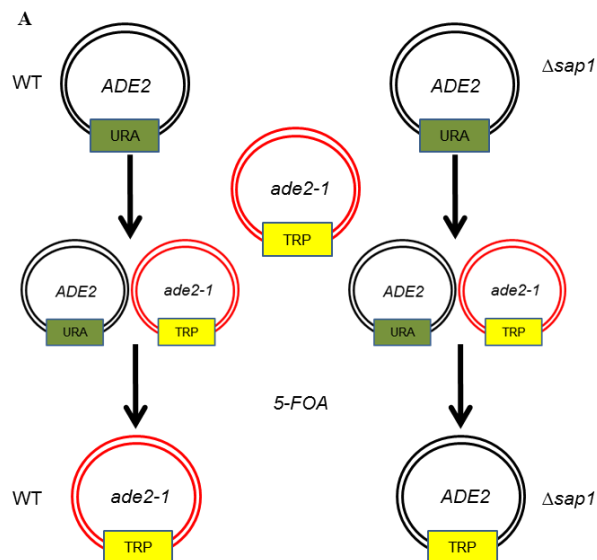
Figure 3.13: Complementation of $\Delta sap1$ by different variants of Sap1. Chromosomal variants of WT Sap1 and mutants (*I236A*, ΔSIM , and *K651A*) with *prp8-101* mutant did not revert to temperature/cold sensitivity consistently. Although the WT Sap1 variant shows sensitivity at lower temperature, it grew well at higher temperature. The SIM mutants show similar inconsistency and the *K651A* ATPase mutant showed growth at all temperatures.

3.3.13 Sap1-Snu66 in homologous recombination

After sequencing the *prp8-101* plasmid, we found that it had the WT sequence instead of the mutation and speculated whether Sap1 might be involved in the homologous recombination pathway. To check it, we designed an *ADE2* based reporter assay. We cloned *ADE2* and *ade2-1* gene in vectors with *URA3* and *TRP1* selection markers, respectively. First, we transformed WT and $\Delta sap1$ with the *ADE2-URA3* plasmid and, subsequently, the *ade2-1-TRP1* plasmid. The cells had both the wild type and mutant copy of Ade2, and we put them

on 5-FOA to shuffle out the *URA3* plasmid (Figure 3.14A). Now, if Sap1 regulated homologous recombination, the *ade2-1* might change to a wild type copy, which could be observed and quantified based on the number of white and pink colonies that appeared on shuffling out the WT-*URA3* plasmid. We observed that the WT (W303) strain hardly gave any white colonies after shuffling out the *ura3* plasmid, but $\Delta sap1$ had a mixture of white and pink colonies. Quantification showed a recombination efficiency of 60% for $\Delta sap1$ (Figure 3.14B). To verify the reporter's credibility, we checked the assay using already reported regulators of homologous recombination and found that they all showed the presence of pink and white mixed colonies but with different recombination efficiencies suggesting that our reporter assay was functional (Figure 3.14C).

At last, we checked the recombination of the *ADE2* reporter in *Snu66* mutants, including HIND and *Snu66-CM* (*Sap1* binding mutant). We observed that the different mutants showed different efficiency of recombination. The *RRAA* mutant had the highest amount, followed by *D533A* and $\Delta snu66-CM$. The *K546A* mutant showed negligible efficiency of recombination (Figure 3.14D). These results indicated that *Snu66* was not only critical for RNA splicing, but it might also regulate homologous recombination by binding to the AAA-ATPase *Sap1*.



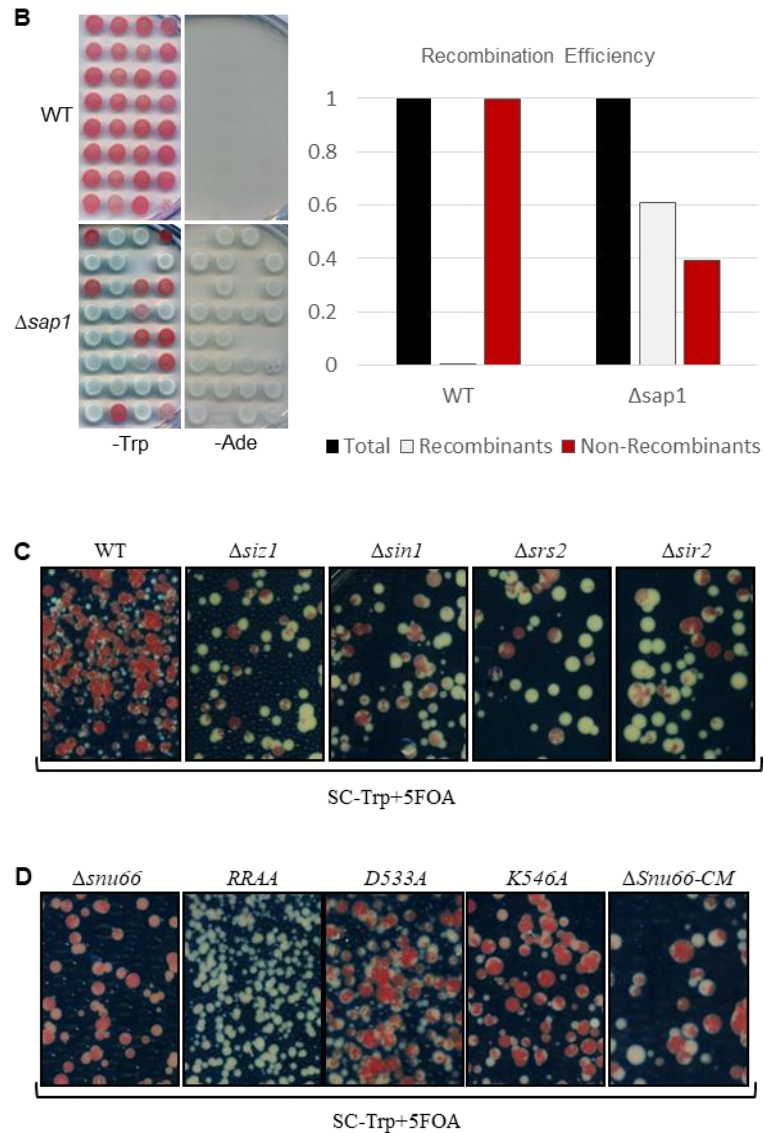


Figure 3.13 Sap1-Snu66 complex in homologous recombination (HR). (A) Schematic flowchart of the *ADE2* reporter experiment. (B) Recombination of *ADE2* containing plasmids in WT and $\Delta sap1$ represented by pink and white colonies. Pink colonies are Ade2 mutant, and white colonies are Ade2 wild type. By contrast to 2% efficiency in WT, the quantification shows a 60% recombination efficiency for $\Delta sap1$ (C). The previously known regulator of HR verified the working of Ade2 reporter and showed varying levels of HR efficiency. (D) Recombination efficiency in different mutants of Snu66. The Deletion of Snu66 and *K546A* mutant show almost no recombination. By contrast, *D533A* and $\Delta Snu66-CM$ show a moderate amount of recombination, and the *RRA4* mutant shows the highest recombination efficiency.

3.4 Conclusion and Discussion

The general splicing factor Snu66 interacts with a SUMO-binding AAA-ATPase Sap1 via its conserved and essential C-terminal motif (Snu66-CM see Chapter 2). Two protein isoforms of Sap1 full-length 100kDa protein (Sap1) and the shorter form 50kDa protein (Sap1_C) were expressed from alternatively transcribed mRNAs in a carbon source-dependent manner. We, for the first time, report the presence of the shorter isoform, which expressed only after the diauxic shift when grown in glucose-containing media. However, in non-fermentable carbon sources (conditions that mimic diauxic shift), Sap1_C was expressed constitutively. The two proteins are expressed from two mRNA transcripts by alternate transcription, a rare mechanism in yeast. Such mechanisms are more prevalent in mammalian (human) systems where isoforms thus generated are often tissue-specific. Genes under such regulation have been shown to have a crucial role in the development and cell differentiation. This is one example of the conservation of the alternate transcription pathway from lower to higher eukaryote and its significance in generating proteome diversity.

One of the modes of alternate transcription is the presence of alternate promoters. Alternate promoters can generate isoforms with different start sites like in the case for Sap1. What is more interesting is that Sap1_C had an alternate 'internal' promoter which lay within the ORF of the full-length protein. Why the cells needed such an unusual and interesting mode of expression for Sap1 is yet to be understood. The expression of Sap1_C is regulated by the conserved transcriptional co-repressor Tup1, which usually functions with a partner repressor protein. But, in the case of Sap1_C, Tup1 bound the internal promoter without a partner and repressed it. Here, Tup1's activity depended only on the status of its own sumoylation. We report that the sumoylation of Tup1, which is important for its activity, depends on the stage of cell growth. We showed that level of Tup1's sumoylation reduces on the diauxic shift, which results in the expression of Sap1_C. This sumoylation based repressor activity of Tup1 might be critical for alternate promoter based transcription expressing alternating protein isoforms.

Interestingly, the Sap1 isoforms localised very distinctly from one another; the full-length protein localized at the bud neck, whereas the shorter form diffused throughout the cytoplasm and nucleus. With such distinct localisation, the two isoforms might have a different function. The constitutively expressed full-length protein, which has an unstructured N terminus, a SIM domain, and the AAA-ATPase domain at C-terminus, might be needed during the cell division/proliferation phase. The change in localization of the full-length protein in septin sumoylation inhibited cells also indicated a role during cell cycle or budding in cells. Whereas the shorter form with only the AAA-ATPase C terminal domain expressed after diauxic shift might be needed by cells to adapt to stationary phase changes. Its diffused localisation and a strong affinity with Snu66 indicated a probable nuclear role of the isoform.

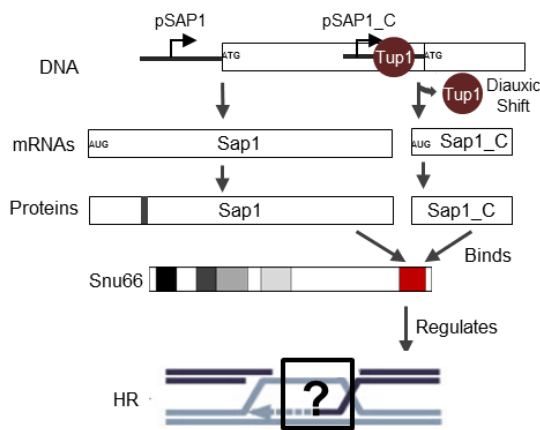


Figure 3.14: The Sap1-Snu66 complex.

Mechanism of Sap1 and Sap1_C. The isoforms interact to Snu66-CM and might regulate HR. The mechanism of their function remains to be explored.

In context to Snu66 interaction, although we could not find the role of the complex or Sap1 in RNA splicing, we confirmed the validity of the interaction by *in.vitro* studies. We observed that Snu66 homolog in *S. pombe* and humans also interacted with Sap1, which indicated at the conservation of the interaction. However, we did not find a confirmed homolog of Sap1 in other organisms yet. Its functional role with Snu66 could be performed by a conserved AAA-ATPase. It is also possible that due to the absence of budding in the higher organism, the function of full-length Sap1 is not required, and it evolved to be just the shorter isoform. Based on the preliminary *ADE2* report assay, we propose that the Sap1-Snu66 complex might have a novel and intriguing role in homologous recombination. Since the shorter form expressed after the diauxic shift, we speculated that the Sap1-Snu66 complex might be required to maintain the level rDNA circles (formed by homologous recombination of tandemly repeated sequence) in the aging cells. However, this remains unclear and needs to be explored for further understanding.

Chapter 4

SRC1 Alternative Splicing Factors and Mechanism

4.1 Introduction

Alternative splicing of pre-mRNAs produces more than one protein-coding mRNAs. This is achieved by recognition of cis-acting splicing signals in pre-mRNAs by trans-acting factors of the spliceosome¹³⁶. The highly diverse splicing signals in metazoans, including 5' splice site (ss), 3' splice site, branch site, splicing enhancers, and silencers, bring about distinct mechanisms of alternative splicing, including exon skipping, intron-retention, and competing splice sites^{137,138}. Spliceosomes complete different types of alternative splicing with the help of distinct trans-acting factors¹³⁹. Fewer events of alternative splicing have been reported in fungi, possibly because of smaller numbers of intron-containing genes¹⁴⁰, but a larger number of events are likely to be present^{141,142}. Nevertheless, alternative splicing is important for virulence and stress survival in fungi¹⁴³. While intron-retention is the common form of alternative splicing in yeast, *S. cerevisiae SRC1* undergoes alternative splicing using two competing 5'ss which produces two proteins.

SRC1 pre-mRNA has one intron with two overlapping 5'ss //GCAA//GUGAGU (bent lines show exon-1/intron boundaries, the upstream 5'ss is underlined). Splicing using the downstream 5'ss GUGAGU is constitutive and generates Src1-L encoding transcript while splicing using the upstream 5'ss GCAAGU is alternative and generates Src1-S encoding transcript¹⁴⁴. The transcripts contain complete exons, but the alternatively spliced transcript acquires an in-frame stop codon, thereby translating into a shorter protein. The two proteins have common N-termini but differ in their C-termini and have different topologies in the inner nuclear membrane. The longer Src1-L is a double pass membrane protein, and the

shorter Src1-S is a single-pass membrane protein. These proteins control the expression of sub-telomeric genes¹⁴⁴.

The two 5'ss in *SRC1* intron are non-canonical and weak (GUAUGU/GUAAGU are canonical 5'ss in yeast) and compete for the spliceosome. This arrangement of 5' splice sites is essential for *SRC1* alternative splicing. Strengthening any of the two 5'ss abolished the competition and led to its preferential usage by the spliceosome. Canonical 5'ss also abolished usage of the other 5'ss and led to a loss of alternative splicing^{48,145}. Splicing using these 5'ss requires the ubiquitin-like protein Hub1 and its non-covalent associations with the general splicing factor Snu66 and the RNA helicase Prp5. *SRC1* alternative splicing thereby also requires Hub1 complexes with Snu66 and Prp5⁴⁹.

Through its Asp22 surface, Hub1 binds conserved Arginine in the Hub1 interaction domain (HIND) of Snu66 (SART1 in mammals), and through its His63 surface, Hub1 binds and activates the helicase activity of Prp5. As a result, yeast strains with *hub1* knockout, or *hub1(D22A)* mutation that abolished its interactions with Snu66, or *hub1(H63L)* mutation that abolished its interaction with Prp5, were normal in *SRC1* constitutive splicing but were defective in alternative splicing. Whereas the general splicing factor Snu66 was required for splicing from both 5'ss, Hub1 binding defective *snu66-HIND* mutants showed defects in *SRC1* alternative splicing. On the contrary, higher levels of Hub1 did not lead to the dominant usage of alternative 5'ss for producing Src1-S protein⁴⁸. Instead, they made the spliceosome error-prone allowing usage of suboptimal and cryptic 5'ss⁴⁹. Nevertheless, Hub1 activity is regulated by a negative feedback loop by inducing splicing from a cryptic 5'ss in *PRP5* and decreasing its protein level^{49,146,147}.

The genetic approach has been the key to studying *SRC1* alternative splicing. In this study using yeast genetics, we have identified the roles of additional factors in alternative splicing. By tethering *hub1(D22A)* to a subset of spliceosomal core proteins in *hub1* knockout strain, we identified potential roles of spliceosomal complex B proteins Prp6 and Prp3, besides the

previously reported proteins Prp38 and Prp8. The role of Prp8 was elucidated following the identification of the *prp8-101* allele, specifically defective in *SRC1* alternative splicing. We further identified the involvement of RES complex subunits by screening *S. cerevisiae* haploid deletion strains using LacZ reporter fusions of *SRC1* intron. The collective list of *SRC1* alternative splicing factors indicates manifold spliceosomal controls during alternative splicing.

4.2 Objective

***SRC1* alternative splicing factors in *S. cerevisiae*:** To screen, identify, and study splicing factors that promote alternative splicing of *SRC1* in *S. cerevisiae*. We also studied the mechanism of *SRC1* alternative splicing via the two overlapping 5' ss.

4.3 Results

4.3.1 Specific spliceosomal proteins promote *SRC1* alternative splicing

SRC1 alternative splicing is experimentally monitored by detecting the protein's two isoforms by N-terminal epitope tags or by sequencing of cDNAs arising from the two mRNAs. Further, genetic interactions, biochemical and *in vitro* splicing assays have revealed roles of Hub1, Snu66, and Prp5 in *SRC1* alternative splicing. Also, roles of spliceosomal complex B proteins Snu66, Prp38, and Prp8 was revealed by artificially increasing their proximity to Hub1, by creating linear fusions of splicing factors with *hub1(D22A)* and testing restoration of *SRC1* alternative defects in a *hub1*-knockout strain (Figure 4.1). In its free form, this HIND-binding-deficient mutant showed defective *SRC1* alternative splicing but could restore the defect when fused to the N- or C-termini of Snu66, or the C-termini of Prp38 or Prp8. The chimeras worked likely by bypassing the need for Hub1 recruitment and/or incorporation to the complex of its action, thereby indicating that Hub1 worked in proximity to Snu66, Prp38, and Prp8 in *SRC1* alternative splicing^{48,49}.

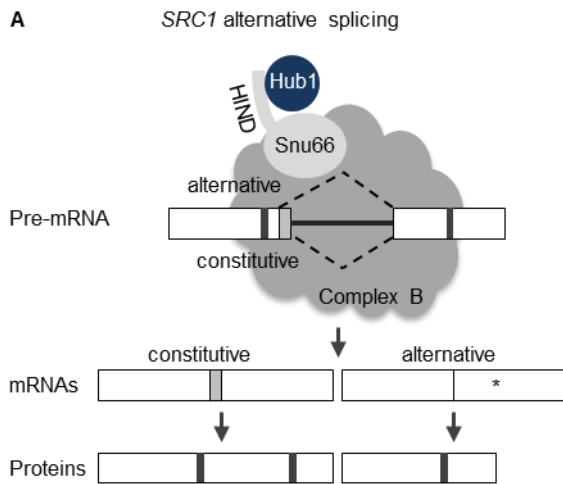


Figure 4.1: Mechanism of *SRC1* alternative splicing from⁴⁸. Splicing using the alternative 5' ss removes four extra nucleotides from exon-1, causing a translational frame-shift, thereby producing the shorter Src1-S protein.

To identify more splicing factors involved in *SRC1* alternative splicing, we tested for restoration of the defect in *hub1Δ* strain by probing with *hub1* (*D22A*) fusion to a set of spliceosomal proteins (Figure 4.2A). We chromosomally tagged *SRC1* with TAP epitope at N-terminus for monitoring its two protein isoforms by anti-TAP western blot assays. Yeast strains were made with C-terminal fusions of *hub1*(*D22A*) to selected splicing factors of U1, U2, and tri- snRNP complexes in *TAP-SRC1 hub1Δ* backgrounds. Anti-TAP western blots showed that *SRC1* alternative splicing was restored in *hub1Δ* by *hub1*(*D22A*) fusions to Prp3 and Prp6, besides the previously reported proteins Snu66, Prp8, and Prp38. The fusions to other proteins of U1-, U2-, or tri- snRNPs did not restore alternative splicing; this could be due to the unsuitability of the fusion-probing approach on these factors or their Hub1-independent roles in alternative splicing (see later). These results suggested that Hub1 might act in proximity to a specific set of tri-snRNP factors for promoting alternative splicing of *SRC1* (Figure 4.2B)

74

A

Yeast strains	<i>SRC1</i> pre-mRNA splicing	
	Constitutive	Alternative
Wild type Hub1	✓	✓
$\Delta hub1$	✓	-
$\Delta hub1 + hub1(D22A)$	✓	-
$\Delta hub1 + Snu66/Prp38/Prp8-hub1(D22A)$	✓	✓
$\Delta hub1 + Splicing\ factors-hub1(D22A)$?	?

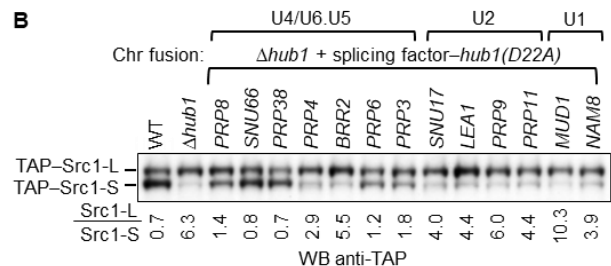


Figure 4.2: Proximity probing of splicing factors with *hub1(D22A)* to monitor their role in *SRC1* alternative splicing. (A) The HIND-binding-deficient *hub1(D22A)* defective in *SRC1* alternative splicing restores the alternative splicing defect in *hub1Δ* when fused linearly to Snu66, Prp38, and Prp8⁴⁸. This strategy is used to probe similar splicing factors from U1, U2, and tri-snRNP complexes in (B). A linear fusion to Prp6 and Prp3 also restores the defect as seen by the gain of the alternative Src1-S protein in anti-TAP western blot assays. Src1-L/Src1-S signal ratio for each strain is quantified below the blot.

In contrast to *hub1* knockout, Hub1 overexpression did not change the *SRC1* alternative splicing pattern or did not lead to preferential usage of the alternative 5'ss⁴⁸. Also, stress treatments that are reported to induce Hub1 expression¹⁴⁷ did not alter the alternative splicing pattern (Figure 4.3A, B). This lacking effect of increased Hub1 level was not due to its restricted incorporation in the spliceosome, as enhancing spliceosomal Hub1 by fusing *hub1(D22A)* to both Snu66 and Prp38 concurrently did not alter *SRC1* alternative splicing pattern. Thus, Hub1 activity on the alternative 5'ss does not dominate over spliceosomal activity on the constitutive 5'ss.

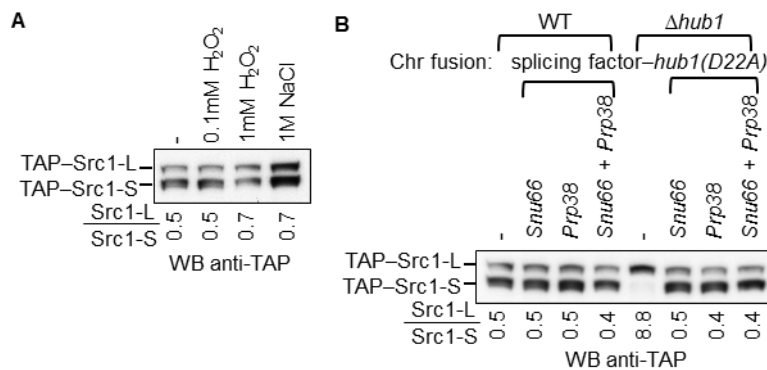


Figure 4.3: Excess of Hub1 does not alter *SRC1* alternative splicing pattern. (A) Stress treatments known to induce Hub1 expression does not alter the alternative splicing pattern. Src1-L/Src1-S signal ratio for each treatment is quantified below the blot. (B) Excess of Hub1 in spliceosome by linear fusions to Snu66, Prp38, or both does not alter the alternative splicing pattern. Src1-L/Src1-S signal ratio for each strain is quantified below the blot.

4.3.2 *SRC1* alternative splicing is defective in *prp8-101* allele

From the outcome of *hub1(D22A)* fusion-probing, we presumed that *SRC1* alternative splicing defects might exist in specific alleles/mutants of essential spliceosomal core factors. We tested this presumption for Prp8 by screening from a large number of previously reported Prp8 alleles^{135,148}. We TAP-tagged *SRC1* in yJU75 yeast genetic background (the strain suitable for studying *prp8* alleles¹⁴⁹ and monitored *SRC1* alternative splicing in a different class of Prp8 mutants by anti-TAP western blots. Strikingly, the alternatively spliced Src1-S protein was completely missing in the *prp8-101* (E1960K) allele, but the constitutively spliced Src1-L protein remained normal. Other *prp8* alleles were normal in alternative splicing, and the ratio of constitutively spliced Src1-L and Src1-S remained similar to the wild type control (Figure 4.4A). We validated *prp8-101*-specific alternative splicing defects by cDNA sequencing of *SRC1* transcripts. Electropherograms showed peaks for both transcripts in wild type yeast, but peaks for the alternative transcript was almost completely missing in *prp8-101*. These results confirmed the role of a specific Prp8 surface in alternative splicing (Figure 4.4B).

Hub1 genetically interacted with two Prp8 alleles: *prp8-101* and *prp8** (P1384L), but unlike *hub1Δ* and *prp8-101*, the *prp8** allele was normal in alternative splicing. Splicing assays using *ACT1-CUP1* reporters⁹⁶ showed that the three mutants, *hub1Δ*, *prp8**, and *prp8-101*, were defective in using 5'ss GUCUGU, but only *hub1Δ* and *prp8** were defective in using GUAUAU, whereas *prp8-101* used this 5'ss similar to wild type strain. Thus, with respect to 5'ss usage and alternative splicing, *prp8-101* and *prp8** surfaces likely perform non-overlapping functions.

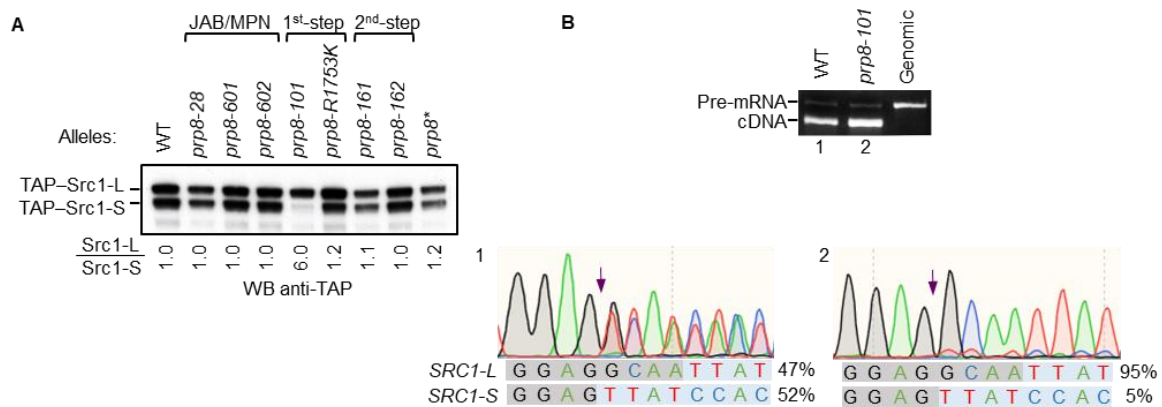


Figure 4.4: *SRC1* alternative splicing requires a functional *Prp8-101* surface. (A) *SRC1* alternative splicing was monitored in different alleles of *Prp8*. Quantitation below the blot shows normal alternative splicing in all alleles except for *prp8-101*. (B) RT-PCR assay doesn't show obvious defects in *SRC1* splicing, but the alternative splicing defects become obvious after sequencing the cDNAs in the electropherogram from wildtype (WT) shows mixed peaks after *SRC1* exon-exon junction (marked with an arrow). By contrast, cDNA from the *prp8-101* allele shows sequencing peaks exclusively for Src1-L isoform.

4.3.3 The RES complex promotes *SRC1* alternative splicing

We searched for other factors participating in *SRC1* alternative splicing from *S. cerevisiae* haploid deletion library of genes not essential for viability by expressing β -galactosidase reporters similar to RP51-LacZ¹⁵⁰ containing *SRC1* intron within a portion of its exons fused to LacZ. Two reporter chimeras monitored splicing from alternative and constitutive 5'ss, when Src1 and LacZ came in frame only after splicing (Figure 4.5A). The screen was done following synthetic genetic array (SGA) screening protocol¹⁵¹. The alternative splicing specific reporter was expressed in the bait strain, which was mated with the yeast deletion library, and following sporulation of the diploids, haploid deletion strains expressing the reporter were obtained. X-gal overlay on solid media plates was used to estimate LacZ activity, and duplicate spots with altered blue colour were considered putative positive. We analysed the splicing of the two reporters in putative positive mutants by measuring β -galactosidase activities by X-gal overlay assay on solid media (Figure 4.5B) and a more sensitive ONPG assay performed with cells grown and harvested from liquid cultures (Figure 4.5C).

Defective usage of the alternative 5' splice sites was observed in deletion mutants of the RES complex subunits: Snu17, Bud13, Pml1, and Urn1.

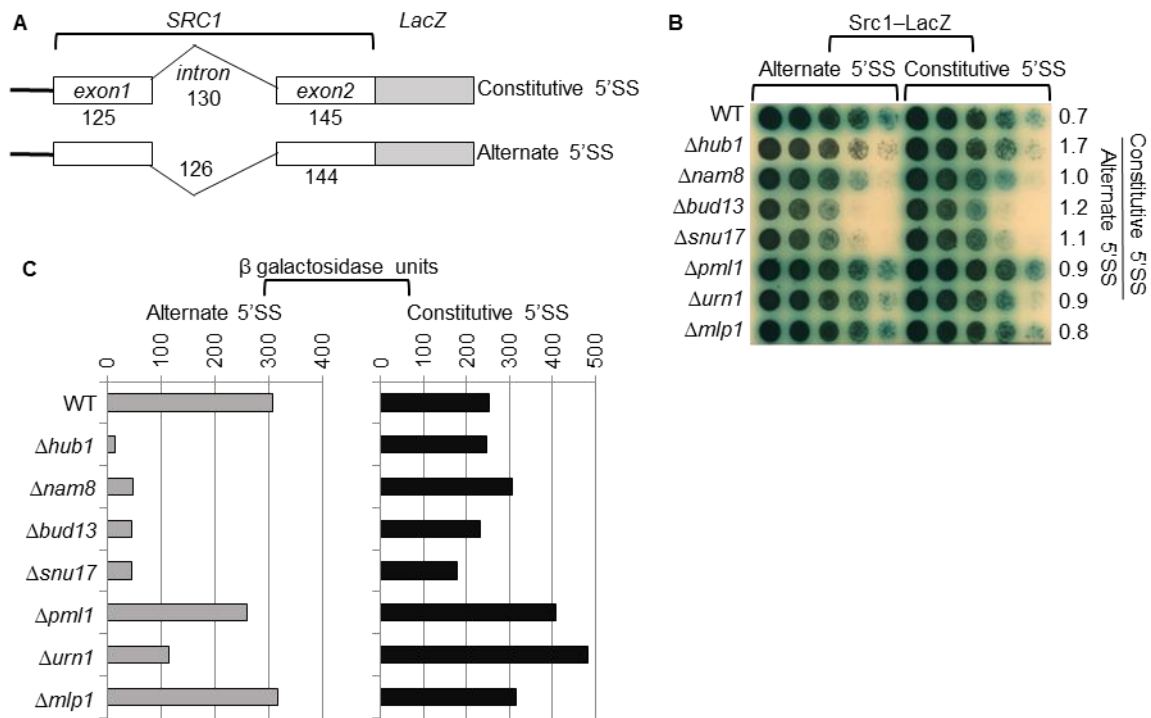


Figure 4.5: Screening for factors involved in *SRC1* alternative splicing. (A) The design of *SRC1-LacZ* reporters is such that the two transcript isoforms would generate in-frame *LacZ* only after the excision of the intron. (B) X-gal overlay assay on solid agar plates shows activities of the two reporters in indicated yeast strains. The ratio of blue colours obtained for the two reporters is shown on the right. (C) ONPG assay performed from cultures grown in liquid media essentially recapitulates the results in (B). This assay, however, was more sensitive and quantitative than X-gal overlay assay in (B).

We validated the roles of the proteins identified from the screen, including of the RES complex subunits, by cDNA sequencing of *SRC1* transcripts (Figure 4.6A, B), and western blot assays of Src1 proteins in respective deletion mutants chromosomally TAP-tagged at *SRC1* N-terminus (Figure 4.6C, D). Similar to the reporter assays, the Src1 protein pattern was also altered in the RES mutants and *ecm2A* (facilitates the formation of U2/U6 snRNA helix) strains.

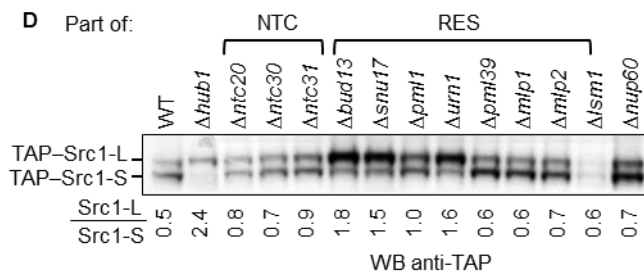
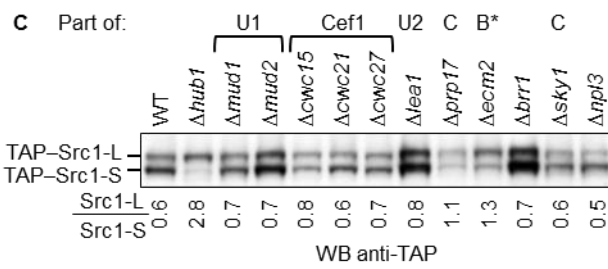
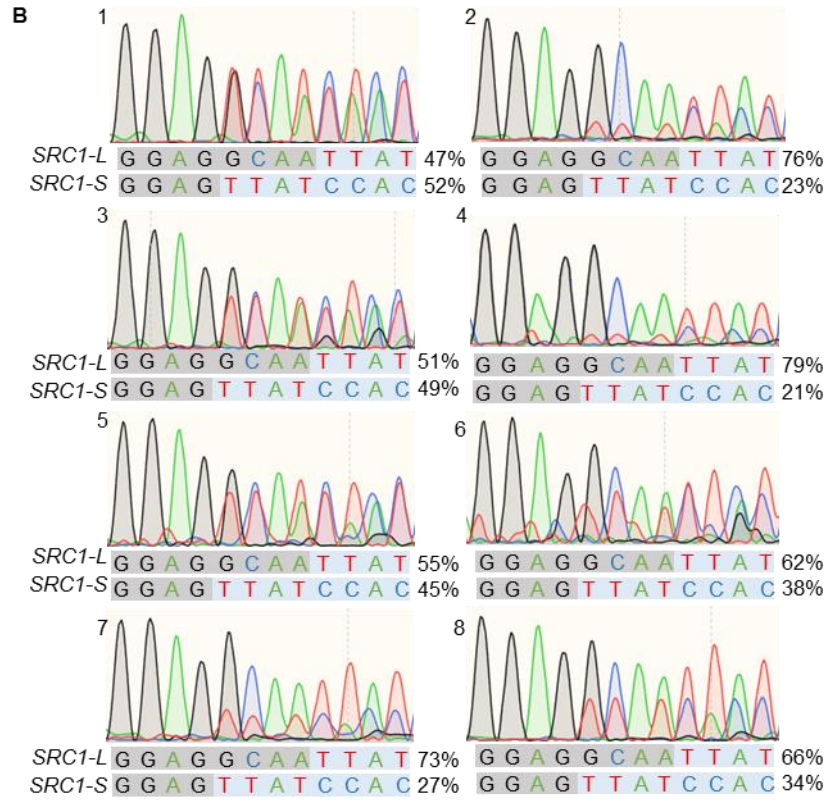
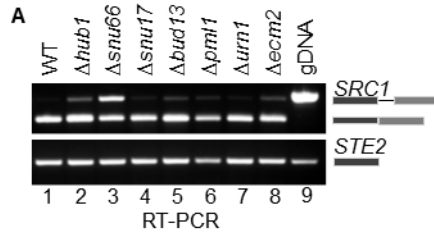


Figure 4.7: Mutants defective in mRNA export do not show *SRC1* alternative splicing defects.

(A) Spot assays monitoring the growth of indicated yeast strains show negative genetic interaction between *hub1Δ* and THO/TREX complex mutants *sem1Δ*, *mft1Δ*, and *thp2Δ*. (B) Anti-TAP western blot monitoring Src1 protein isoforms in indicated yeast strains does not show obvious defects in its alternative splicing. Src1-L/Src1-S signal ratio for each strain is quantified below the blot.

We next tested whether the above proteins showed phenotypes overlapping with Hub1 by monitoring (i) general splicing defects for endogenous *ACT1* in above mutants by RT-PCR assays (Figure 4.8A, C), and (ii) defects in the usage of non-canonical 5'ss by plasmid-borne *act1* 5'ss mutant GUCUGU (Figure 4.8B, D) (*hub1Δ* was defective in the usage of non-canonical 5'ss but did not show general splicing defects). Not only the RES complex mutants but also *ecm2Δ* showed defects distinct from *hub1Δ* in general splicing and 5'ss usage. These results suggested that the newly identified proteins work in *SRC1* alternative splicing by mechanisms independent of Hub1 (Table 4.1).

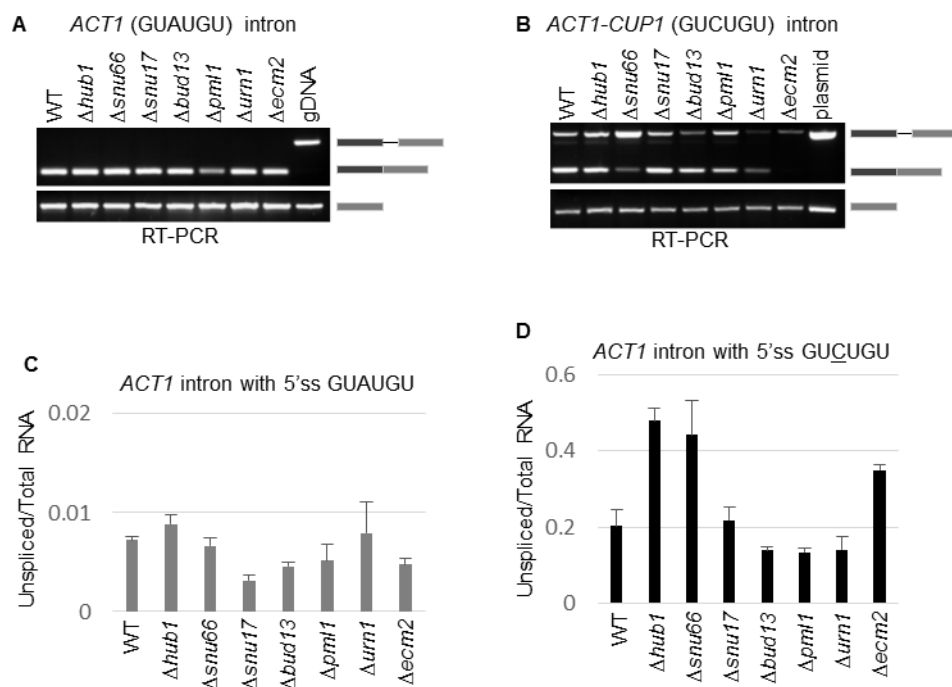


Figure 4.8: Splicing defects in RES complex mutants is distinct from *hub1Δ*. Splicing efficiency of *ACT1* pre-mRNA (A) and its 5'ss mutant GUCUGU (B) monitored by real-time PCR assay (C, D) are shown as the ratio of unspliced to total transcripts. RES mutants did not show splicing defects similar to *hub1Δ*.

Table 4.1: *SRC1* alternative splicing factors and proposed mechanisms

Protein/Complex	Human homologs	Known mechanism pre-mRNA splicing relevant to the proposed role in <i>SRC1</i> alternative splicing
Hub1-Prp5	UBL5-DDX46	Hub1-stimulated helicase/ATPase activity of Prp5 promotes usage of non-canonical and cryptic 5'ss ⁴⁹ ; <i>the complex may promote usage of non-canonical SRC1 5'ss</i>
Hub1-Snu66	UBL5-SART1	Hub1 binding to Snu66-HIND promotes usage of non-canonical 5'ss ⁴⁸ ; <i>Snu66 functioning in Hub1 proximity may slow down spliceosomes on SRC1 5'ss, Hub1 may independently promote usage of non-canonical SRC1 5'ss by stimulating Prp5 helicase</i>
Prp38	UBL5-PRPF38A	Prp38 has HIND in certain organisms ⁴⁸ , found in close proximity to Snu66 in the spliceosome ²³ ; <i>functions in Hub1 proximity may slow down spliceosomes on SRC1 5'ss</i>
Prp8 allele <i>prp8-101</i> (E1960K)	PRPF8	Prp8 allele, which quickens first step catalysis ^{135,152,153} , E1960 lies in the RNase H domain responsible for splicing catalysis ^{154,155} ; <i>prp8-101 is defective in splicing of non-canonical 5'ss GUCUGU (this study), Prp8 functions in Hub1 proximity, may slow down spliceosomes on SRC1 5'ss, may help spliceosome attain a conformation accommodating both SRC1 5'ss</i>
Prp3, Prp6	PRPF3, PRPF6	U4/U6.U5 tri-snRNP components, in complex with Snu66 and Prp3; <i>function in Hub1 proximity, may help spliceosome attain a conformation accommodating SRC1 5'ss</i>
RES complex: Snu17, Pml1, Bud13, Urn1	RBMX2, SNIP1, BUD13, TCERG1	Nuclear retention and splicing of selected pre-mRNAs, important in the conversion of pre-catalytic B complex to B ^{act} complex by controlling Prp2 incorporation ¹⁶⁰⁻¹⁶³ ; <i>may not function in Hub1 proximity; may slow down spliceosomes on SRC1 5'ss</i>
Ecm2/Slt11	RBM22	Activates spliceosome by facilitating U2/U6 helix II formation ^{164,165} ; <i>may help spliceosome attain a conformation accommodating SRC1 5'ss</i>

4.3.4 Mechanism of *SRC1* alternative splicing

To understand the mechanism of *SRC1* splice site selection, we made different mutants that are altered in their U1, U5, and U6 binding efficiency and checked for Src1 protein expression (summarised in Table 4.2). Sample **A** represents the *SRC1* splice site in WT case scenario and its binding to U1, U5, and U6 snRNAs. We observed that changing the binding efficiency of the alternative or constitutive splice site to U1, U5, and U6 affected the expression of each of the isoforms. Strengthening the binding efficiency of one of the splice

sites to the U5 or U6 snRNAs increased the preference for the use of that splice site. For example, in mutant **B** (GCAAGU-GUAAGU) and **C** (GCAAGU-GCAUGU), increasing the binding efficiency of alternative 5'ss to U6 resulted in the expression of only Src1-S and abolished the expression of the constitutive Src1-L. Also, in mutant **D** (GAGGCAAGU-GAUGAAAGU) and **F** (GCAAGU-GAAAGU), increasing the binding efficiency of constitutive 5'ss to U5 resulted in the expression of only constitutive Src1-L. However, there was no significant effect of change in binding efficiency to U1 snRNA such as in mutant **E** (GAGGCAAGU-GAAGCAAGU).

Along with these *cis*-acting elements, the *trans*-acting factors also regulated the efficient alternative splicing of *SRC1*. The different mutants behave and respond to the different mutation of the 5'ss distinctly. Considering mutant **H** (GCAAGU-GUCUGU), we showed that increasing the binding efficiency of alternative 5'ss to U6 by this change does not rescue the defects in *hub1* and *ecm2* deletions whereas in WT cells it results in expression of Src1 -S. Similarly in mutant **G** (GUGAGU-GUCUGU), we increased the efficiency of U6 binding of constitutive 5'ss, which leads to expression of only Src1-L in wild-type cells, but in an intron retained protein Src1-I in *hub1* and *ecm2* deletion. We analysed other *SRC1* alternative splicing factors (Snu17, Urn1, etc.) and showed different deletions behaved and rescued the effect of different 5'ss mutants in different ways and to different levels.

This suggest that the two 5'ss of *SRC1* are maintained at a thermodynamic equivalence in the cell. The stronger U5 pairing and weak U6 pairing of the alternative ss and the weak U5 pairing and stronger U6 pairing of the constitutive ss helps to maintain the balance. Whenever there is a change in this binding efficiency balance the expression of Src1 protein changes. If you make the binding of any of the ss to U5 and U6 stronger it prefers that splice site and if you make the binding weaker than the spliceosome favours the other splice site. And these alternative splicing regulators help in maintaining of achieving this thermodynamic balance for these overlapping competing 5'ss of *SRC1*.

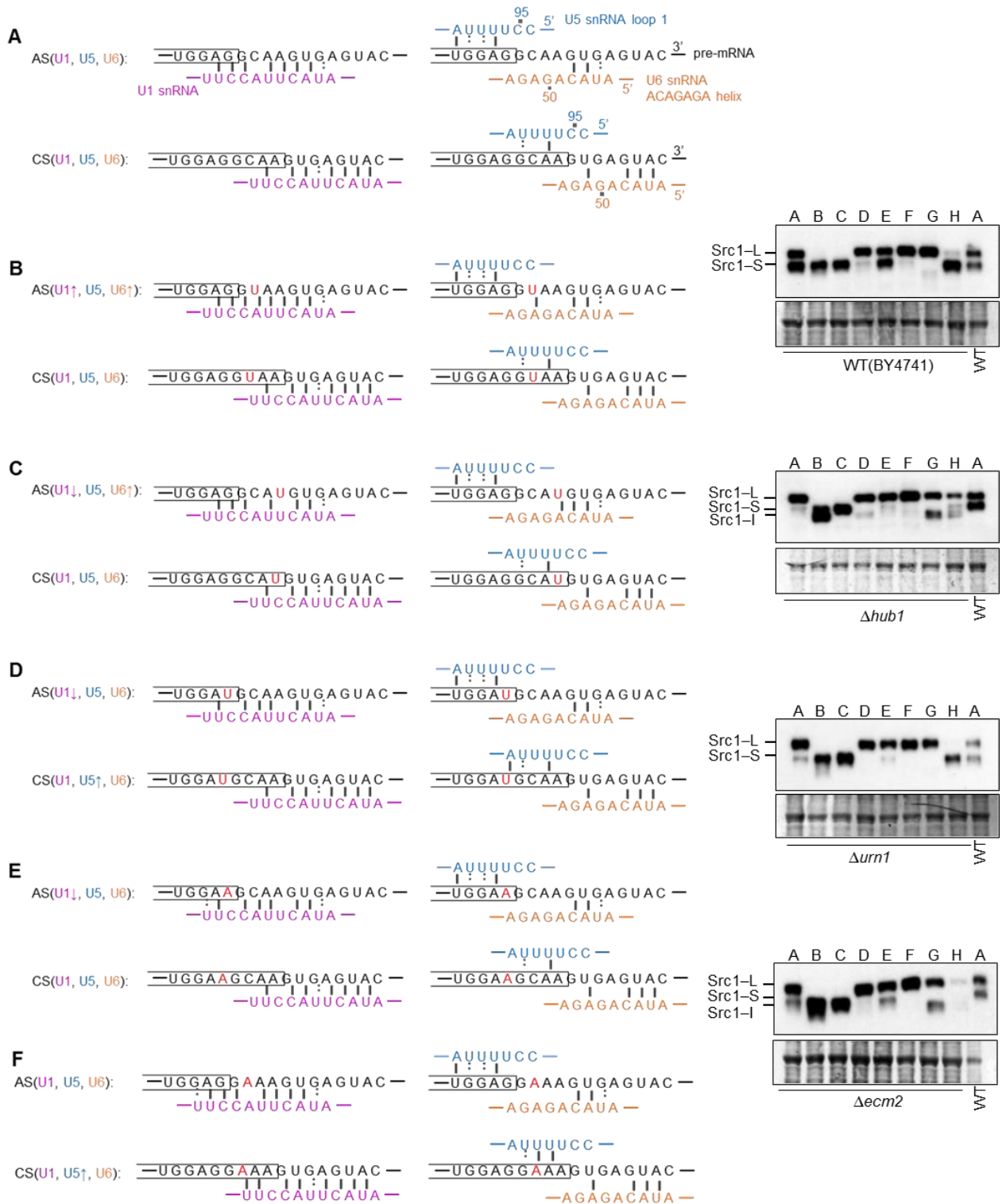




Figure 4.9: U1, U5, and U6 snRNA binding of *SRC1* 5'ss. Splicing of *SRC1* overlapping 5'ss with (A) wild-type (GCAAGUGAGU) ss, (B) GCAAGU-GUAAGU (C) GCAAGU-GCAUGU (D) GAGGCAAGU-GAUGAAAGU (E) GAGGCAAGU-GAAGCAAGU (F) GCAAGU-GAAAGU (G) GUGAGU-GUCUGU (H) GCAAGU-GUCUGU mutant 5'ss monitored by anti-MYC western blot in different splicing factor mutant strains. The last lane in each blot is control of wild-type *SRC1* splicing in wild type cell used as a marker for size of Src1-L, Src1-S, and intron retained smaller protein. The panel on left shows the snRNAs (U1, U5, and U6) and their binding to the *SRC1* pre-mRNA in each variant/mutant.

Table 4.2 Affinity of *SRC1* 5'ss binding to U1, U5, and U6 snRNAs (red boxes show weakening of binding, green boxes show strengthening of binding and UA denotes unaltered binding in mutants compared to WT. Number of '+' and '-' shows the difference in fold of binding).

Variants	5'ss	U1 binding	U5 binding	U6 binding	Splicing
GAGGCAAGTGTGAGT	AS	Optimal	Optimal	Optimal	Expressed
	CS	Optimal	Optimal	Optimal	Expressed
GCAAGU-GUAAGU	AS	+	UA	+	Expressed
	CS	UA	UA	UA	
GCAAGU-GCAUGU	AS	-	UA	+	Expressed
	CS	UA	UA	UA	
GAGGCAAG-GAUGAAAG	AS	-	UA	UA	
	CS	UA	+	UA	Expressed
GAGGCAAG-GAAGCAAG	AS	-	UA	UA	Expressed
	CS	UA	UA	UA	Expressed
GCAAGU-GAAAGU	AS	UA	UA	UA	
	CS	UA	+	UA	Expressed
GUGAGU-GUCUGU	AS	UA	UA	-	
	CS	UA	+	+	Expressed

GCAAGU-GUCUGU	AS	-	UA	+	Expressed
	CS	-	-	UA	

4.4 Conclusion and Discussion

SRC1 alternative splicing factors

A distinct set of core splicing factors and regulators facilitate *SRC1* alternative splicing (Table 4.1). Roles of Hub1, Snu66, Prp5, Prp8, and Prp38 has also been reported earlier^{48,49}. The function of the factors identified in this study was elucidated by: (i) probing Hub1 proximity to core splicing factors, (ii) testing different types of *prp8* mutants, and (iii) screening yeast mutants with *SRC1* alternative splicing reporter. The majority of *SRC1* alternative splicing factors evidently have a common phenotype; they show negative genetic interactions with Hub1 as *hub1Δ* strain showed synthetic sick phenotype with respective mutants^{48,166,167}. Although *hub1Δ* was defective in using alternative 5'ss (and normal in using constitutive 5'ss), excess of Hub1 in the spliceosome did not increase usage of the alternative 5'ss.

The RES complex is required for nuclear pre-mRNA retention and splicing^{163,168,169}. The pre-mRNA splicing function of this complex appears to be critical for *SRC1* alternative splicing, as other mutants of mRNA export did not show similar defects. Nevertheless, the alternative splicing defects in RES mutants were not as pronounced as *hub1Δ* or *prp8-101*. Similar to the *prp8-101* allele, alleles of Prp38, Prp3, and Prp6 defective, specifically in *SRC1* alternative splicing, are likely to be found.

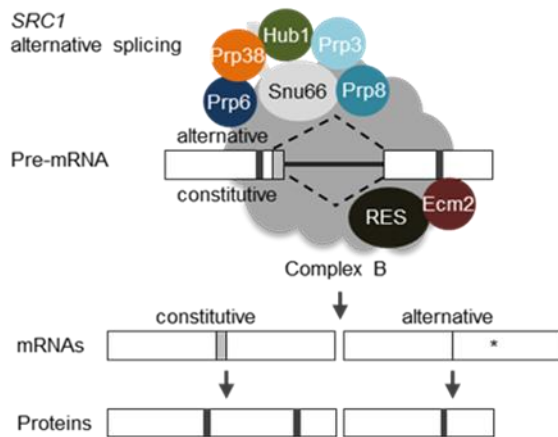


Figure 4.10: Mechanism of *SRC1* alternative splicing with additional factors Proteins that promote *SRC1* alternative splicing in *Saccharomyces cerevisiae*: Ecm2, Hub1, Prp3, Prp6, Prp8, Prp38, Snu66, and the RES complex subunits: Snu17, Pml1, Bud13, and Urn1 (* translation stop codon).

Proposed mechanism of *SRC1* alternative splicing

Since splicing via constitutive 5'ss was normal in the mutants of *SRC1* alternative splicing factors, the spliceosome was competent for the first trans-esterification reaction between branch adenosine and 'G' of the constitutive 5'ss. However, alternative splicing factors are needed for presenting the alternative 'G' to the branch adenosine. The process would require conformational changes in the spliceosome^{31,32}, which may occur by Hub1 dependent and independent mechanisms. The Hub1-dependent mechanism depends on its proximity to selected tri-snRNP factors, including Snu66, Prp38, Prp3, Prp6, and Prp8. Among these proteins, Snu66 and Prp38 are unique, as Hub1-binding HIND elements are found in Snu66 and/or Prp38. Other core components of the spliceosome, Prp3, Prp6, and Prp8, further revealed alternative splicing-specific activity of the machinery, which was also supported by finding of the alternative splicing-specific defective *prp8-101* allele. *prp8-101* is the first-step alleles of Prp8, which allows spliceosomes to attain the first catalytic conformation faster but the second catalytic conformation slower¹³⁵. This might cause spliceosomes to skip the weaker of the two competing 5'ss, the alternative 5'ss GCAAGU. Thus, wild type Prp8 may be slowing the spliceosome on the competing 5'ss leading to the usage of both 5'ss.

The RES complex, by contrast, appears to function by Hub1-independent mechanisms, as Hub1 proximity to the RES subunit Snu17 did not support *SRC1* alternative splicing. Spliceosomes lacking RES are suggested to be aberrant, which get activated prematurely¹⁶⁰; this hastened activation possibly causes skipping of the weaker 5'ss similar to the *prp8-101* allele. *SRC1* alternative splicing factors appear to slow down spliceosome in a conformation

that allows usage of non-canonical and competing 5'ss. Since these factors are conserved in humans, they might, in general, promote alternative splicing involving competing 5'ss. These factors belong to spliceosomal core and regulators and appear to function by different mechanisms (Figure 4.10). Their diversity suggests that other forms of alternative splicing might similarly require distinct sets of splicing factors and regulators.

The affinity of the 5'ss binding to U1, U5, and U6 snRNAs is also mechanistically important for such alternative splicing. The preferred expression of one of the forms of Src1 is determined by (i) strength of the binding of the competing 5'ss to mostly U5, and U6 (ii) balance between the strength of binding of a splice site to the different snRNAs (iii) presence of the *trans*-acting proteins modulating the efficiency of ss and snRNA pairing. These all features are maintained in a thermodynamically balanced state in wild type cells to allow expression of both the isoforms of Src1 at an optimal level and any deviation from those results in preference of one isoform expression over another or in the complete intron retention.

Methods

5.1 Materials

5.1.1 Chemicals and plastic wares

Fine chemicals, reagents, and media components were obtained from commercial sources like Sigma-Aldrich, Himedia, Merck. Ltd, and, Formedium. All chemicals were either of analytical quality or molecular biology grade. Plastic wares were obtained from Abdos lebtech, Tarsons, and, Genexy.

5.1.2 Molecular biology reagents

Enzymes such as restriction enzymes, T4 DNA ligase, Phusion polymerase, Taq polymerase, Vent polymerase, rSAP were purchased from New England Biolabs (NEB), Pfu Turbo was purchased from Aligent, and reverse transcriptase was purchased from Invitrogen and Thermo. dNTPs and Salmon sperm DNA were purchased from Invitrogen and Thermo. DNA molecular weight markers from Thermo scientific and protein molecular weight markers from Biorad were used. Plasmid extraction miniprep kit and gel/PCR purification kit from Bioneer and Favorgen were used.

5.1.3 Antibodies and antibody-coupled beads

Antibodies used in the study are as follows: anti-haemagglutinin, raised in rabbit (HA, polyclonal), anti-MYC, raised in rabbit (polyclonal); HRP coupled anti-mouse (goat), anti-rabbit (goat) secondary antibodies were obtained from Sigma-Aldrich. Antibody coupled beads (anti-HA and anti-MYC) were also obtained from the same source. The IgG (goat) coupled beads used as a control was generated in the lab.

5.1.4 Media

- i) *Luria-Bertain (LB) broth and plates*: 10g tryptone, 5g yeast extract, and 10g NaCl were dissolved in 1000ml of distilled water and autoclaved. For plates- 10g tryptone, 5g yeast extract, 10g NaCl, and 20g agar were dissolved in 1000 ml distilled water and autoclaved. Desired antibiotic was added in a specified concentration just before pouring the plates at a temperature around 45°C - 50°C.
- ii) *YPAD broth and plates*: 5g yeast extract, 10g peptone, 20mg adenine in 250ml distilled water, and 10g glucose in 250ml distilled water were dissolved and autoclaved separately. The two solutions were mixed after autoclaving. For plates, 5g yeast extract, 10g peptone, 20mg adenine in 100ml distilled water, 10g glucose in 100 ml distilled water, and 10g agar in 300ml of distilled water were dissolved and autoclaved. After autoclaving, the three solutions were mixed and poured into plates. For antibiotic-containing plates, desired antibiotics (Nat. G418 or hygromycin) in specified concentrations were added to the mixture before pouring into plates.
- iii) *Synthetic defined media broth and plates*: 6.7g yeast nitrogen base, 2g required supplement dropout mixture were added in 500ml water and 20g glucose in 500ml water and autoclaved. For plates, 20g agar was added in addition to the above-mentioned ingredients, such as to make a total volume of 1L, autoclaved, and mixed before pouring into plates.

5.1.5 Buffers and stock solutions

50X TAE buffer:

Tris Base	242 g
Glacial acetic acid	57.1 ml
500mM EDTA (pH 8)	100 ml
Water	600.9 ml

10X SDS Running Buffer (pH 8.3):

Tris Base	30 g
Glycine	144 g
SDS	10 g
Water	1000 ml

20X MOPS buffer (pH 7.7):

MOPS	50 mM
Tris Base	50 mM
SDS	0.1 %
EDTA	1 mM

93

10X Semi-dry Transfer Buffer:

Glycine	29.3 g
Tris Base	58.2 g
SDS	4 g
Water	1000 ml

For transfer 1X buffer with 5-20 % methanol was used.

10X Tris-Buffer Saline (TBS) (pH 7.6):

Tris Base	24.2 g
NaCl	80 g
Water	1000 ml

Sterilised by autoclaving. For washing, 1X TBS with 0.1% tween 20 was used.

10X Phosphate Buffer Saline (PBS) (pH 7.4)

NaCl	80 g
KCl	2 g
Na ₂ HPO ₄	14.4 g

K ₂ HPO ₄	2.4 g
Water	1000 ml

Sterilized by autoclave and diluted to 1X for use.

40% PEG mix: filter sterilized and stored at 4°C

Lithium acetate	100 mM
Tris-HCL	10 mM
EDTA (pH 8)	1 mM
PEG	40%

SORB (pH 8):

Lithium acetate	100 mM
Tris-HCL (pH 8)	10 mM
EDTA (pH 8)	1 mM
Sorbitol	1M

Filter sterilized and stored at room temperature.

Lysis Buffer for DNA isolation:

94

Triton X 100	2%
SDS	1%
NaCl	100 mM
Tris-Cl (pH 8)	10 mM
EDTA	1 mM

HU-Buffer

8 M Urea	96 g
5% SDS	10 g
200mM Tris pH 6.8	40ml of 1M
MilliQ	200ml
Bromo-phenol blue	10 mg
Add to 900µl of HU 1.5% DTT	100 µl of 15%

5.1.6 Yeast strains and plasmids

Table 5.1: Strains used for Chapter 2

Strain	Relevant genotype	Methods	Reference
BY4741	<i>ura3Δ0 leu2Δ0 his3Δ1 met15Δ0</i>	Obtained from Euroscarf	¹⁵¹
W303	<i>ade2-1 his3-11, 15 leu2-3, 112 ura3 trp1-1 ssd1 can1-100</i>	Gift from K. Nasmyth	
Sc9	<i>W303 snu66::KanMX6</i>	PCR-based deletion in W303	
Sc 113	<i>W303 Snu66-3HA::natNT2</i>	Cassette based replacement of selection marker with WT/mutant Snu66 in Sc9	This study
Sc114	<i>W303 snu66RRAA-3HA::natNT2</i>	Cassette based replacement of selection marker with WT/mutant Snu66	This study
Sc115	<i>W303 snu66K546A-3HA::natNT2</i>	Cassette based replacement of selection marker with WT/mutant Snu66	This study
Sc116	<i>W303 snu66ΔSnu66-CM-3HA::natNT2</i>	Cassette based replacement of selection marker with WT/mutant Snu66	This study
YJU75	<i>MATa ade2 cup1□::ura3 his3 leu2 lys2 prp8□::LYS2 trp1; pJU169 (PRP8 URA3 CEN ARS)</i>	Gift from C. Guthrie	¹⁴⁹
YJU75	<i>YJU75 snu66::hisMX6</i>	PCR-based deletion in YJU75	This study
Sc105	<i>W303 Snu66-3HA::natNT2; Prp4-9MYC::KanMX6</i>	PCR-based C-terminal tagging of <i>Prp4</i>	This study
Sc106	<i>W303 snu66RRAA-6HA::natNT2; Prp4-9MYC::KanMX6</i>	PCR-based C-terminal tagging of <i>Prp4</i>	This study
Sc107	<i>W303 snu66K546A-6HA::natNT2; Prp4-9MYC::KanMX6</i>	PCR-based C-terminal tagging of <i>Prp4</i>	This study
Sc108	<i>W303 snu66ΔSnu66-CM-6HA::natNT2; Prp4-9MYC::KanMX6</i>	PCR-based C-terminal tagging of <i>Prp4</i>	This study
Sc109	<i>W303 Snu66-6HA::natNT2; Brr2-9MYC::KanMX6</i>	PCR-based C-terminal tagging of <i>Brr2</i>	This study
Sc110	<i>W303 snu66RRAA-6HA::natNT2; Brr2-9MYC::KanMX6</i>	PCR-based C-terminal tagging of <i>Brr2</i>	This study
Sc111	<i>W303 snu66K546A-6HA::natNT2; Brr2-9MYC::KanMX6</i>	PCR-based C-terminal tagging of <i>Brr2</i>	This study
Sc112	<i>W303 snu66ΔSnu66-CM-6HA::natNT2; Brr2-9MYC::KanMX6</i>	PCR-based C-terminal tagging of <i>Brr2</i>	This study
Sc104	<i>W303 Prp4-9MYC::KanMX6</i>	PCR-based C-terminal tagging of <i>Prp4</i>	This study
SP8	<i>snu66K613A(snu66-1)</i>		This study
SP42	<i>cdc5-6HA::KanMX6</i>	PCR-based C-terminal tagging of <i>cdc5</i>	¹⁷⁰
SP194	<i>snu66K613A(snu66-1); cdc5-6HA::KanMX6</i>	PCR-based C-terminal tagging of <i>cdc5</i>	This study

Table 5.2: Strains used for Chapter 3

Strain	Relevant genotype	Methods	Reference
pJ69-7a			
SC9	<i>W303 snu66::KanMX6</i>	PCR-based deletion in W303	
SC16	<i>W303 sap1::natNT2</i>	PCR-based deletion in W303	This study
SC54	<i>W303 Sap1-9MYC::KanMX62</i>	PCR-based C-terminal tagging in W303	This study
SC29	<i>Cen.PK</i>	Gift from S. Laxman	
SC34	<i>Cen.PK sap1::natNT2</i>	PCR-based deletion in Cen.PK	This study
SC42	<i>Cen.PK gin4::KanMX6</i>	PCR-based deletion in Cen.PK	This study
SC43	<i>Cen.PK elm1::KanMX6</i>	PCR-based deletion in Cen.PK	This study
SC44	<i>Cen.PK cla4::KanMX6</i>	PCR-based deletion in Cen.PK	This study
SC123	<i>Cen.PK sap1::natNT2 gin4::KanMX6</i>	By mating and dissection of	This study
SC124	<i>Cen.PK sap1::natNT2 cla4::KanMX6</i>	By mating and dissection of	This study
SC125	<i>Cen.PK sap1::natNT2 elm1::KanMX6</i>	By mating and dissection of	This study
SC36	<i>Cen.PK pADH-GFP-Sap1::NatNT2</i>	PCR-based N-terminal tagging of Sap1	This study
SC37	<i>Cen.PK pADH-GFP-Sap1_C::NatNT2</i>	PCR-based N-terminal tagging of Sap1_C	This study
SC63	<i>BY4741 pADH-GFP-Sap1::NatNT2, siz1::KanMX6</i>	PCR-based deletion of Siz1 in	This study
SC55	<i>BY4741 Cdc3-6HA</i>	PCR-based C-terminal tagging of Cdc3	This study
SC56	<i>BY4741 Cdc3-6HA sap1::KanMX6</i>	PCR-based C-terminal tagging of Cdc3	This study
SC57	<i>BY4741 Cdc3-6HA siz1::KanMX6</i>	PCR-based C-terminal tagging of Cdc3	This study
SC10	<i>W303 Prp8*</i>		48
SC80	<i>W303 Prp8* sap1::NatNT2;</i>	PCR-based deletion of Sap1	This study
SC86	<i>YJU75 sap1::hisMX6</i>	PCR-based deletion of Sap1	This study
SC100	<i>YJU75 Sap1-NatNT2</i>	Cassette based replacement of selection marker with Sap1 variant	This study
SC101	<i>YJU75 Sap1I236A-NatNT2</i>	Cassette based replacement of selection marker with mutant Sap1	This study
SC102	<i>YJU75 Sap1ΔSIM-NatNT2</i>	Cassette based replacement of selection marker with mutant Sap1	This study
SC103	<i>YJU75 Sap1ΔK651A-NatNT2</i>	Cassette based replacement of selection marker with mutant Sap1	This study
SC117	<i>W303 Sap1-NatNT2</i>	Cassette based replacement of selection marker with Sap1 variant	This study
SC118	<i>W303 Sap1I236A-NatNT2</i>	Cassette based replacement of selection marker with mutant Sap1	This study
SC119	<i>W303 Sap1ΔSIM-NatNT2</i>	Cassette based replacement of selection marker with mutant	This study

		Sap1	
SC120	<i>W303 Sap1K651A-NatNT2</i>	Cassette based replacement of selection marker with mutant Sap1	This study
SC59	<i>W303 TAD3 pLGS5-ura3</i>	Reporter plasmid transformed in <i>W303</i>	This study
SC60	<i>W303 Tup1-6HA::NatNT2</i>	PCR-based C-terminal tagging of Tup1	This study
SC61	<i>W303 Tup1-6HA::NatNT2 Sap1-9MYC::KanMX6</i>	PCR-based tagging of Tup1 in SC54	This study
SC64	<i>W303 tup1::NatNT2 Sap1-9MYC::KanMX6</i>	PCR-based deletion of <i>tup1</i> in SC54	This study
SC70	<i>W303 Tup1-6HA, 6His-Smt3</i>	6His tagging of Smt3 by integrative plasmid	This study
SC132	<i>W303 srs2::KanMX6</i>	PCR based deletion from deletion library	This study
SC133	<i>W303 sir2::KanMX6</i>	PCR based deletion from deletion library	This study
SC134	<i>W303 siz1::KanMX6</i>	PCR based deletion from deletion library	This study
SC136	<i>W303 sin1::KanMX6</i>	PCR based deletion from deletion library	This study
SC87	<i>YJU75 hub1::KanMX6</i>	PCR-based deletion of Hub1	This study
SC88	<i>W303 hub1::KanMX6 sap1::natNT2</i>	PCR-based deletion of Hub1 and Sap1	This study
	<i>BY4741, siz1::KanMX6</i>	Deletion library euroscarf	

Table 5.3: Strains used for Chapter 4

Strain	Relevant genotype	Methods	Reference
BY4741	BY4741 deletion strains: <i>tex1::KanMX6; thp1::KanMX6; lrp1::KanMX6; sem1::KanMX6; mft1::KanMX6; hrb1::KanMX6; tho2::KanMX6; gbp2::KanMX6; sac3::KanMX6; hpr1::KanMX6; thp2::KanMX6</i>	Obtained from Euroscarf	151
YSKM443	<i>W303a P_{CUP1-1}TAP-SRC1::natNT2</i>	PCR-based N-terminal tagging of <i>SRC1</i> in <i>W303a</i>	48
YSKM449	<i>W303a P_{CUP1-1}TAP-SRC1::KanMX6</i>	PCR-based N-terminal tagging of <i>SRC1</i> in <i>W303a</i>	48
YSKM452	<i>W303a P_{CUP1-1}TAP-SRC1::KAN Prp38-hub1(D22A)</i>	PCR-based C-terminal tagging of <i>PRP38</i> with <i>HUB1(D22A)</i> in YSKM449	48
YSKM461	<i>W303a P_{CUP1-1}TAP-SRC1::KAN Snu66-hub1(D22A)</i>	PCR-based C-terminal tagging of <i>SNU66</i> with <i>HUB1(D22A)</i> in YSKM449	48
YSKM464	<i>BY4741 lea1::KanMX6 P_{CUP1-1}TAP-SRC1::natNT2</i>	PCR-based N-terminal tagging of <i>SRC1</i> in <i>BY4741 lea1::KanMX6</i>	This study
YSKM466	<i>BY4741 ecm2::KanMX6 P_{CUP1-1}TAP-SRC1::natNT2</i>	PCR-based N-terminal tagging of <i>SRC1</i> in <i>BY4741 ecm2::KanMX6</i>	This study
YSKM467	<i>BY4741 bud13::KanMX6 P_{CUP1-1}TAP-SRC1::natNT2</i>	PCR-based N-terminal tagging of <i>SRC1</i> in <i>BY4741 bud13::KanMX6</i>	This study

YSKM468	<i>BY4741 pml1::KanMX6 P_{CUP1}-_iTAP-SRC1::natNT2</i>	PCR-based N-terminal tagging of <i>SRC1</i> in <i>BY4741 pml1::KanMX6</i>	This study
YSKM469	<i>BY4741 cwf27::KanMX6 P_{CUP1}-_iTAP-SRC1::natNT2</i>	PCR-based N-terminal tagging of <i>SRC1</i> in <i>BY4741 cwf27::KanMX6</i>	This study
YSKM470	<i>W303a hub1::HIS3MX6 P_{CUP1}-_iTAP-SRC1::KanMX6</i>	PCR-based deletion of <i>HUB1</i> and N-terminal tagging of <i>SRC1</i> in <i>W303a</i>	48
YSKM472	<i>W303 □ hub1::HIS3MX6 P_{CUP1}-_iTAP-SRC1::KanMX6 PRP38-hub1(D22A):: natNT2</i>	PCR-based C-terminal tagging of <i>PRP38</i> with <i>HUB1(D22A)</i> in YSKM470	48
YSKM475	<i>W303a hub1::HIS3MX6 P_{CUP1}-_iTAP-SRC1::KanMX6 PRP8-hub1(D22A):: natNT2</i>	PCR-based C-terminal tagging of <i>PRP8</i> with <i>HUB1(D22A)</i> in YSKM470	48
YSKM479	<i>W303 □ hub1::HIS3MX6 P_{CUP1}-_iTAP-SRC1::KanMX6 SNU66-hub1(D22A):: natNT2</i>	PCR-based C-terminal tagging of <i>SNU66</i> with <i>HUB1(D22A)</i> in YSKM470	48
YSKM488	<i>BY4741 nup60::KanMX6 P_{CUP1}-_iTAP-SRC1::natNT2</i>	PCR-based N-terminal tagging of <i>SRC1</i> in <i>BY4741 nup60::KanMX6</i>	This study
YSKM489	<i>BY4741 lsm1::KanMX6 P_{CUP1}-_iTAP-SRC1::natNT2</i>	PCR-based N-terminal tagging of <i>SRC1</i> in <i>BY4741 lsm1::KanMX6</i>	This study
YSKM490	<i>BY4741 sky1::KanMX6 P_{CUP1}-_iTAP-SRC1::natNT2</i>	PCR-based N-terminal tagging of <i>SRC1</i> in <i>BY4741 sky1::KanMX6</i>	This study
YSKM491	<i>BY4741 snu17::KanMX6 P_{CUP1}-_iTAP-SRC1::natNT2</i>	PCR-based N-terminal tagging of <i>SRC1</i> in <i>BY4741 snu17::KanMX6</i>	This study
YSKM492	<i>BY4741 mlp2::KanMX6 P_{CUP1}-_iTAP-SRC1::natNT2</i>	PCR-based N-terminal tagging of <i>SRC1</i> in <i>BY4741 mlp2::KanMX6</i>	This study
YSKM493	<i>BY4741 mlp1::KanMX6 P_{CUP1}-_iTAP-SRC1::natNT2</i>	PCR-based N-terminal tagging of <i>SRC1</i> in <i>BY4741 mlp1::KanMX6</i>	This study
YSKM494	<i>BY4741 pml39::KanMX6 P_{CUP1}-_iTAP-SRC1::natNT2</i>	PCR-based N-terminal tagging of <i>SRC1</i> in <i>BY4741 pml39::KanMX6</i>	This study
YSKM495	<i>BY4741 brr1::KanMX6 P_{CUP1}-_iTAP-SRC1::natNT2</i>	PCR-based N-terminal tagging of <i>SRC1</i> in <i>BY4741 brr1::KanMX6</i>	This study
YSKM496	<i>BY4741 mud2::KanMX6 P_{CUP1}-_iTAP-SRC1::natNT2</i>	PCR-based N-terminal tagging of <i>SRC1</i> in <i>BY4741 mud2::KanMX6</i>	This study
YSKM497	<i>BY4741 mud1::KanMX6 P_{CUP1}-_iTAP-SRC1::natNT2</i>	PCR-based N-terminal tagging of <i>SRC1</i> in <i>BY4741 mud1::KanMX6</i>	This study
YSKM498	<i>BY4741 prp17::KanMX6 P_{CUP1}-_iTAP-SRC1::natNT2</i>	PCR-based N-terminal tagging of <i>SRC1</i> in <i>BY4741 prp17::KanMX6</i>	This study
YSKM499	<i>BY4741 npl3::KanMX6 P_{CUP1}-_iTAP-SRC1::natNT2</i>	PCR-based N-terminal tagging of <i>SRC1</i> in <i>BY4741 npl3::KanMX6</i>	This study
YSKM500	<i>BY4741 cwf15::KanMX6 P_{CUP1}-_iTAP-SRC1::natNT2</i>	PCR-based N-terminal tagging of <i>SRC1</i> in <i>BY4741 cwf15::KanMX6</i>	This study
YSKM501	<i>BY4741 cwf21::KanMX6 P_{CUP1}-_iTAP-SRC1::natNT2</i>	PCR-based N-terminal tagging of <i>SRC1</i> in <i>BY4741</i>	This study

		<i>cwf21::KanMX6</i>	
YSKM502	<i>BY4741 ntc20::KanMX6 P_{CUP1}-_jTAP-SRC1::natNT2</i>	PCR-based N-terminal tagging of <i>SRC1</i> in <i>BY4741 ntc20::KanMX6</i>	This study
YSKM503	<i>BY4741 ntc30::KanMX6 P_{CUP1}-_jTAP-SRC1::natNT2</i>	PCR-based N-terminal tagging of <i>SRC1</i> in <i>BY4741 ntc30::KanMX6</i>	This study
YSKM504	<i>BY4741 ntc31::KanMX6 P_{CUP1}-_jTAP-SRC1::natNT2</i>	PCR-based N-terminal tagging of <i>SRC1</i> in <i>BY4741 ntc31::KanMX6</i>	This study
YSKM505	<i>BY4741 P_{CUP1}-_jTAP-SRC1::natNT2</i>	PCR-based N-terminal tagging of <i>SRC1</i>	48
YSKM506	<i>BY4741 hub1::KanMX6 P_{CUP1}-_jTAP-SRC1::natNT2</i>	PCR-based N-terminal tagging of <i>SRC1</i> in <i>BY4741 hub1::KanMX6</i>	This study
YSKM527	<i>W303? P_{CUP1}-_jTAP-SRC1::KAN Snu66-hub1(D22A) Prp38-hub1(D22A)</i>	Mating of YSKM452 with YSKM479, diploid selection on mating type tester plates, dissection of tetrads, western blotting	This study
YSKM528	<i>W303? □hub1::HIS P_{CUP1}-_jTAP-SRC1::KAN Snu66-hub1(D22A) Prp38-hub1(D22A)</i>	Mating of YSKM452 with YSKM479, diploid selection on mating type tester plates, dissection of tetrads, western blotting	This study
YSKM535	<i>W303a hub1::HIS3MX6 P_{CUP1}-_jTAP-SRC1::KanMX6 SNU17-hub1(D22A):: natNT2</i>	PCR-based C-terminal tagging of <i>SNU17</i> with <i>HUB1(D22A)</i> in YSKM470	This study
YSKM547	<i>W303a hub1::HIS3MX6 P_{CUP1}-_jTAP-SRC1::KanMX6 PRP4-hub1(D22A):: natNT2</i>	PCR-based C-terminal tagging of <i>PRP4</i> with <i>HUB1(D22A)</i> in YSKM470	This study
YSKM548	<i>W303a hub1::HIS3MX6 P_{CUP1}-_jTAP-SRC1::KanMX6 BRR2-hub1(D22A):: natNT2</i>	PCR-based C-terminal tagging of <i>BRR2</i> with <i>HUB1(D22A)</i> in YSKM470	This study
YSKM549	<i>W303a hub1::HIS3MX6 P_{CUP1}-_jTAP-SRC1::KanMX6 PRP6-hub1(D22A):: natNT2</i>	PCR-based C-terminal tagging of <i>PRP6</i> with <i>HUB1(D22A)</i> in YSKM470	This study
YSKM550	<i>W303a hub1::HIS3MX6 P_{CUP1}-_jTAP-SRC1::KanMX6 PRP3-hub1(D22A):: natNT2</i>	PCR-based C-terminal tagging of <i>PRP3</i> with <i>HUB1(D22A)</i> in YSKM470	This study
YSKM551	<i>W303a hub1::HIS3MX6 P_{CUP1}-_jTAP-SRC1::KanMX6 LEA1-hub1(D22A):: natNT2</i>	PCR-based C-terminal tagging of <i>LEA1</i> with <i>HUB1(D22A)</i> in YSKM470	This study
YSKM552	<i>BY4741 hub1::natNT2</i>	PCR-based deletion of <i>HUB1</i> in <i>BY4741</i>	This study
YSKM553	<i>W303a hub1::HIS3MX6 P_{CUP1}-_jTAP-SRC1::KanMX6 PRP9-hub1(D22A):: natNT2</i>	PCR-based C-terminal tagging of <i>PRP9</i> with <i>HUB1(D22A)</i> in YSKM470	This study
YSKM554	<i>W303a hub1::HIS3MX6 P_{CUP1}-_jTAP-SRC1::KanMX6 PRP11-hub1(D22A):: natNT2</i>	PCR-based C-terminal tagging of <i>PRP11</i> with <i>HUB1(D22A)</i> in YSKM470	This study
YSKM555	<i>W303a hub1::HIS3MX6 P_{CUP1}-_jTAP-SRC1::KanMX6 MUD1-hub1(D22A):: natNT2</i>	PCR-based C-terminal tagging of <i>MUD1</i> with <i>HUB1(D22A)</i> in YSKM470	This study
YSKM560	<i>BY4741 hub1::natNT2 tex1::KanMX6</i>	PCR-based deletion of <i>HUB1</i> in <i>BY4741 tex1::KanMX6</i>	This study
YSKM561	<i>BY4741 hub1::natNT2 sem1::KanMX6</i>	PCR-based deletion of <i>HUB1</i> in <i>BY4741 sem1::KanMX6</i>	This study
YSKM562	<i>BY4741 hub1::natNT2</i>	PCR-based deletion of <i>HUB1</i>	This study

	<i>mft1::KanMX6</i>	<i>in BY4741 mft1::KanMX6</i>	
YSKM563	<i>BY4741 hub1::natNT2 hrb1::KanMX6</i>	PCR-based deletion of <i>HUB1</i> <i>in BY4741 hrb1::KanMX6</i>	This study
YSKM564	<i>BY4741 hub1::natNT2 tho2::KanMX6</i>	PCR-based deletion of <i>HUB1</i> <i>in BY4741 tho2::KanMX6</i>	This study
YSKM565	<i>BY4741 hub1::natNT2 gbp2::KanMX6</i>	PCR-based deletion of <i>HUB1</i> <i>in BY4741 gbp2::KanMX6</i>	This study
YSKM566	<i>BY4741 hub1::natNT2 thp2::KanMX6</i>	PCR-based deletion of <i>HUB1</i> <i>in BY4741 thp2::KanMX6</i>	This study
YSKM567	<i>BY4741 hub1::natNT2 lrp1::KanMX6</i>	PCR-based deletion of <i>HUB1</i> <i>in BY4741 lrp1::KanMX6</i>	This study
YSKM568	<i>BY4741 hub1::natNT2 sac3::KanMX6</i>	PCR-based deletion of <i>HUB1</i> <i>in BY4741 sac3::KanMX6</i>	This study
YSKM569	<i>BY4741 tex1::KanMX6 P_{CUP1}- iTAP-SRC1::natNT2</i>	PCR-based N-terminal tagging of <i>SRC1</i> in <i>BY4741</i> <i>tex1::KanMX6</i>	This study
YSKM570	<i>BY4741 lrp1::KanMX6 P_{CUP1}- iTAP-SRC1::natNT2</i>	PCR-based N-terminal tagging of <i>SRC1</i> in <i>BY4741</i> <i>lrp1::KanMX6</i>	This study
YSKM571	<i>BY4741 sem1::KanMX6 P_{CUP1}- iTAP-SRC1::natNT2</i>	PCR-based N-terminal tagging of <i>SRC1</i> in <i>BY4741</i> <i>sem1::KanMX6</i>	This study
YSKM572	<i>BY4741 mft1::KanMX6 P_{CUP1}- iTAP-SRC1::natNT2</i>	PCR-based N-terminal tagging of <i>SRC1</i> in <i>BY4741</i> <i>mft1::KanMX6</i>	This study
YSKM573	<i>BY4741 hrb1::KanMX6 P_{CUP1}- iTAP-SRC1::natNT2</i>	PCR-based N-terminal tagging of <i>SRC1</i> in <i>BY4741</i> <i>hrb1::KanMX6</i>	This study
YSKM574	<i>BY4741 gbp2::KanMX6 P_{CUP1}- iTAP-SRC1::natNT2</i>	PCR-based N-terminal tagging of <i>SRC1</i> in <i>BY4741</i> <i>gbp2::KanMX6</i>	This study
YSKM575	<i>BY4741 sac3::KanMX6 P_{CUP1}- iTAP-SRC1::natNT2</i>	PCR-based N-terminal tagging of <i>SRC1</i> in <i>BY4741</i> <i>sac3::KanMX6</i>	This study
YSKM576	<i>BY4741 thp2::KanMX6 P_{CUP1}- iTAP-SRC1::natNT2</i>	PCR-based N-terminal tagging of <i>SRC1</i> in <i>BY4741</i> <i>thp2::KanMX6</i>	This study
YSKM577	<i>BY4741 hub1::natNT2 thp1::KanMX6</i>	PCR-based deletion of <i>HUB1</i> <i>in BY4741 thp1::KanMX6</i>	This study
YSKM578	<i>BY4741 hub1::natNT2 hpr1::KanMX6</i>	PCR-based deletion of <i>HUB1</i> <i>in BY4741 hpr1::KanMX6</i>	This study
YSKM579	<i>BY4741 thp1::KanMX6 P_{CUP1}- iTAP-SRC1::natNT2</i>	PCR-based N-terminal tagging of <i>SRC1</i> in <i>BY4741</i> <i>thp1::KanMX6</i>	This study
YSKM580	<i>BY4741 hpr1::KanMX6 P_{CUP1}- iTAP-SRC1::natNT2</i>	PCR-based N-terminal tagging of <i>SRC1</i> in <i>BY4741</i> <i>hpr1::KanMX6</i>	This study
YSKM581	<i>BY4741 tho2::KanMX6 P_{CUP1}- iTAP-SRC1::natNT2</i>	PCR-based N-terminal tagging of <i>SRC1</i> in <i>BY4741</i> <i>tho2::KanMX6</i>	This study
YSKM591	<i>YJU75 P_{CUP1}-iTAP-SRC1::natNT2</i>	PCR-based N-terminal tagging of <i>SRC1</i> in <i>YJU75</i>	This study
YSKM593	<i>BY4741 bud31::KanMX6 P_{CUP1}- iTAP-SRC1::natNT2</i>	PCR-based N-terminal tagging of <i>SRC1</i> in <i>BY4741</i> <i>bud31::KanMX6</i>	This study

Table 5.4: Plasmids used for Chapter 2

Name	Description	Reference
p121	<i>S. cerevisiae</i> SNU66 in <i>YEplac112</i>	This study
p133	<i>S. cerevisiae</i> <i>snu66RRAA</i> in <i>YEplac122</i>	This study
p122	<i>S. cerevisiae</i> <i>snu66Δ75-87</i> in <i>YEplac122</i>	This study
p123	<i>S. cerevisiae</i> <i>snu66Δ102-113</i> in <i>YEplac122</i>	This study
p124	<i>S. cerevisiae</i> <i>snu66Δ126-128</i> in <i>YEplac122</i>	This study
p125	<i>S. cerevisiae</i> <i>snu66Δ161-183</i> in <i>YEplac122</i>	This study
p130	<i>S. cerevisiae</i> <i>snu66Δ273-295</i> in <i>YEplac122</i>	This study
p129	<i>S. cerevisiae</i> <i>snu66Δ297-320</i> in <i>YEplac122</i>	This study
p128	<i>S. cerevisiae</i> <i>snu66Δ321-351</i> in <i>YEplac122</i>	This study
p127	<i>S. cerevisiae</i> <i>snu66Δ365-394</i> in <i>YEplac122</i>	This study
p126	<i>S. cerevisiae</i> <i>snu66Δ437-460</i> in <i>YEplac122</i>	This study
p131	<i>S. cerevisiae</i> <i>snu66ΔSnu66-CM</i> in <i>YEplac122</i>	This study
p132	<i>S. cerevisiae</i> <i>ΔHIND-Snu66-CM</i> in <i>YEplac122</i>	This study
p057	<i>S. cerevisiae</i> SNU66 in <i>YCplac111</i>	This study
p058	<i>S. cerevisiae</i> <i>snu66Y531A</i> in <i>YCplac111</i>	This study
p059	<i>S. cerevisiae</i> <i>snu66D533A</i> in <i>YCplac111</i>	This study
p060	<i>S. cerevisiae</i> <i>snu66E534A</i> in <i>YCplac111</i>	This study
p061	<i>S. cerevisiae</i> <i>snu66L539A</i> in <i>YCplac111</i>	This study
p062	<i>S. cerevisiae</i> <i>snu66K542A</i> in <i>YCplac111</i>	This study
p063	<i>S. cerevisiae</i> <i>snu66E543A</i> in <i>YCplac111</i>	This study
p064	<i>S. cerevisiae</i> <i>snu66K546A</i> in <i>YCplac111</i>	This study
p065	<i>S. cerevisiae</i> <i>snu66L548A</i> in <i>YCplac111</i>	This study
p066	<i>S. cerevisiae</i> <i>snu66S549A</i> in <i>YCplac111</i>	This study
p068	<i>S. cerevisiae</i> <i>snu66ΔSnu66-CM</i> in <i>YCplac111</i>	This study
D022	ACT1-CUP1(GUAUGU) splicing reporter	

D023	ACT1-CUP1(GUCUGU) splicing reporter	
D024	ACT1-CUP1(GUAUUAU) splicing reporter	
p136	<i>S. cerevisiae</i> <i>Snu66</i> C terminally tagged with 9MYC in pYM17 for chromosomal replacement	This study
p137	<i>S. cerevisiae</i> <i>snu66RRAA</i> C terminally tagged with 9MYC in Pym17 for chromosomal replacement	This study
p139	<i>S. cerevisiae</i> <i>snu66K546A</i> C terminally tagged with 9MYC in pYM17 for chromosomal replacement	This study
p140	<i>S. cerevisiae</i> Δ <i>Snu66-CM</i> C terminally tagged with 9MYC in pYM17 for chromosomal replacement	This study
p135	<i>S. pombe</i> <i>tho5-i1</i> splicing reporter 5' ss mutant (GTATAT)	This study
	<i>S. pombe</i> <i>tho5-i1</i> splicing reporter WT	Anil et al
	<i>S. pombe</i> <i>tho5-i1</i> splicing reporter 3'ss mutant (AAG)	Anil et al
	<i>S. pombe</i> <i>tho5-i1</i> splicing reporter bp mutant (TTAAC)	Anil et al
	<i>S. pombe</i> <i>tho5-i1</i> splicing reporter bp mutant (CTAAA)	Anil et al

Table 5.6: Plasmids used for Chapter 3

Name	Description	Reference
p001	<i>S. cerevisiae</i> Sap1 in <i>pGADC1</i>	This study
p002	<i>S. cerevisiae</i> Sap1I236A in <i>pGADC1</i>	This study
p023	<i>S. cerevisiae</i> Sap1 Δ SIM in <i>pGADC1</i>	This study
p003	<i>S. cerevisiae</i> Sap1K651A in <i>pGADC1</i>	This study
p004	<i>S. cerevisiae</i> Sap1 521-end in <i>pGADC1</i>	This study
p025	<i>S. cerevisiae</i> Sap1 568-end in <i>pGADC1</i>	This study
p024	<i>S. cerevisiae</i> Sap1 583-end in <i>pGADC1</i>	This study
p005	<i>S. cerevisiae</i> <i>snu66</i> in <i>pGBDUC1</i>	This study
p006	<i>S. cerevisiae</i> <i>snu66</i> Δ HIND in <i>pGBDUC1</i>	This study
p007	<i>S. cerevisiae</i> <i>snu66</i> 162-587 in <i>pGBDUC1</i>	This study
p008	<i>S. cerevisiae</i> <i>snu66</i> 267-587 in <i>pGBDUC1</i>	This study

p009	<i>S. cerevisiae</i> <i>snu66</i> 412-587 in <i>pGBDUC1</i>	This study
p010	<i>S. cerevisiae</i> <i>snu66</i> Δ <i>Snu66-CM</i> in <i>pGBDUC1</i>	This study
p026	<i>S. cerevisiae</i> <i>snu66</i> 525-554 in <i>pGBDUC1</i>	This study
p027	<i>S. cerevisiae</i> <i>snu66</i> 518-554 in <i>pGBDUC1</i>	This study
p028	<i>S. cerevisiae</i> <i>snu66</i> 531-554 in <i>pGBDUC1</i>	This study
D019	<i>pLGSD5</i>	This study
3743	<i>S. cerevisiae</i> Prp8 in <i>YCplac22</i>	This study
3745	<i>S. cerevisiae</i> <i>prp8-101</i> in <i>YCplac22</i>	This study
pSKM509	<i>S. cerevisiae</i> <i>Hub1</i> in <i>YEplac181</i>	This study
pSKM360	<i>S. cerevisiae</i> <i>Sap1</i> in <i>YEplac195</i>	This study
3658	<i>S. cerevisiae</i> <i>pGAL1-10</i> 3MYC- <i>Src1</i> in <i>YCplac111</i>	This study
	6His- <i>Smt3</i> in <i>YIplac128</i>	Ivan Psakhye
p090	<i>S. cerevisiae</i> <i>Ade2</i> in <i>YCplac33</i>	This study
p091	<i>S. cerevisiae</i> <i>Ade2-1</i> in <i>YCplac22</i>	This study
D153	<i>S. cerevisiae</i> <i>Sap1</i> in <i>YCplac111</i>	This study
p030	<i>S. cerevisiae</i> <i>Sap1I236A</i> in <i>YCplac111</i>	This study
p031	<i>S. cerevisiae</i> <i>Sap1</i> Δ <i>SIM</i> in <i>YCplac111</i>	This study
p032	<i>S. cerevisiae</i> <i>Sap1K651A</i> in <i>YCplac111</i>	This study
pSKM231	<i>pDPP1-lacZ</i> (-500) <i>pSL9</i>	This study
p049	<i>S. cerevisiae</i> <i>Sap1</i> promoter and terminator in <i>pFA6a-NatNT2</i> for chromosomal replacement	This Study
p050	<i>S. cerevisiae</i> <i>Sap1 I236A</i> promoter and terminator in <i>pFA6a-NatNT2</i> for chromosomal replacement	This Study
p051	<i>S. cerevisiae</i> <i>Sap1</i> Δ <i>SIM</i> , promoter and terminator in <i>pFA6a-NatNT2</i> for chromosomal replacement	This Study
p052	<i>S. cerevisiae</i> <i>Sap1 K651A</i> , promoter and terminator in <i>pFA6a-NatNT2</i> for chromosomal replacement	This Study

5.1.7 Primers

Table 5.7: Primers used for RT-PCR and CHIP assay

Number	Name	Sequence (5'-3')
SKM_PR13	<i>act1</i> F	CCCCTAGAGCTGTATTCCC
SKM_PR14	<i>act1</i> R	CCAGTGGTACGACCAGAGG
SKM_PR41	<i>STE2</i> F	AAAGGATCCATGTCTGATGCGGCTCCTTC
SKM_PR62	<i>STE2</i> R	CTCCATCTGCAGCGGCGTTTTTCTGCTTCTC
SKM_PR214	<i>TAD3</i> intron 1 F	GTATGTATCTATGAGATCTAACAG
SKM_PR215	<i>TAD3</i> exon 2 R	CTATTACTTTCTTCGAGTCTCTTGG
SKM_PR216	<i>TAD3</i> intron 2 F	CATGGAAGTAAACTAACTAGTAAAG
SKM_PR217	<i>TAD3</i> exon 3 F	GCTAATTCGAAACGATTTTCAG
SKM_PR218	<i>TAD3</i> exon 3 R	GCACTTCGATATCATCACTCAG
SKM_PR326	<i>SpSPBP16F5.02</i> <i>Exon3</i> R	TTTCGGAAGCACTGTTTGACAATC
SKM_PR327	<i>SpSPBP16F5.02</i> <i>Exon1</i> F	GCACTTTCTTCCGCTCTTTCC
SKM_PR499	<i>SpSPBC1778.02</i> <i>E2F</i>	AGAGAGAACTGTTCACCTTAGAAG
SKM_PR502	<i>SpSPBC1778.02</i> <i>E3R</i>	CTTATAATGTTGCCGCCAGG
SKM_PR1010	Sap1 CHIP F1	GGCCAGGGTTTACAAGACAAAAGC
SKM_PR1011	SAP1CHIP R1	CCATGGCTTTTTGAGCTTCTAAGC
SKM_PR1012	SAP1 CHIP F2	GAGTGAAGTCAATACTGACGAAC
SKM_PR1013	SAP1 CHIP R2	GCAAACGCTTTTAGTTTTCTTTCCAG
SKM_PR1014	SAP1 CHIP F3	GATAAAAAGGTCCCTTCCAAGG
SKM_PR1015	SAP1 CHIP R3	CCTGCTCACCTAGGATTAGCTC
SKM_PR1016	SAP1 CHIP F4	GGAACACAAAAACATACTGTGGCC
SKM_PR1017	SAP1 CHIP R4	GCCTGTGATATGTCTAGAATACATAGGG

SKM_PR1018	SAP1 CHIP F5	CCTTTCAAGTCTTCAGCACTTATG
SKM_PR1019	SAP1 CHIP R5	CAGCCTCTTATGACCGTGAATC
SKM_PR1020	SAP1 CHIP F6	GCAACCGGCTCCCAAGAAC
SKM_PR1021	SAP1 CHIP R6	GAAAAATTGCGTTTGTAGCTGC
SKM_PR1022	SAP1 CHIP F7	CTTTC ACTCGTGCGGTTTTAC
SKM_PR1023	SAP1 CHIP R7	GTCTCATTGGCAATTCTACTGTAAAG
SKM_PR1024	SAP1 CHIP F8	GCATTGCAAGGATGGAAAGC
SKM_PR1025	SAP1 CHIP R8	CAAAAAATTGGTCCGAGAAGAGC
SKM_PR1026	SAP1 CHIP F9	CAGCCTCTTATGACCGTGAATC
SKM_PR1027	SAP1 CHIP R9	GTTTTCATCATTCTTCCGGGAAC
SKM_PR1028	SAP1 CHIP F10	GCGGCTATAAAACCGCATAAC
SKM_PR1029	SAP1 CHIP R10	GCTGTCTGCTTGCATTGTTG
SKM_PR1030	SAP1 CHIP F11	GCTGTCTGCTTGCATTGTTG
SKM_PR1031	SAP1 CHIP R11	CGTTGTGTCTTTTTAAAATGCCG
SKM_PR1032	SAP1 CHIP F12	GTGATGGTTTCGAGTTTGATGTG
SKM_PR1033	SAP1 CHIP R12	GACAAGTCAGACATTTGCTGTTG
SKM_PR1034	SAP1 CHIP F13	CTACGTCCAGTAATAAGAGTGTAAG
SKM_PR1035	SAP1 CHIP R13	CTTAGAGCGCCAGTGCTG
SKM_PR1036	SAP1 CHIP F14	CTACTACTATGGATTCATCAAAGATTAGG
SKM_PR1037	SAP1 CHIP R14	CTTTTTGATCTTGTAATAAATGTTGGCG
SKM_PR1038	SAP1 CHIP F15	CCAATCATCAAATCCAATGCATCG
SKM_PR1039	SAP1 CHIP R15	CTTCGTAGTGTTTAATGCGGG
SKM_PR1040	SAP1 CHIP F16	GAGTCACCCCATTTTGAAATCC
SKM_PR1041	SAP1 CHIP F16	CGTTTTACTCATAGACGTGGTTTG
SKM_PR1042	SAP1 CHIP R17	CGTTTCTCCAAAAATAGAAGATGTTGG
SKM_PR1043	SAP1 CHIP F17	GCAGCTTGCCTATCTACACC

SKM_PR1044	SAP1 CHIP R18	GAAATCGTAGTGCACGGAGATG
SKM_PR1045	SAP1 CHIP F18	CAAATAAGAGCATCCCCCTGAC
SKM_PR1046	SAP1 CHIP R19	CCAGGTACAGGTAAAACAATGC
SKM_PR1047	SAP1 CHIP F19	GGCAATTGCAAATAGTGCCC
SKM_PR1048	SAP1 CHIP R20	GACTCTATCATGGGTAGTAGGAATAACG
SKM_PR1049	SAP1 CHIP F20	CGCCATTGGTGTCAGAATTG
SKM_PR1050	SAP1 CHIP R21	CTGGTACTTGCCGCGACAAAC
SKM_PR1051	SAP1 CHIP F21	GTGCTTTTGTATGGGAAAGAAGC
SKM_PR1052	SAP1 CHIP F22	GATTACTGAGGGCTATTCAGGAAG
SKM_PR1053	SAP1 CHIP R22	GGGCTTGATATACACTAAACTGTTC
SKM_PR1054	SAP1 CHIP F23	CAGGACGGATTAGTGAAGTACG
SKM_PR1055	SAP1 CHIP R23	GATCCGCTTATGTGCACACAG
SKM_PR1056	SAP1 CHIP Control F	GGTGGGTCAACGTGAGGCAG
SKM_PR1057	SAP1 CHIP Control R	GGGCAAAAACCATTTCTTGAAGG
SKM_PR1354	<i>ypt5</i> Exon 1 F	ATGGCATCAAATACAGCTCC
SKM_PR1355	<i>ypt5</i> Exon 4 R	CAAATTTTCGAGTTTTACGGAAGTG
SKM_PR1356	<i>kap114</i> Exon 1 F	ATGGTTGAAAGCAAATCATTAAAGC
SKM_PR1357	<i>kap114</i> Exon 3 R	GCAAGTTGAGGTGCAATAATAAAG
SKM_PR1463	<i>mug161</i> splicing check F	CAAGCGTACAACACTAGTGCGG
SKM_PR1464	<i>mug161</i> splicing check R	AATGGACTCTGGCAAACCAGC
SKM_PR1551	<i>RPL14A</i> F	CCACCGATTCTATTGTCAAGG
SKM_PR1552	<i>RPL14A</i> R	GCCTTAGCCAAAGCCTTCTTG
SKM_PR1553	<i>RPL7A</i> F	AAAATCTTGACCCCAGAATCTC
SKM_PR1554	<i>RPL7A</i> R	GTTCATGGACTTAACCAATTTGTTG

SKM_PR1555	<i>RPL34B</i> F	ATGGCTCAACGTGTTACTTTCAG
SKM_PR1556	<i>RPL34B</i> R	CTTCTTTTCAGACTTCTTAGCAGC
SKM_PR1557	<i>SNR17B</i> F	CTTTTTACTAAAAAATTGTGCGACGTACTTC
SKM_PR1558	<i>SNR17B</i> R	CTTGTCAGACTGCCATTTGTACC
SKM_PR1559	<i>RPL30</i> F	CTTATTCAATTAATCAATATACGCAGAGAT
SKM_PR1560	<i>RPL30</i> R	GCCAAGGTGGTCAAGATATC
SKM_PR1561	<i>RPL43B</i> F	CAGCATAGATAATCAAACAAAAAAT
SKM_PR1562	<i>RPL43B</i> R	GCTTCAACCATTTCTCTTAATCTTC
SKM_PR1681	<i>SRC1</i> F	CGAGAGTGGTATGACGGAAG
SKM_PR1682	<i>SRC1</i> R	CATTAGCCATATTGGCCTTTG
SKM_PR2594	<i>pst2</i> F	ATGGAACAAACACTAGCGATATTAA
SKM_PR2595	<i>pst2</i> R	GAAGTTGGCACCGCTATTCG
SKM_PR2598	<i>zas1</i> F	CCCTGTGGGTCTATCAAGC
SKM_PR2599	<i>zas1</i> R	CATTTCCCTTGGATAATAATTGTTGTATG
SKM_PR2600	<i>clr6</i> F	GGGCTGTACGAATTTTGTTTC
SKM_PR2601	<i>clr6</i> R	CCTGTTCCAATTCCGGTGTC
SKM_PR2602	<i>clr6</i> F	GACACCGGAATTGGAACAGG
SKM_PR2603	<i>clr6</i> R	CGAATCAAGATACTGCCGAG
SKM_PR2606	<i>cdk9</i> F	GAAACGCTCAAGCAGCGTTTC
SKM_PR2607	<i>cdk9</i> R	GAACCACGACGTCGATGCTTC
SKM_PR2280	<i>hri2</i> -F	GCGGATGCTTTTAACTGCTTTG
SKM_PR2281	<i>hri2</i> -R	TCAAATACATTGGTGGGATCGG
SKM_PR2282	<i>Sp mms1</i> -F	GCAACTCCCAAGAGATTACTTG
SKM_PR2283	<i>Sp mms1</i> -R	GCGAAGTTCTATAGCATTGCTG
SKM_PR2400	<i>hse1 I2</i> F	ATGTTTCGAGGAAAACCCAAC
SKM_PR2401	<i>hse1 I2</i> R	GAGTCACTAGCTATTTTCAAAGAG

SKM_PR2624	<i>Act1-Cup1</i> E1 F	CGAAAATTTACTGAATTAACAATGGATTCTG
SKM_PR2625	<i>Act1-Cup1</i> I F	GGAATAAATAGGGGCTTGAAATTTGG
SKM_PR2626	<i>Act1-Cup1</i> E2 F	GGTTGCTGCTTTGGTTATTG
SKM_PR2627	<i>Act1-Cup1</i> E2 R	CAGGGGCATTTGTCGTCGCTG
SKM_PR2654	<i>Sc ACT1</i> E1 F	GAAAATTTACTGAATTAACAATGGATTCTG
SKM_PR2655	<i>Sc ACT1</i> E2 R	CTTTTTGACCCATACCGACC

5.2 Methods

5.2.1 Strain maintenance

Yeast and bacterial strains were grown overnight in YPAD/ Selection media and LB broth to reach the stationary phase at 30°C and 37°C, respectively. The overnight grown cultures were then mixed in 1:3 ratios with 50% (v/v) sterile glycerol and stored at -80°C. Cells for later experiments could be revived from the stock on YPAD and LB plates.

5.2.2 Yeast genomic DNA isolation

Cells were grown over-night in 5ml rich media broth at 30°C. Cells were harvested by centrifugation at 3000 rpm for 5 mins at room temperature. 200 µl of lysis buffer and 200 µl phenol:chloroform:isoamyl alcohol (PCI) was added. Cells were lysed by adding glass beads and vortexing for 5 min with incubation of 1 min of ice. 200 µl of TE (Tris-Cl, EDTA) buffer was added to the mixture and centrifuged at maximum speed at room temperature for 10 mins. The supernatant was transferred to a new tube and 200µl of chloroform was added. The mixture was vortexed and centrifuged again at maximum speed at room temperature for 5 mins. The aqueous layer was transferred to a new tube with 1 ml 100% ethanol. The mixture was incubated for 20 min at -20°C and then centrifuged at maximum speed at 4°C for 10 mins. The supernatant was discarded and the pellet was dissolved in 200 µl TE buffer. 1 µl of RNase A was added and mixture was incubated at 37°C for 1.5 hours. 1 µl of proteinase K was added to it and again incubated at 37°C for another 1.5 hours. Then 20 µl of 4 m ammonium acetate with 1ml 100% ethanol was added to the tube and incubate at -20°C for 1 hour for precipitation. After precipitation, the tube was centrifuged at 4°C for 10 mins at maximum speed. The supernatant was discarded and the pellet washed with 70% ethanol by centrifugation. The supernatant was discarded and tubewas completely dried to remove any ethanol. Lastly, the pellet was dissolved in 50 µl of water and store at -20°C.

5.2.3 Yeast competent cell preparation

Cells were grown overnight in 5ml synthetic or rich media at 30°C. 50ml rich media was re-inoculated to an OD₆₀₀ 0.2. Cells were incubated at 30°C till OD₆₀₀ reaches 0.6-0.8. Cells were harvested by centrifugation at 3000 rpm for 5 mins at room temperature. The supernatant was discarded and the pellet was washed with half volume of sterile water. Next, the pellet was washed with one-tenth volume of SORB by centrifugation. The supernatant was discarded. 360ul of SORB and 40ul of denatured salmon sperm DNA (10mg/ml stock solution) were added and the pellet resuspended in it. Cells were aliquoted in MCTs and stored at -80°C.

5.2.4 Yeast transformation

10 µl of competent cell and 1-2 µl of a plasmid were mixed in a sterile tube. 6 fold sterile 40% PEG mix was added. The components were vortexed and incubated at 30°C for 30 mins. The sample was given a heat shock at 42°C for 25 min (*S. cerevisiae*) or 5 mins (*S. pombe*). Following heat shock, cells were kept on ice 5 mins. The complete mixture was spread on the selection plate and incubated at 30°C till colonies appear.

5.2.5 QuikChange Site-directed mutagenesis

All site-directed point mutations, insertions, and deletions on plasmids were done by following this protocol (Agilent). We used specific primers that harbour the desired mutation and high fidelity *Pfu* DNA polymerase. The flanking unmodified nucleotide sequences annealed to the opposite strands of the plasmid and amplified the plasmid with the incorporation of the mutation. The mutagenesis PCR ran for 18 cycles and had a denaturation at 98°C, annealing of 1 min at 55°C and an extension of 2 mins/kb of plasmid at 68°C. The amplified mixture was then treated with 1µl Dpn1 for 3 hours or more at 37°C to cleave off the parent template. At last, 5-10 µl of the Dpn1 treated product was transformed in 100 µl of XL1-blue competent cell and plated to selection media plates.

5.2.6 Overlap extension (SOE) PCR

Some of the mutants of *Sap1*, *Snu66*, and *SRC1* ss were generated by overlap extension (SOE) PCR method¹⁷¹. Two fragments of a gene were amplified by Phusion polymerase PCR with overlapping regions that incorporated the desired mutation. Then, SOE PCR with vent polymerase was performed using a mixture of amplicons of initial PCRs as templates with primers having restriction enzyme sites. Subsequently, the final SOE amplicon was cloned in the required plasmid and for assays.

5.2.7 Deletion and tagged strain generation

PCR-based deletion and tagging were done as per the protocol reported in ¹⁷². Perform a PCR with long primers with flanking regions of genes to be tagged or deleted using a selection marker cassette. Precipitate the PCR products with 3M NaOAc (pH 5.3) and 100% ethanol over-night at -20°C. Transform competent cells with 10µl of precipitated product and incubate at 30°C for 3-4 days.

Mating based deletion or tagging was used to generate double mutants or double-tagged strain. Use the opposite mating type of single mutants or tagged strains to obtain diploids. Once you have generated heterozygous diploids, put them on potassium acetate sporulation media (broth/plate) and incubate at 25°C for 4-5 days. Check for spores under a microscope at 60X magnification. Once the cells sporulate, due to stress, dissect them into individual spores with a dissection microscope. To prepare the cells for dissection, dissolve some cells from potassium acetate media into 9µl of 1M sorbitol and add 1µ of zymolyase. Incubate at 37°C for 15-20 mins. This will loosen the cell wall around the spore, making it easier to separate the spores during dissection. Put on ice for 5 mins to spot reaction. Add 50-100µl MQ to dilute the cells. Put 10-12µl on YPAD plate and roll down the cells to make a smear. Proceed for dissection.

5.2.8 Trichloroacetic acid (TCA) precipitation

Cells were grown to log phase and 1 OD₆₀₀ cells were harvested by centrifugation at 5000 rpm for 5 min. Pellet was resuspended in freshly prepared 1 ml solution of 2N NaOH and 7.5% β-mercaptoethanol. The components were mixed by vortexing and kept on ice for 10 mins. 200ul of 55% TCA solution was added and mixed by vortexing. Mixture was kept on ice for another 10 mins. Mixture was centrifuged at 14000 rpm at 4°C for 15 mins. Supernatant was discarded and tube was spun for 2 mins. Remaining TCA was removed by vaccusip. 50ul HU buffer with 1.5% DTT was added and the pellet was heated at 65°C for 10 mins at 1300 rpm. The sample was vortexed and centrifuged at 14000 rpm at room temperature for 5 mins and load 10ul on an SDS-PAGE gel.

5.2.9 Western blot assays (WB)

10 µl of isolated protein was loaded on SDS-PAGE and run at 100V. Proteins were transferred from gel to PVDF membrane using a semi-dry transfer method for 2.5 hour at 110mA. Following transfer, membrane was blocked with 5% skimmed milk on rotation for 1 hour at room temperature. The membrane was washed once with TBST and primary antibody (diluted in TBST) was added to it. It was then incubated for 3 hours on rotation at room temperature or over-night at 4°C with sodium azide. The membrane was washed with TBST 3 times 5 min each on rotation. HRP conjugated secondary antibody (diluted in skimmed milk) was added to membrane and incubated for 1 hour on rotation at room temperature. The membrane was washed with TBST 3 times 5 min each. Membrane was treated with ECL solution A (luminol) and B (peroxide) for 1 min and proceed to develop blot.

5.2.10 Co-immunoprecipitation (Co-IP) assay

Culture was grown to O.D₆₀₀ 0.8 (secondary culture). 100 O.D₆₀₀ cells were harvested at 3000 rpm for 10 mins at 4°C. Cells were washed once with 1X PBS at 3000 rpm for 10 mins at 4°C. Cell pellet was resuspended in 500µl lysis buffer (1µM PMSF, protease inhibitor cocktail, and 1% triton X 100) and freeze in liquid nitrogen and store at -80°C.

Mortar and pestle wash cleaned with 80% ethanol and cool down with liquid nitrogen. Pellet was quickly thawed by adding 300µl lysis buffer (1µM PMSF, protease inhibitor cocktail, and 1% triton X 100). Cell suspension was dropped into liquid nitrogen containing mortar and grinded until fine powder; liquid nitrogen was added if needed. After thawing the lysate was transferred in a MCT. The mortar was rinsed with 200 µl lysis buffer, and transferred to the MCT. The lysate was cleared by centrifugation at 5000 rpm for 10 mins at 4°C.

Transfer supernatant to another MCT. 20 µl of supernatant was separated as input control, to which 20µl HU buffer was added and denatured at 65°C for 10 mins. To the rest of the supernatant, 15 µl antibody beads (HA or MYC) to each tube (Dilute bead in lysis buffer and distribute 50µl), was added and kept on rotation for 3-4 hr at 4°C. Samples were washed 1X with 800 µl lysis buffer (1µM PMSF, protease inhibitor cocktail, and 1% triton X 100) diluted 10, 3X with 800 µl lysis buffer with 1% triton X 100, and 1X with 800 µl lysis buffer at 3000 rpm for 2 mins at 4°C. Supernatant was removed completely with vaccusip. 20 µl HU buffer was added to pellet and denatured at 65°C for 10 mins. Samples were loaded on SDS-PAGE and proceed to western blot.

Lysis Buffer:

Sodium Chloride (150mM)	0.876
Magnesium Chloride (5mM)	0.101
Tris pH 7.5 (50mM)	5 ml
Glycerol (10%)	5 ml
MilliQ	Up to 100 ml

5.2.11 RNA isolation and RT-PCR

RNA precipitation:

Secondary culture till O.D₆₀₀ 0.5 was grown, heat shocked at 37°C for 15 mins and 5 O.D₆₀₀ cells were filter-collected. Samples were frozen in liquid nitrogen and stored at -80°C to proceed later.

The pellet was resuspended in 2ml acid phenol; then 2ml AES buffer (50mM NaOAc(5.3), 10mM EDTA, 1% SDS) was added and vortexed well. Samples were incubated 5-7 minutes in 65°C water bath, and vortexed every minute. Incubate on ice for 5 mins. During incubation, 15ml phase-lock tubes were spun briefly at 4750 rpm at 4°C. 1ml chloroform was added to the phase lock tubes. The cell mixture was transferred to the pre-spun phase-lock tubes. The tubes were spun at 4750 rpm for 5 mins at 4°C. 2ml Phenol:Chloroform:IAA (25:24:1) was added and mixed by inverting tubes 3-4 times. The tubes were spun again at 4750 rpm for 5 mins at 4°C. 2ml chloroform was added to the tube, mixed by inverting, and spun again at 4750 rpm for 5 mins at 4°C. The supernatant was poured into a fresh 15ml falcon, and 200µl 3M NaOAc (5.3), and 2.4ml isopropanol was added (can be stored at -20°C). 2ml RNA precipitate was transferred in an MCT and precipitated at 14,000 rpm for 20 min at 4°C. The supernatant was discarded and pellet was washed with 1ml 70% ethanol by centrifuging at 14,000 rpm for 5 mins at 4°C. The supernatant was discarded and pellet was dried in speed vac at 25°C 2000 rpm for 10-15 mins. The RNA pellet was dissolved in 50µl water and concentration was measured.

114

DNase treatment:

To treat 20µg of RNA in a 50µl reaction volume, added:

RNA - 20µg

DNase - 5µl

10X DNase buffer - 5µl

Nuclease free water (NFW) – made volume up to 50µl.

The mixture was vortexed and incubated at room temperature for 15 mins. 5-7 volumes of RNA binding buffer (2M guanidium-HCl, 75% isopropanol) was added and vortexed. Zymo spin column was assembled. The sample mixture was transferred and spun for 1 min at 14,000 rpm and flow-through was discarded. 200µl wash buffer (10mM Tris pH 8.5, 80% ethanol) was added and spun again for 1 min at 14,000 rpm. The flow-through was discarded

and step was repeated once more. A dry spin for 1 min at 14,000 rpm was given to remove any residual ethanol. A column was placed in a fresh 1.5ml MCT, and 30µl NFW was added. The sample was incubated for 1 min, and then spun for 1 min at 14,000 rpm. Concentration was measured and proceeded with cDNA synthesis.

cDNA synthesis:

To synthesize cDNA for 3µg RNA in 30µl reaction volume, added:

RT buffer- 3 µl

Hexameric primers- 3 µl

DNase treated RNA- 3 µg

NFW- made volume up to 26 µl

The mixture was incubated at 60°C for 5 mins to denature RNA secondary structure and anneal primers to RNA. The mixture was kept on ice for 5 mins and dNTP- 3 µl and reverse transcriptase- 1 µl were added. The mixture was incubated at 42°C over-night.

5.2.12 Real-time quantitative PCR

Quantitative-PCRs (qPCR) were performed using SYBR green dye-based reagents from Roche. The reactions were performed in triplicates/quadruples to normalize pipetting or handling errors. *STE2* in *S. cerevisiae* and *act1* in *S. pombe* was used as a control, and relative expression of the gene of interest was normalized with respect to these house-keeping genes' expression.

5.2.13 Splicing reporter assays

The growth of different chromosomal variants of Snu66 in yJU75 genetic background transformed with *ACT1-CUPI* plasmid reporters (harbouring different 5'ss mutations) was monitored in CuSO₄ containing media as described in ⁹⁶. The splicing reporter assays in *S.pombe* were performed as described in Anil et al. (unpublished). Site-directed mutagenesis was used to generate the GUAUUAU variant of the tho5-intron in the splicing reporter.

5.2.14 Growth assay

Dilution spotting: The growth assays for yeast was performed by spotting fivefold serial dilution of indicated strains with or without transformed plasmids. Different conditions were tested using different media plates indicated in the figure and composition described in section

Growth curve: The growth rate experiments were done in liquid media. The over-night grown primary culture was diluted to 0.2 OD₆₀₀ secondary cultures, and OD₆₀₀ was measured every 3 hours for a total of 48 hours. Once the OD₆₀₀ increased, more than the measurable limit of the spectrometer cells was diluted before measuring the OD₆₀₀, and the dilution factor multiplied to the obtained value.

5.2.15 Splicing sensitive microarray

Log-phase cells grown at 30°C, post diauxic shift, 37°C (15 mins), and in glycerol containing media were harvested. Total RNA was isolated by hot acid phenol method and cDNA was synthesized. cDNA from different strains to be compared were labelled with cy3 and cy5 dyes and mixed. A second batch of dyes swapped samples was prepared. Samples were hybridized to splicing sensitive microarrays having intron-, exons, and junction specific probes. The relative abundance of transcripts between wild type and mutant/deletion strain was compared.

5.2.16 ONPG assay

Secondary culture at 0.2 O.D.₆₀₀ from an overnight grown primary culture was inoculated. O.D.₆₀₀ was measured and 1 ml culture was harvested in an MCT for 0, 1, and 3 hour time interval. Samples were harvested in triplicates and the cells were pelleted. Cells were resuspended in 500 µl of Z-buffer. 50 µl of 0.1% SDS was added and vortexed vigorously for 15 secs. 50 µl of chloroform was added and vortexed again for 15 secs. 100 µl of freshly made ONPG (4 µg/ml) was added, vortexed, and incubated at 37°C for 2-30 mins. The reaction was quenched with 500 µl of 1M Na₂CO₃.

The cells were pelleted at maximum speed and the supernatant was carefully removed to a clean tube. O.D₄₂₀ of the supernatant was measured against a blank containing Z-buffer, ONPG, and Na₂CO₃. The incubation time or volume of cells was adjusted if yellow colour developed strongly. The unit of β-galactosidase activity was calculated by the following formula

$$\text{Units of } \beta\text{-galactosidase activity} = 1000 \cdot \text{OD}_{420} / V \cdot t \cdot \text{OD}_{600}$$

Where V=volume of cells and t= time of incubation in mins.

Buffer Z (pH 7.0)

Na ₂ HPO ₄	4.7 g
NaH ₂ PO ₄ .H ₂ O	2.75 g
KCl	0.375 g
MgSO ₄ .7H ₂ O	0.125 g
MilliQ	Up to 500 ml

For working, Z-buffer 0.14 ml of β-mercaptoethanol to 50 ml Z-buffer from stock was added.

5.2.17 Northern blot assay

117

Preparation of template DNA for radiolabelling

A PCR DNA fragment from genomic DNA complementary to your gene of interest was generated. PCR product was purified by clean up kit and measure concentration. DNA from PCR (50 ng) and 30 μl random primer were mixed. The mixture was incubated at 95°C for 5 min, and then cooled on ice. 4 μl dCTP, dGTP, dTTP and 10 μl [α-³²P] dATP, 26 μl water, and 1.5 μl Klenow enzyme buffer were added. 1 μl Klenow enzyme was added and the reaction mixture was incubated for 1 hr at 25°C. 10 μl reaction stop buffer was added. To remove unincorporated radiolabelled nucleotide the mixture was purified using Sephadex G-25 column. 35 μl of 1X TE buffer was added to the mixture and loaded onto G-25 column equilibrated in TE buffer. 30 μl elute was collected in a fresh tube.

Running polyacrylamide-urea gel and blotting

Gel was casted as given below and left overnight. Gel was pre-run for 30-45 mins at 60V, after wells were washed with water, and 1X TBE buffer to remove accumulated urea. Extracted RNA sample was prepared for loading by adding 2X sample buffer (96%

formamide + EDTA + bromophenol blue) and heating at 95°C for 2 mins. The sample was flash cooled on ice for 5 mins. Gel was stopped, wells were rewashed, and 10 µl sample was loaded. The gel was run at 60V till dye reaches the end. Gel was separated and set for transfer on nitro-cellulose membrane sandwiched between layers off Whatman paper, leaving no air bubbles. 0.5% buffer was used at 150mA current for 2 hours. After transfer, RNA was cross-linked on the membrane using UV cross-linker with 1.2J energy. The membrane was put in a roller bottle for pre-hybridization at 42°C for 1-2 hours. The buffer was discarded and fresh hybridization buffer was added with radiolabelled probe and left overnight at 42°C on rolling. Buffer with probe was discarded properly and membrane was washed twice with low stringency (0.1X SSC, 0.1% SDS, and 150 ml water) buffer at 25°C for 10 mins each on rolling. Membrane was washed twice with high stringency buffer (2X SSC, 0.1% SDS, and 50ml water) at 42 for 10 min each on rolling. **(Discard the buffers properly after washes).** Membrane was put in between saran wrap foils and proceeded for blot development. The films were exposed for 1 and 4 hours or as suitable.

Polyacrylamide-Urea Gel (8% gel)

Urea - 4.8 g
 TBE - 2 ml
 Acrylamide - 2 ml
 Water – make volume up to 10 ml
 10% APS – 100 µl
 TEMED – 15 µl

5X TBE

Tris base	54 g
Boric acid	27.5 g
0.5M EDTA (pH 8)	20 ml
MilliQ	Up to 1000 ml

20X SSC Buffer (pH 7)

3M NaCl	175 g
0.3M sodium citrate	88 g
MilliQ	Up to 1000 ml

Sterilize by autoclaving.

5.2.18 Microscopy

5 ml of secondary culture of tagged cells were grown till 0.5-0.6 OD₆₀₀. 1µl DAPI was added to the cell for 30 mins. 100µl of cells were harvested by centrifugation and washed 2 times with PBS. Cells were dissolved in 100µl of synthetic media so that cells don't die. To prepare slides little agarose was heated in 1ml of water, and after it dissolved, 20µl was put on a glass slide. A second glass slide was put on top of it and pressed gently such that the agarose forms a thin layer. Once the agarose solidified, the slide on top was pushed away very gently and carefully. Now 10µl of cells were put on the agarose layer such that it covers the complete thin layer. A cover slide was placed carefully on top and proceeded with visualization.

5.2.19 Ni-NTA pull-down assay

Cells (100 OD) were harvested at 3000 rpm for 10 min at 4°C (harvest 1OD for TCA-prep as input control). The supernatant was discarded and washed with water at 2500g for 5 mins at 4°C. Pellets were frozen in liquid nitrogen and stored in -80°C.

The cells were lysed on ice with 6 ml 1.91 N NaOH (45ml) and 7.5% (v/v) β-mercaptoethanol (5ml), vortexed, and incubated 15 min on ice. An equal volume of 55% TCA was added, vortexed, and incubated again for 15 mins on ice. The mixture was centrifuge for 15 mins at 2500g at 4°C. The pellet was washed 2X with 5ml acetone (pre-chilled at -20°C) for 5 min 2500g at 4°C. The pellet was resuspended with 12ml buffer A/ 0.05% tween 20 by pipetting up and down with 10ml pipette. The mixture was transferred in Oakridge centrifuge tube, shaken for 1 hour at room temperature at 15 rpm on rotator wheel. It was then centrifuged for 30 min at the highest speed at 4°C. The supernatant was transferred in 14ml falcon by decanting carefully. 48µl 5M imidazole (20mM) was added. 50µl Ni-NTA magnetic agarose beads (Qiagen) were added. The sample was rotate for 1 hour at room temperature at 10 rpm. A magnetic rack was used to pellet the bead, the supernatant was sucked off, and the beads were transfred into 1.5ml MCT. The sample was washed 3X with 800µl buffer A, 0.05% tween 20, 20mM imidazole. Then the sample was washed 5X with 800µl buffer C. 0.05% tween 20. The sample was transferred into a new tube with 100µl buffer C, put on a magnetic rack, and the supernatant sucked off. The sample was eluted with 30µl 1% SDS for 10 mins at 65°C. The tube was placed on a magnetic rack to precipitate beads, and elute was transferred to a new tube. The elute was dried in speed vac at 45°C for 25

mins. 10µl water was added to dissolve the pellet. 25µl HU buffer was added, and the pellet was denatured at 65°C for 10 mins. The sample was loaded on SDS-PAGE.

Buffer A

6 M Guanidium Chloride	573.24 g
100mM NaH ₂ PO ₄ ·2H ₂ O	15.6 g
10mM tris	5ml (2M)/1.21 g
pH (NaOH)	8.0
MilliQ	1000 ml

Buffer C

8 M Urea	240.2 g
100mM NaH ₂ PO ₄ ·H ₂ O	6.9 g
10mM tris	2.5ml (2M)/0.606 g
pH (HCl)	6.3
MilliQ	500 ml

5.2.20 Chromatin immunoprecipitation (Ch-IP) assay

120 Secondary culture was grown until it reaches the log phase (0.8-1.0) OD₆₀₀ and 37% formaldehyde was added such that the final concentration in culture is 1%. The culture was incubated at room temperature with occasional shaking for 15-40 mins (needs to be optimized to maximize signal to noise ratios).

2.5M glycine was added to a final concentration of 125 mM and the mixture was incubated at room temperature for 5 mins. Cells were spun down and suspended in 30-40 ml ice-cold TBS (20mM Tris-HCl pH7.5, 150mM NaCl). Cells were washed for 3-4 times to completely remove formaldehyde. Cells were resuspended in 2 ml lysis buffer and proceeded for sonication using. Cell lysate was spun down and debris was removed for 5 min at full speed. Pre-immuno-precipitate sample were separated (1/20 volume of total). The rest of the supernatant was transferred to fresh MCT and suspension of antibody beads was added. The sample was rotated for 4 hours at 4°C. Before adding the beads were washed 2 times with 1ml lysis buffer, 2 times with 1ml lysis buffer + 360mM NaCl, 2 times with 1ml wash buffer, and once with 1ml TE buffer.

The sample was spun for 3 mins at 5000 rpm and the supernatant was completely discarded. 250µl elution buffer was added and the sample was incubated at 65°C for 10 min on shaking. The sample was spun at room temperature for 10 secs, 30µl of supernatant was transferred to new MCT, and proceeded with reversion of crosslinking. To the remaining elute, the same volume of HU buffer was added. The sample was incubated at 95°C for 30 min. 230µl of TE, 1% SDS was added to sample and incubated at 65°C overnight. 140µl of TE, 2µ of 10mg/ml glycogen, and 7.5µl of 20mg/ml proteinase K was added to sample, and incubated at 37°C for 2 hours. The sample was washed twice with Phenol:Chloroform:IAA and once with chloroform. 50µl 3M NaOAc and 2 volume of ethanol was added. The mixture was vortexed and incubated at -20°C for 15 min. The mixture was spun at 4° at 12000 rpm for 10 mins. The supernatant was discarded and the pellet was washed with 70% ethanol. The pellet was dried completely and dissolved in 30µl TE containing RNase A. The sample was incubate at 37°C for 1 hour and proceeded for PCR.

Appendix



Thank you for your order!

Dear Ms. Poulami Choudhuri,

Thank you for placing your order through Copyright Clearance Center's RightsLink® service.

Order Summary

Licensee:	Ms. Poulami Choudhuri
Order Date:	Oct 15, 2020
Order Number:	4930061122009
Publication:	Science
Title:	Structure of a yeast step II catalytically activated spliceosome
Type of Use:	Thesis / Dissertation
Order Total:	0.00 USD

123

View or print complete [details](#) of your order and the publisher's terms and conditions.

Sincerely,

Copyright Clearance Center

Tel: +1-855-239-3415 / +1-978-646-2777
customercare@copyright.com
<https://myaccount.copyright.com>



RightsLink®



Thank you for your order!

Dear Ms. Poulami Choudhuri,

Thank you for placing your order through Copyright Clearance Center's RightsLink[®] service.

Order Summary

Licensee:	Ms. Poulami Choudhuri
Order Date:	Oct 15, 2020
Order Number:	4930061292389
Publication:	Science
Title:	Structure of a human catalytic step I spliceosome
Type of Use:	Thesis / Dissertation
Order Total:	0.00 USD

View or print complete [details](#) of your order and the publisher's terms and conditions.

124

Sincerely,

Copyright Clearance Center

Tel: +1-855-239-3415 / +1-978-646-2777
customercare@copyright.com
<https://myaccount.copyright.com>



RightsLink[®]

SPRINGER NATURE

Thank you for your order!

Dear Ms. Poulami Choudhuri,

Thank you for placing your order through Copyright Clearance Center's RightsLink® service.

Order Summary

Licensee: Ms. Poulami Choudhuri
Order Date: Oct 19, 2020
Order Number: 4932300061097
Publication: Nature
Title: Cryo-EM structure of the yeast U4/U6.U5 tri-snRNP at 3.7 Å resolution
Type of Use: Thesis/Dissertation
Order Total: 0.00 USD

125

View or print complete [details](#) of your order and the publisher's terms and conditions.

Sincerely,

Copyright Clearance Center

Tel: +1-855-239-3415 / +1-978-848-2777
customer@copyright.com
<https://myaccount.copyright.com>



RightsLink®



Thank you for your order!

Dear Ms. Poulami Choudhuri,

Thank you for placing your order through Copyright Clearance Center's RightsLink® service.

Order Summary

Licensee: Ms. Poulami Choudhuri
Order Date: Oct 19, 2020
Order Number: 4932291056793
Publication: Science
Title: Structure of the Cdo48 segregase in the act of unfolding an authentic substrate
Type of Use: Thesis / Dissertation
Order Total: 0.00 USD

126

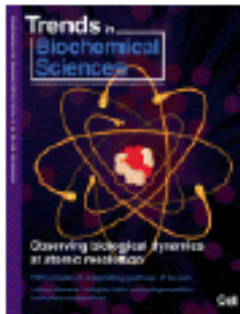
View or print complete [details](#) of your order and the publisher's terms and conditions.

Sincerely,

Copyright Clearance Center

Tel: +1-855-239-3415 / +1-978-646-2777
customercare@copyright.com
<https://myaccount.copyright.com>





Thank you for your order!

Dear Ms. Poulami Choudhuri,

Thank you for placing your order through Copyright Clearance Center's RightsLink® service.

Order Summary

Licensee:	Ms. Poulami Choudhuri
Order Date:	Oct 19, 2020
Order Number:	4932480169598
Publication:	Trends in Biochemical Sciences
Title:	Staying on message: ensuring fidelity in pre-mRNA splicing
Type of Use:	reuse in a thesis/dissertation
Order Total:	0.00 USD

127

View or print complete [details](#) of your order and the publisher's terms and conditions.

Sincerely,

Copyright Clearance Center

Tel: +1-855-239-3415 / +1-978-646-2777
customer@copyright.com
<https://myaccount.copyright.com>



RightsLink®

References

1. Brody, E. & Abelson, J. The ‘spliceosome’: yeast pre-messenger RNA associates with a 40S complex in a splicing-dependent reaction. *Science* (80-.). **228**, 963 LP – 967 (1985).
2. Lin, R. J., Newman, A. J., Cheng, S. C. & Abelson, J. Yeast mRNA splicing in vitro. *J. Biol. Chem.* **260**, 14780–14792 (1985).
3. Parker, R. & Guthrie, C. A point mutation in the conserved hexanucleotide at a yeast 5' splice junction uncouples recognition, cleavage, and ligation. *Cell* **41**, 107–118 (1985).
4. Domdey, H. *et al.* Lariat structures are in vivo intermediates in yeast pre-mRNA splicing. *Cell* **39**, 611–621 (1984).
5. Jurica, M. S. & Moore, M. J. Pre-mRNA Splicing: Awash in a Sea of Proteins. *Mol. Cell* **12**, 5–14 (2003).
6. Matera, A. G. & Wang, Z. A day in the life of the spliceosome. *Nat. Rev. Mol. Cell Biol.* **15**, 108–121 (2014).
7. De Conti, L., Baralle, M. & Buratti, E. Exon and intron definition in pre-mRNA splicing. *Wiley Interdisciplinary Reviews: RNA* **4**, 49–60 (2013).
8. Burke, J. E., Sashital, D. G., Zuo, X., Wang, Y.-X. & Butcher, S. E. Structure of the yeast U2/U6 snRNA complex. *RNA* **18**, 673–683 (2012).
9. Absmeier, E., Santos, K. F. & Wahl, M. C. Functions and regulation of the Brr2 RNA helicase during splicing. *Cell Cycle* **15**, 3362–3377 (2016).
10. de Almeida, R. A. & O’Keefe, R. T. The NineTeen Complex (NTC) and NTC-associated proteins as targets for spliceosomal ATPase action during pre-mRNA splicing. *RNA Biol.* **12**, 109–114 (2015).
11. Fourmann, J.-B. *et al.* Dissection of the factor requirements for spliceosome disassembly and the elucidation of its dissociation products using a purified splicing system. *Genes Dev.* **27**, 413–428 (2013).
12. Chathoth, K. T., Barrass, J. D., Webb, S. & Beggs, J. D. A Splicing-Dependent Transcriptional Checkpoint Associated with Prespliceosome Formation. *Mol. Cell* **53**, 779–790 (2014).
13. Semlow, D. R. & Staley, J. P. Staying on message: ensuring fidelity in pre-mRNA splicing. *Trends Biochem. Sci.* **37**, 263–273 (2012).
14. Cordin, O. & Beggs, J. D. RNA helicases in splicing. *RNA Biol.* **10**, 83–95 (2013).
15. Liang, W.-W. & Cheng, S.-C. A novel mechanism for Prp5 function in prespliceosome formation and proofreading the branch site sequence. *Genes Dev.* **29**, 81–93 (2015).
16. Strauss, E. J. & Guthrie, C. PRP28, a ‘DEAD-box’ protein, is required for the first step of mRNA splicing in vitro. *Nucleic Acids Res.* **22**, 3187–3193 (1994).
17. Staley, J. P. & Guthrie, C. An RNA Switch at the 5' Splice Site Requires ATP and the

DEAD Box Protein Prp28p. *Mol. Cell* **3**, 55–64 (1999).

18. Maeder, C., Kutach, A. K. & Guthrie, C. ATP-dependent unwinding of U4/U6 snRNAs by the Brr2 helicase requires the C terminus of Prp8. *Nat. Struct. Mol. Biol.* **16**, 42–48 (2009).
19. Hahn, D., Kudla, G., Tollervey, D. & Beggs, J. D. Brr2p-mediated conformational rearrangements in the spliceosome during activation and substrate repositioning. *Genes Dev.* **26**, 2408–2421 (2012).
20. Bao, P., Höbartner, C., Hartmuth, K. & Lührmann, R. Yeast Prp2 liberates the 5' splice site and the branch site adenosine for catalysis of pre-mRNA splicing. *RNA* **23**, 1770–1779 (2017).
21. King, D. S. & Beggs, J. D. Interactions of PRP2 protein with pre-mRNA splicing complexes in *Saccharomyces cerevisiae*. *Nucleic Acids Res.* **18**, 6559–6564 (1990).
22. Zhang, X. *et al.* Structure of the human activated spliceosome in three conformational states. *Cell Res.* **28**, 307–322 (2018).
23. Plaschka, C., Lin, P.-C. & Nagai, K. Structure of a pre-catalytic spliceosome. *Nature* **546**, 617–621 (2017).
24. Tseng, C.-K., Liu, H.-L. & Cheng, S.-C. DEAH-box ATPase Prp16 has dual roles in remodeling of the spliceosome in catalytic steps. *RNA* **17**, 145–154 (2011).
25. Schwer, B. & Meszaros, T. RNA helicase dynamics in pre-mRNA splicing. *EMBO J.* **19**, 6582–6591 (2000).
26. Schwer, B. A conformational rearrangement in the spliceosome sets the stage for Prp22-dependent mRNA release. *Mol. Cell* **30**, 743–754 (2008).
27. Fourmann, J.-B., Tauchert, M. J., Ficner, R., Fabrizio, P. & Lührmann, R. Regulation of Prp43-mediated disassembly of spliceosomes by its cofactors Ntr1 and Ntr2. *Nucleic Acids Res.* **45**, 4068–4080 (2017).
28. Tauchert, M. J., Fourmann, J.-B., Lührmann, R. & Ficner, R. Structural insights into the mechanism of the DEAH-box RNA helicase Prp43. *Elife* **6**, e21510 (2017).
29. Fourmann, J.-B. *et al.* The target of the DEAH-box NTP triphosphatase Prp43 in *Saccharomyces cerevisiae* spliceosomes is the U2 snRNP-intron interaction. *Elife* **5**, e15564 (2016).
30. Nguyen, T. H. D. *et al.* CryoEM structure of the yeast U4/U6.U5 tri-snRNP at 3.7 Å resolution. *Nature* **530**, 298–302 (2016).
31. Yan, C. *et al.* Structure of a yeast spliceosome at 3.6-angstrom resolution. *Science (80-.)*. **349**, 1182–1191 (2015).
32. Yan, C., Wan, R., Bai, R., Huang, G. & Shi, Y. Structure of a yeast activated spliceosome at 3.5 Å resolution. *Science (80-.)*. **353**, 904 LP – 911 (2016).
33. Rauhut, R. *et al.* Molecular architecture of the Saccharomyces cerevisiae activated spliceosome. *Science (80-.)*. **353**, 1399 LP – 1405

- (2016).
34. Wan, R., Yan, C., Bai, R. & Huang, G. Structure of a yeast catalytic step I spliceosome at 3.4 Å resolution. **1941**, (2014).
 35. Zhan, X., Yan, C., Zhang, X., Lei, J. & Shi, Y. Structure of a human catalytic step I spliceosome. *Science (80-.)*. **359**, 537 LP – 545 (2018).
 36. Yan, C., Wan, R., Bai, R., Huang, G. & Shi, Y. Structure of a yeast step II catalytically activated spliceosome. *Science (80-.)*. **355**, 149 LP – 155 (2017).
 37. Bertram, K. *et al.* Cryo-EM structure of a human spliceosome activated for step 2 of splicing. *Nature* **542**, 318–323 (2017).
 38. Li, X. *et al.* A unified mechanism for intron and exon definition and back-splicing. *Nature* **573**, 375–380 (2019).
 39. Gelfman, S. *et al.* Changes in exon–intron structure during vertebrate evolution affect the splicing pattern of exons. *Genome Res.* **22**, 35–50 (2012).
 40. Keren, H., Lev-Maor, G. & Ast, G. Alternative splicing and evolution: diversification, exon definition and function. *Nat. Rev. Genet.* **11**, 345–355 (2010).
 41. Koç, A., Wheeler, L. J., Mathews, C. K. & Merrill, G. F. Hydroxyurea Arrests DNA Replication by a Mechanism That Preserves Basal dNTP Pools. *J. Biol. Chem.* **279**, 223–230 (2004).
 42. Xu, Y.-Z. & Query, C. C. Competition between the ATPase Prp5 and branch region-U2 snRNA pairing modulates the fidelity of spliceosome assembly. *Mol. Cell* **28**, 838–849 (2007).
 43. Yang, F. *et al.* Splicing proofreading at 5' splice sites by ATPase Prp28p. *Nucleic Acids Res.* **41**, 4660–4670 (2013).
 44. Mayas, R. M., Maita, H. & Staley, J. P. Exon ligation is proofread by the DExD/H-box ATPase Prp22p. *Nat. Struct. Mol. Biol.* **13**, 482–490 (2006).
 45. Koodathingal, P., Novak, T., Piccirilli, J. A. & Staley, J. P. The DEAH box ATPases Prp16 and Prp43 cooperate to proofread 5' splice site cleavage during pre-mRNA splicing. *Mol. Cell* **39**, 385–395 (2010).
 46. Koodathingal, P. & Staley, J. P. Splicing fidelity: DEAD/H-box ATPases as molecular clocks. *RNA Biol.* **10**, 1073–1079 (2013).
 47. Smith, D. J., Query, C. C. & Konarska, M. M. 'Nought may endure but mutability': spliceosome dynamics and the regulation of splicing. *Mol. Cell* **30**, 657–666 (2008).
 48. Mishra, S. K. *et al.* Role of the ubiquitin-like protein Hub1 in splice-site usage and alternative splicing. *Nature* **474**, 173–178 (2011).
 49. Karaduman, R., Chanarat, S., Pfander, B. & Jentsch, S. Error-Prone Splicing Controlled by the Ubiquitin Relative Hub1. *Mol. Cell* **67**, 423-432.e4 (2017).
 50. Wang, Y. *et al.* Mechanism of alternative splicing and its regulation. *Biomed. reports* **3**, 152–158 (2015).

51. Kelemen, O. *et al.* Function of alternative splicing. *Gene* **514**, 1–30 (2013).
52. Jin, Y., Yang, Y. & Zhang, P. New insights into RNA secondary structure in the alternative splicing of pre-mRNAs. *RNA Biol.* **8**, 450–457 (2011).
53. McManus, C. J. & Graveley, B. R. RNA structure and the mechanisms of alternative splicing. *Curr. Opin. Genet. Dev.* **21**, 373–379 (2011).
54. Zhan, X., Yan, C., Zhang, X., Lei, J. & Shi, Y. Structures of the human pre-catalytic spliceosome and its precursor spliceosome. *Cell Res.* **28**, 1129–1140 (2018).
55. Iyer, L. M., Leipe, D. D., Koonin, E. V & Aravind, L. Evolutionary history and higher order classification of AAA+ ATPases. *J. Struct. Biol.* **146**, 11–31 (2004).
56. Walker, J. E., Saraste, M., Runswick, M. J. & Gay, N. J. Distantly related sequences in the alpha- and beta-subunits of ATP synthase, myosin, kinases and other ATP-requiring enzymes and a common nucleotide binding fold. *EMBO J.* **1**, 945–951 (1982).
57. Hishida, T., Iwasaki, H., Ohno, T., Morishita, T. & Shinagawa, H. A yeast gene, MGS1, encoding a DNA-dependent AAA(+) ATPase is required to maintain genome stability. *Proc. Natl. Acad. Sci. U. S. A.* **98**, 8283–8289 (2001).
58. Ogura, T. & Wilkinson, A. J. AAA+ superfamily ATPases: Common structure-diverse function. *Genes to Cells* **6**, 575–597 (2001).
59. Snider, J., Thibault, G. & Houry, W. A. The AAA+ superfamily of functionally diverse proteins. *Genome Biol.* **9**, 216 (2008).
60. Herruzo, E. *et al.* The Pch2 AAA+ ATPase promotes phosphorylation of the Hop1 meiotic checkpoint adaptor in response to synaptonemal complex defects. *Nucleic Acids Res.* **44**, 7722–7741 (2016).
61. Babst, M., Wendland, B., Estepa, E. J. & Emr, S. D. The Vps4p AAA ATPase regulates membrane association of a Vps protein complex required for normal endosome function. *EMBO J.* **17**, 2982–2993 (1998).
62. Numata, N. *et al.* Molecular mechanism of force generation by dynein, a molecular motor belonging to the AAA+ family. *Biochem. Soc. Trans.* **36**, 131 LP – 135 (2008).
63. Xia, D., Tang, W. K. & Ye, Y. STRUCTURE AND FUNCTION OF THE AAA+ ATPASE p97/Cdc48p. *Gene* **583**, 64–77 (2016).
64. Bodnar, N. O. & Rapoport, T. A. Molecular Mechanism of Substrate Processing by the Cdc48 ATPase Complex. *Cell* **169**, 722-735.e9 (2017).
65. Braun, R. J. & Zischka, H. Mechanisms of Cdc48/VCP-mediated cell death — from yeast apoptosis to human disease. *Biochim. Biophys. Acta - Mol. Cell Res.* **1783**, 1418–1435 (2008).
66. Bodnar, N. & Rapoport, T. Toward an understanding of the Cdc48/p97 ATPase. *F1000Research* **6**, 1318 (2017).
67. Banerjee, S. *et al.* 2.3 Å resolution cryo-EM structure of human p97 and mechanism of

- allosteric inhibition. *Science* (80-.). **351**, 871–875 (2016).
68. Davies, J. M., Brunger, A. T. & Weis, W. I. Improved Structures of Full-Length p97, an AAA ATPase: Implications for Mechanisms of Nucleotide-Dependent Conformational Change. *Structure* **16**, 715–726 (2008).
 69. Watts, G. D. J. *et al.* Inclusion body myopathy associated with Paget disease of bone and frontotemporal dementia is caused by mutant valosin-containing protein. *Nat. Genet.* **36**, 377 (2004).
 70. Saugar, I., Parker, J. L., Zhao, S. & Ulrich, H. D. The genome maintenance factor Mgs1 is targeted to sites of replication stress by ubiquitylated PCNA. *Nucleic Acids Res.* **40**, 245–257 (2012).
 71. Hishida, T., Ohno, T., Iwasaki, H. & Shinagawa, H. *Saccharomyces cerevisiae* MGS1 is essential in strains deficient in the RAD6-dependent DNA damage tolerance pathway. *EMBO J.* **21**, 2019–2029 (2002).
 72. Sung, P. & Klein, H. Mechanism of homologous recombination: mediators and helicases take on regulatory functions. *Nat. Rev. Mol. Cell Biol.* **7**, 739–750 (2006).
 73. Wu, H.-Y. & Burgess, S. M. Two distinct surveillance mechanisms monitor meiotic chromosome metabolism in budding yeast. *Curr. Biol.* **16**, 2473–2479 (2006).
 74. Szostak, J. W., Orr-Weaver, T. L., Rothstein, R. J. & Stahl, F. W. The double-strand-break repair model for recombination. *Cell* **33**, 25–35 (1983).
 75. Wright, W. D., Shah, S. S. & Heyer, W.-D. Homologous recombination and the repair of DNA double-strand breaks. *J. Biol. Chem.* **293**, 10524–10535 (2018).
 76. Miura, T. *et al.* Homologous recombination via synthesis-dependent strand annealing in yeast requires the Irc20 and Srs2 DNA helicases. *Genetics* **191**, 65–78 (2012).
 77. Bhargava, R., Onyango, D. O. & Stark, J. M. Regulation of Single-Strand Annealing and its Role in Genome Maintenance. *Trends Genet.* **32**, 566–575 (2016).
 78. Aylon, Y. & Kupiec, M. New insights into the mechanism of homologous recombination in yeast. *Mutat. Res. Mutat. Res.* **566**, 231–248 (2004).
 79. McEachern, M. & Haber, J. Break-Induced Replication and Recombinational Telomere Elongation in Yeast. *Annu. Rev. Biochem.* **75**, 111–135 (2006).
 80. Pâques, F. & Haber, J. E. Multiple pathways of recombination induced by double-strand breaks in *Saccharomyces cerevisiae*. *Microbiol. Mol. Biol. Rev.* **63**, 349–404 (1999).
 81. Yashiroda, H. & Tanaka, K. Hub1 is an essential ubiquitin-like protein without functioning as a typical modifier in fission yeast. *Genes to Cells* **9**, 1189–1197 (2004).
 82. Stevens, S. W. *et al.* Biochemical and genetic analyses of the U5, U6, and U4/U6 x U5 small nuclear ribonucleoproteins from *Saccharomyces cerevisiae*. *RNA* **7**, 1543–1553 (2001).
 83. Ammon, T. *et al.* The conserved ubiquitin-like protein Hub1 plays a critical role in

splicing in human cells. *J. Mol. Cell Biol.* **6**, 312–323 (2014).

84. Wan, R. *et al.* The 3.8 Å structure of the U4/U6.U5 tri-snRNP: Insights into spliceosome assembly and catalysis. *Science* (80-.). **351**, 466 LP – 475 (2016).
85. Makarova, O. V, Makarov, E. M. & Lührmann, R. The 65 and 110 kDa SR-related proteins of the U4/U6·U5 tri-snRNP are essential for the assembly of mature spliceosomes. *EMBO J.* **20**, 2553–2563 (2001).
86. Narita, M. *et al.* Induction of antigen-specific cytotoxic T lymphocytes by using monocyte-derived DCs transfected with in vitro-transcribed WT1 or SART1 mRNA. 429–436 (2009). doi:10.1007/s12032-008-9142-3
87. Koh, M. Y., Darnay, B. G. & Powis, G. Hypoxia-associated factor, a novel E3-ubiquitin ligase, binds and ubiquitinates hypoxia-inducible factor 1alpha, leading to its oxygen-independent degradation. *Mol. Cell. Biol.* **28**, 7081–7095 (2008).
88. Tanaka, S. *et al.* Expression of tumor-rejection antigens in gynecologic cancers. *Jpn. J. Cancer Res.* **91**, 1177–1184 (2000).
89. Schmidt-Kastner, R. *et al.* Hypoxia-regulated components of the U4/U6.U5 tri-small nuclear riboprotein complex: possible role in autosomal dominant retinitis pigmentosa. *Mol. Vis.* **14**, 125–135 (2008).
90. Wheatley, A. P., Bolland, D. J., Hewitt, J. E., Dewar, J. C. & Hall, I. P. Identification of the autoantigen SART-1 as a candidate gene for the development of atopy. *Hum. Mol. Genet.* **11**, 2143–2146 (2002).
91. Li, Z. *et al.* Rational extension of the ribosome biogenesis pathway using network-guided genetics. *PLoS Biol.* **7**, e1000213–e1000213 (2009).
92. Baryshnikova, A. *et al.* Chapter 7 - Synthetic Genetic Array (SGA) Analysis in *Saccharomyces cerevisiae* and *Schizosaccharomyces pombe*. in *Guide to Yeast Genetics: Functional Genomics, Proteomics, and Other Systems Analysis* **470**, 145–179 (Academic Press, 2010).
93. Caspary, F. & Séraphin, B. The yeast U2A'/U2B complex is required for pre-spliceosome formation. *EMBO J.* **17**, 6348–6358 (1998).
94. Noble, S. M. & Guthrie, C. Transcriptional pulse-chase analysis reveals a role for a novel snRNP-associated protein in the manufacture of spliceosomal snRNPs. *EMBO J.* **15**, 4368–4379 (1996).
95. Liu, Q., Fischer, U., Wang, F. & Dreyfuss, G. The Spinal Muscular Atrophy Disease Gene Product, SMN, and Its Associated Protein SIP1 Are in a Complex with Spliceosomal snRNP Proteins. *Cell* **90**, 1013–1021 (1997).
96. Lesser, C. F. & Guthrie, C. Mutational analysis of pre-mRNA splicing in *Saccharomyces cerevisiae* using a sensitive new reporter gene, CUP1. *Genetics* **133**, 851–863 (1993).
97. Liberzon, A., Shpungin, S., Bangio, H., Yona, E. & Katcoff, D. J. Association of yeast SAP1, a novel member of the 'AAA' ATPase family of proteins, with the chromatin protein SIN1. *FEBS Lett.* **388**, 5–10 (1996).

98. Hannich, J. T. *et al.* Defining the SUMO-modified proteome by multiple approaches in *Saccharomyces cerevisiae*. *J. Biol. Chem.* **280**, 4102–4110 (2005).
99. Silva, S. *et al.* SUMOylation of Rad52–Rad59 synergistically change the outcome of mitotic recombination. *DNA Repair (Amst)*. **42**, 11–25 (2016).
100. Crickard, J. B. & Greene, E. C. Helicase Mechanisms During Homologous Recombination in *Saccharomyces cerevisiae*. *Annu. Rev. Biophys.* **48**, 255–273 (2019).
101. Mimitou, E. P. & Symington, L. S. DNA end resection: many nucleases make light work. *DNA Repair (Amst)*. **8**, 983–995 (2009).
102. Shim, E. Y. *et al.* *Saccharomyces cerevisiae* Mre11/Rad50/Xrs2 and Ku proteins regulate association of Exo1 and Dna2 with DNA breaks. *EMBO J.* **29**, 3370–3380 (2010).
103. Mimitou, E. P. & Symington, L. S. Sae2, Exo1 and Sgs1 collaborate in DNA double-strand break processing. *Nature* **455**, 770–774 (2008).
104. Shinohara, A., Ogawa, H. & Ogawa, T. Rad51 protein involved in repair and recombination in *S. cerevisiae* is a RecA-like protein. *Cell* **69**, 457–470 (1992).
105. Sung, P. Catalysis of ATP-dependent homologous DNA pairing and strand exchange by yeast RAD51 protein. *Science (80-.)*. **265**, 1241 LP – 1243 (1994).
106. Egger, A. L., Inman, R. B. & Cox, M. M. The Rad51-dependent Pairing of Long DNA Substrates Is Stabilized by Replication Protein A. *J. Biol. Chem.* **277**, 39280–39288 (2002).
107. Shinohara, A. & Ogawa, T. Stimulation by Rad52 of yeast Rad51-mediated recombination. *Nature* **391**, 404–407 (1998).
108. Wright, W. D. & Heyer, W.-D. Rad54 functions as a heteroduplex DNA pump modulated by its DNA substrates and Rad51 during D loop formation. *Mol. Cell* **53**, 420–432 (2014).
109. Pfander, B., Moldovan, G.-L., Sacher, M., Hoegge, C. & Jentsch, S. SUMO-modified PCNA recruits Srs2 to prevent recombination during S phase. *Nature* **436**, 428–433 (2005).
110. Bronstein, A., Bramson, S., Shemesh, K., Liefshitz, B. & Kupiec, M. Tight Regulation of Srs2 Helicase Activity Is Crucial for Proper Functioning of DNA Repair Mechanisms. *G3 (Bethesda)*. **8**, 1615–1626 (2018).
111. Krejci, L. *et al.* DNA helicase Srs2 disrupts the Rad51 presynaptic filament. *Nature* **423**, 305–309 (2003).
112. Symington, L. S., Rothstein, R. & Lisby, M. Mechanisms and regulation of mitotic recombination in *Saccharomyces cerevisiae*. *Genetics* **198**, 795–835 (2014).
113. DeRisi, J. L., Iyer, V. R. & Brown, P. O. Exploring the Metabolic and Genetic Control of Gene Expression on a Genomic Scale. *Science (80-.)*. **278**, 680 LP – 686 (1997).
114. Edman, P. Method for determination of the amino acid sequence in peptides. *Acta*

chem. scand **4**, 283–293 (1950).

115. Gaytán, B. D. *et al.* Functional profiling discovers the dieldrin organochlorinated pesticide affects leucine availability in yeast. *Toxicol. Sci.* **132**, 347–358 (2013).
116. O'Connor, S. T. F. *et al.* Genome-Wide Functional and Stress Response Profiling Reveals Toxic Mechanism and Genes Required for Tolerance to Benzo[a]pyrene in *S. cerevisiae*. *Front. Genet.* **3**, 316 (2013).
117. Versele, M. & Thorner, J. Septin collar formation in budding yeast requires GTP binding and direct phosphorylation by the PAK, Cla4. *J. Cell Biol.* **164**, 701 LP – 715 (2004).
118. Moore, J. K., Chudalayandi, P., Heil-Chapdelaine, R. A. & Cooper, J. A. The spindle position checkpoint is coordinated by the Elm1 kinase. *J. Cell Biol.* **191**, 493–503 (2010).
119. Mortensen, E. M., McDonald, H., Yates 3rd, J. & Kellogg, D. R. Cell cycle-dependent assembly of a Gin4-septin complex. *Mol. Biol. Cell* **13**, 2091–2105 (2002).
120. Byers, B. & Goetsch, L. A highly ordered ring of membrane-associated filaments in budding yeast. *J. Cell Biol.* **69**, 717–721 (1976).
121. Haarer, B. K. & Pringle, J. R. Immunofluorescence localization of the *Saccharomyces cerevisiae* CDC12 gene product to the vicinity of the 10-nm filaments in the mother-bud neck. *Mol. Cell. Biol.* **7**, 3678–3687 (1987).
122. Tamborrini, D. & Piatti, S. Septin clearance from the division site triggers cytokinesis in budding yeast. *Microb. cell (Graz, Austria)* **6**, 295–298 (2019).
123. Takahashi, Y., Toh-e, A. & Kikuchi, Y. A novel factor required for the SUMO1/Smt3 conjugation of yeast septins. *Gene* **275**, 223–231 (2001).
124. Johnson, E. S. & Gupta, A. A. An E3-like Factor that Promotes SUMO Conjugation to the Yeast Septins. *Cell* **106**, 735–744 (2001).
125. Wilkinson, L. E. & Pringle, J. R. Transient G1 arrest of *S. cerevisiae* cells of mating type α by a factor produced by cells of mating type a. *Exp. Cell Res.* **89**, 175–187 (1974).
126. Treitel, M. A. & Carlson, M. Repression by SSN6-TUP1 is directed by MIG1, a repressor/activator protein. *Proc. Natl. Acad. Sci. U. S. A.* **92**, 3132–3136 (1995).
127. Davie, J. K., Trumbly, R. J. & Dent, S. Y. R. Histone-dependent association of Tup1-Ssn6 with repressed genes in vivo. *Mol. Cell. Biol.* **22**, 693–703 (2002).
128. Tzamarias, D. & Struhl, K. Functional dissection of the yeast Cyc8-Tup1 transcriptional co-repressor complex. *Nature* **369**, 758–761 (1994).
129. Nathan, D. *et al.* Histone sumoylation is a negative regulator in *Saccharomyces cerevisiae* and shows dynamic interplay with positive-acting histone modifications. *Genes Dev.* **20**, 966–976 (2006).
130. Sterner, D. E., Nathan, D., Reindle, A., Johnson, E. S. & Berger, S. L. Sumoylation of

- the Yeast Gcn5 Protein. *Biochemistry* **45**, 1035–1042 (2006).
131. Texari, L. *et al.* The Nuclear Pore Regulates GAL1 Gene Transcription by Controlling the Localization of the SUMO Protease Ulp1. *Mol. Cell* **51**, 807–818 (2013).
 132. Ng, C. H. *et al.* Sumoylation controls the timing of Tup1-mediated transcriptional deactivation. *Nat. Commun.* **6**, 6610 (2015).
 133. Gerber, A. P. & Keller, W. An Adenosine Deaminase that Generates Inosine at the Wobble Position of tRNAs. *Science (80-.)*. **286**, 1146 LP – 1149 (1999).
 134. Vijayraghavan, U., Company, M. & Abelson, J. Isolation and characterization of pre-mRNA splicing mutants of *Saccharomyces cerevisiae*. *Genes Dev.* **3**, 1206–1216 (1989).
 135. Liu, L., Query, C. C. & Konarska, M. M. Opposing classes of prp8 alleles modulate the transition between the catalytic steps of pre-mRNA splicing. *Nat. Struct. & Mol. Biol.* **14**, 519 (2007).
 136. Wahl, M. C., Will, C. L. & Lührmann, R. The Spliceosome: Design Principles of a Dynamic RNP Machine. *Cell* **136**, 701–718 (2009).
 137. Ast, G. How did alternative splicing evolve? *Nat Rev Genet* **5**, 773–782 (2004).
 138. Kim, E., Magen, A. & Ast, G. Different levels of alternative splicing among eukaryotes. *Nucleic Acids Res.* **35**, 125–131 (2006).
 139. Lee, Y. & Rio, D. C. Mechanisms and Regulation of Alternative Pre-mRNA Splicing. *Annu. Rev. Biochem.* **84**, 291–323 (2015).
 140. Kempken, F. Alternative splicing in ascomycetes. *Appl. Microbiol. Biotechnol.* **97**, 4235–4241 (2013).
 141. Kawashima, T., Douglass, S., Gabunilas, J., Pellegrini, M. & Chanfreau, G. F. Widespread use of non-productive alternative splice sites in *Saccharomyces cerevisiae*. *PLoS Genet.* **10**, e1004249 (2014).
 142. Stepankiw, N., Raghavan, M., Fogarty, E. A., Grimson, A. & Pleiss, J. A. Widespread alternative and aberrant splicing revealed by lariat sequencing. *Nucleic Acids Res.* **43**, 8488–8501 (2015).
 143. Grützmann, K. *et al.* Fungal alternative splicing is associated with multicellular complexity and virulence: A genome-wide multi-species study. *DNA Res.* **21**, 27–39 (2014).
 144. Grund, S. E. *et al.* The inner nuclear membrane protein Src1 associates with subtelomeric genes and alters their regulated gene expression. *J. Cell Biol.* **182**, 897–910 (2008).
 145. Mishra, S. K. & Thakran, P. Intron specificity in pre-mRNA splicing. *Curr. Genet.* **64**, (2018).
 146. Chanarat, S. & Mishra, S. K. Emerging Roles of Ubiquitin-like Proteins in Pre-mRNA Splicing. *Trends Biochem. Sci.* **43**, 896–907 (2018).

147. Chanarat, S. & Svasti, J. Stress-induced upregulation of the ubiquitin-relative Hub1 modulates pre-mRNA splicing and facilitates cadmium tolerance in *Saccharomyces cerevisiae*. *Biochim. Biophys. Acta - Mol. Cell Res.* **1867**, 118565 (2020).
148. GRAINGER, R. J. Prp8 protein: At the heart of the spliceosome. *RNA* **11**, 533–557 (2005).
149. Umen, J. G. & Guthrie, C. Mutagenesis of the yeast gene PRP8 reveals domains governing the specificity and fidelity of 3' splice site selection. *Genetics* **143**, 723–739 (1996).
150. Jacquier, A., Rodriguez, J. R. & Rosbash, M. A quantitative analysis of the effects of 5' junction and TACTAAC box mutants and mutant combinations on yeast mRNA splicing. *Cell* **43**, 423–430 (1985).
151. Tong, A. H. Y. *et al.* Systematic Genetic Analysis with Ordered Arrays of Yeast Deletion Mutants. *Science (80-.)*. **294**, 2364 LP – 2368 (2001).
152. Anderson, G. J., Bach, M., Lührmann, R. & Beggs, J. D. Conservation between yeast and man of a protein associated with U5 small nuclear ribonucleoprotein. *Nature* **342**, 819–821 (1989).
153. Umen, J. G. & Guthrie, C. A novel role for a U5 snRNP protein in 3' splice site selection. *Genes Dev.* **9**, 855–868 (1995).
154. Galej, W. P., Oubridge, C., Newman, A. J. & Nagai, K. Crystal structure of Prp8 reveals active site cavity of the spliceosome. *Nature* **493**, 638–643 (2013).
155. Fica, S. M. & Nagai, K. Cryo-electron microscopy snapshots of the spliceosome: structural insights into a dynamic ribonucleoprotein machine. *Nat. Struct. Mol. Biol.* **24**, 791–799 (2017).
156. Puig, O., Gottschalk, A., Fabrizio, P. & Séraphin, B. Interaction of the U1 snRNP with nonconserved intronic sequences affects 5' splice site selection. *Genes Dev.* **13**, 569–580 (1999).
157. Qiu, Z. R., Schwer, B. & Shuman, S. Determinants of Nam8-dependent splicing of meiotic pre-mRNAs. *Nucleic Acids Res.* **39**, 3427–3445 (2011).
158. Spingola, M. & Ares, M. A Yeast Intronic Splicing Enhancer and Nam8p Are Required for Mer1p-Activated Splicing. *Mol. Cell* **6**, 329–338 (2000).
159. Li, X. *et al.* CryoEM structure of *Saccharomyces cerevisiae* U1 snRNP offers insight into alternative splicing. *Nat. Commun.* **8**, 1035 (2017).
160. Bao, P., Will, C. L., Urlaub, H., Boon, K.-L. & Lührmann, R. The RES complex is required for efficient transformation of the precatalytic B spliceosome into an activated Bact complex. *Genes Dev.* **31**, 2416–2429 (2017).
161. Zhou, Y. & Johansson, M. J. O. The pre-mRNA retention and splicing complex controls expression of the Mediator subunit Med20. *RNA Biol.* **14**, 1411–1417 (2017).
162. Gottschalk, A., Bartels, C., Neubauer, G., Lührmann, R. & Fabrizio, P. A novel yeast U2 snRNP protein, Snu17p, is required for the first catalytic step of splicing and for

- progression of spliceosome assembly. *Mol. Cell. Biol.* **21**, 3037–3046 (2001).
163. Wyszczanski, P. & Zweckstetter, M. Retention and splicing complex (RES) – the importance of cooperativity. *RNA Biol.* **13**, 128–133 (2016).
 164. Xu, D. & Friesen, J. D. Splicing factor slt11p and its involvement in formation of U2/U6 helix II in activation of the yeast spliceosome. *Mol. Cell. Biol.* **21**, 1011–1023 (2001).
 165. Xu, D. *et al.* Synthetic lethality of yeast slt mutations with U2 small nuclear RNA mutations suggests functional interactions between U2 and U5 snRNPs that are important for both steps of pre-mRNA splicing. *Mol. Cell. Biol.* **18**, 2055–2066 (1998).
 166. Decourty, L. *et al.* Linking functionally related genes by sensitive and quantitative characterization of genetic interaction profiles. *Proc. Natl. Acad. Sci.* **105**, 5821 LP – 5826 (2008).
 167. Costanzo, M. *et al.* The genetic landscape of a cell. *Science (80-.)*. **327**, 425–431 (2010).
 168. Dziembowski, A. *et al.* Proteomic analysis identifies a new complex required for nuclear pre-mRNA retention and splicing. *EMBO J.* **23**, 4847–4856 (2004).
 169. Brooks, M. A. *et al.* Structure of the yeast Pml1 splicing factor and its integration into the RES complex. *Nucleic Acids Res.* **37**, 129–143 (2009).
 170. Thakran, P. *et al.* Sde2 is an intron-specific pre-mRNA splicing regulator activated by ubiquitin-like processing. *EMBO J.* **37**, 89–101 (2018).
 171. Bryksin, A. V & Matsumura, I. Overlap extension PCR cloning: a simple and reliable way to create recombinant plasmids. *Biotechniques* **48**, 463–465 (2010).
 172. Janke, C. *et al.* A versatile toolbox for PCR-based tagging of yeast genes: new fluorescent proteins, more markers and promoter substitution cassettes. *Yeast* **21**, 947–962 (2004).
 173. Praefcke, G. J. K., Hofmann, K. & Dohmen, R. J. SUMO playing tag with ubiquitin. *Trends Biochem. Sci.* **37**, 23–31 (2012).
 174. Geiss-Friedlander, R. & Melchior, F. Concepts in sumoylation: a decade on. *Nat. Rev. Mol. Cell Biol.* **8**, 947 (2007).
 175. Meluh, P. B. & Koshland, D. Evidence that the MIF2 gene of *Saccharomyces cerevisiae* encodes a centromere protein with homology to the mammalian centromere protein CENP-C. *Mol. Biol. Cell* **6**, 793–807 (1995).
 176. Matunis, M. J., Coutavas, E. & Blobel, G. A novel ubiquitin-like modification modulates the partitioning of the Ran-GTPase-activating protein RanGAP1 between the cytosol and the nuclear pore complex. *J. Cell Biol.* **135**, 1457–1470 (1996).
 177. de Klerk, E. & ‘t Hoen, P. A. C. Alternative mRNA transcription, processing, and translation: insights from RNA sequencing. *Trends Genet.* **31**, 128–139 (2015).

Publications

Does genome surveillance explain the global discrepancy between binding and effect of chromatin factors?

Singh A, Choudhuri P, Chandradoss KR, Lal M, Mishra SK, Sandhu KS*
FEBS Lett. 2020 Jan 12. doi: 10.1002/1873-3468.13729

Alternative splicing through competing 5' splice site of *SRCl* requires concerted actions of U1, and U4/U6.U5 tri-snRNPs.

Poulami Choudhuri, Balashankar R., Shravan Kumar Mishra* (Manuscript in preparation)

Uncharacterised C-terminal conserved motif of Snu66 plays critical role in RNA splicing.

Poulami Choudhuri, Balashankar R., Shravan Kumar Mishra* (Manuscript in preparation)

